

Single Image Super-resolution from Transformed Self-Exemplars

Supplementary material

Jia-Bin Huang, Abhishek Singh, and Narendra Ahuja
University of Illinois, Urbana-Champaign
`{jbhuang1, asingh18, nahuja}@illinois.edu`

Abstract

In this supplementary document, we show more single image super-resolution results on a variety of scenes and compare our results against state-of-the-art single image super-resolution algorithms. The results shown in this supplementary material are best viewed on a high-resolution display with adequate zoom.

1. Introduction

1.1. Methods compared

We compare results of the following state-of-the-art single image super-resolution algorithms: ScSR [8], Kim and Kwon [4], SRCNN [1], A+ [7], Sub-band [5], Glasner [3], Sun-Hays [6], and TI-DTV [2].

In Table 1, we list the SR algorithms we compared and links to the publicly available implementations that we use for generating the results.

Table 1. Links to publicly available implementations.

ScSR [8]	http://www.ifp.illinois.edu/~jyang29/ScSR.htm
Kim and Kwon [4]	https://people.mpi-inf.mpg.de/~kkim/supres/supres.htm
SRCNN [1]	http://mmlab.ie.cuhk.edu.hk/projects/SRCNN.html
A+ [7]	http://www.vision.ee.ethz.ch/~timofte/ACCV2014_ID820_SUPPLEMENTARY/index.html
Glasner [3]	Our implementation of [3] http://www.wisdom.weizmann.ac.il/~vision/SingleImageSR.html
Sub-band [5]	Results provided by the authors
Sun and Hays [6]	Results provided by the authors
TI-DTV [2]	http://web.stanford.edu/~cfgranda/TI_DTV_code.zip

1.2. Datasets

In the following sections, we show sample comparisons with state-of-the-art single image super-resolution algorithms on Urban 100, BSD 100, Sun-Hays 80 [6], and test images from [2].

2. Sample comparisons on the *Urban 100* dataset

Here show 30 sample comparisons from the *Urban 100* dataset. As a reference, we show two quantitative evaluation metrics: PSNR and SSIM (computed using the luminance channel) for each method.

Below we show results with SR factor 4x and compare our method with ScSR [8], Kim [4], SRCNN [1], A+ [7], Sub-band [5], Glasner [3], Sun-Hays [6], and TI-DTV [2].

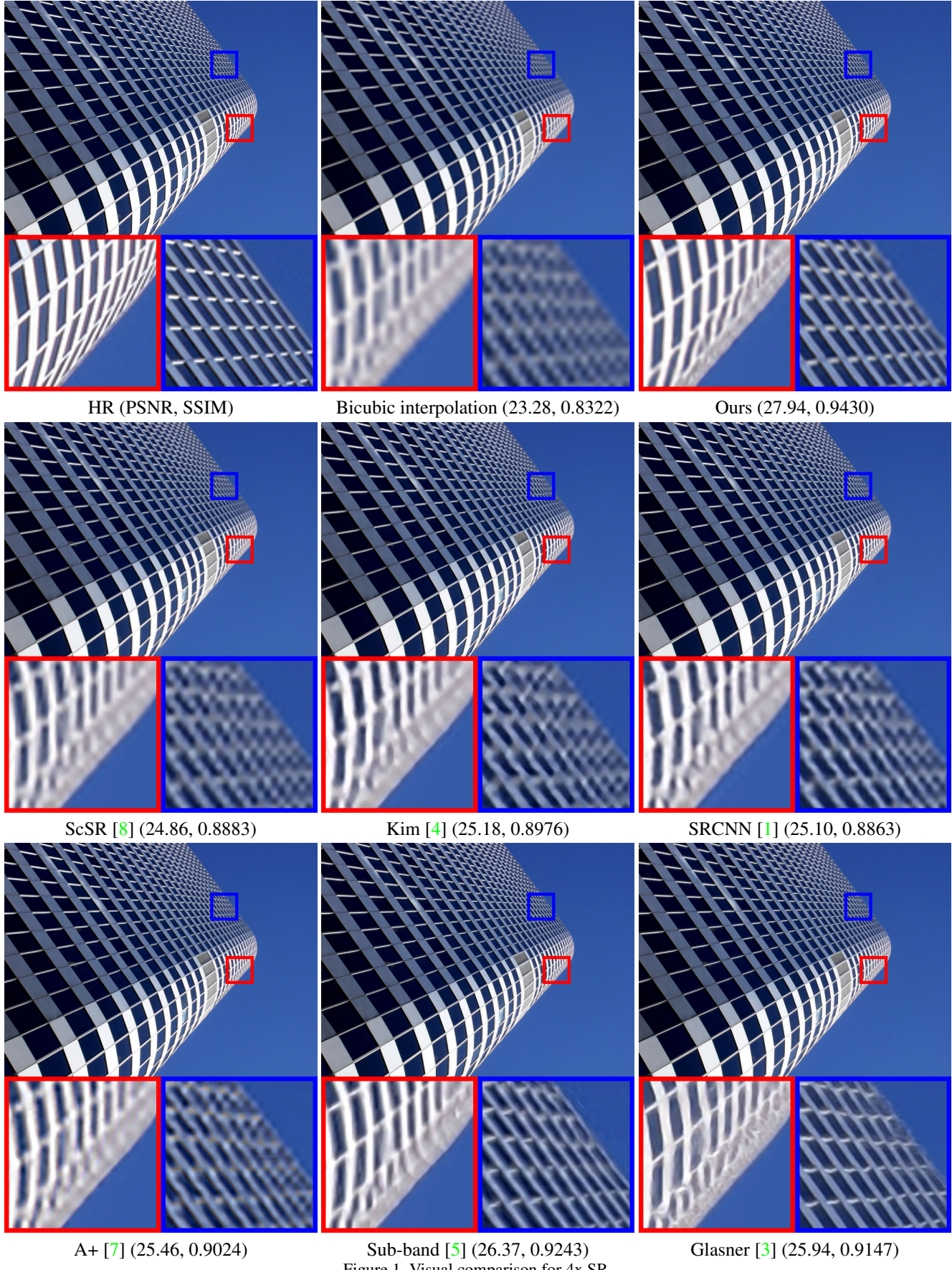


Figure 1. Visual comparison for 4x SR.

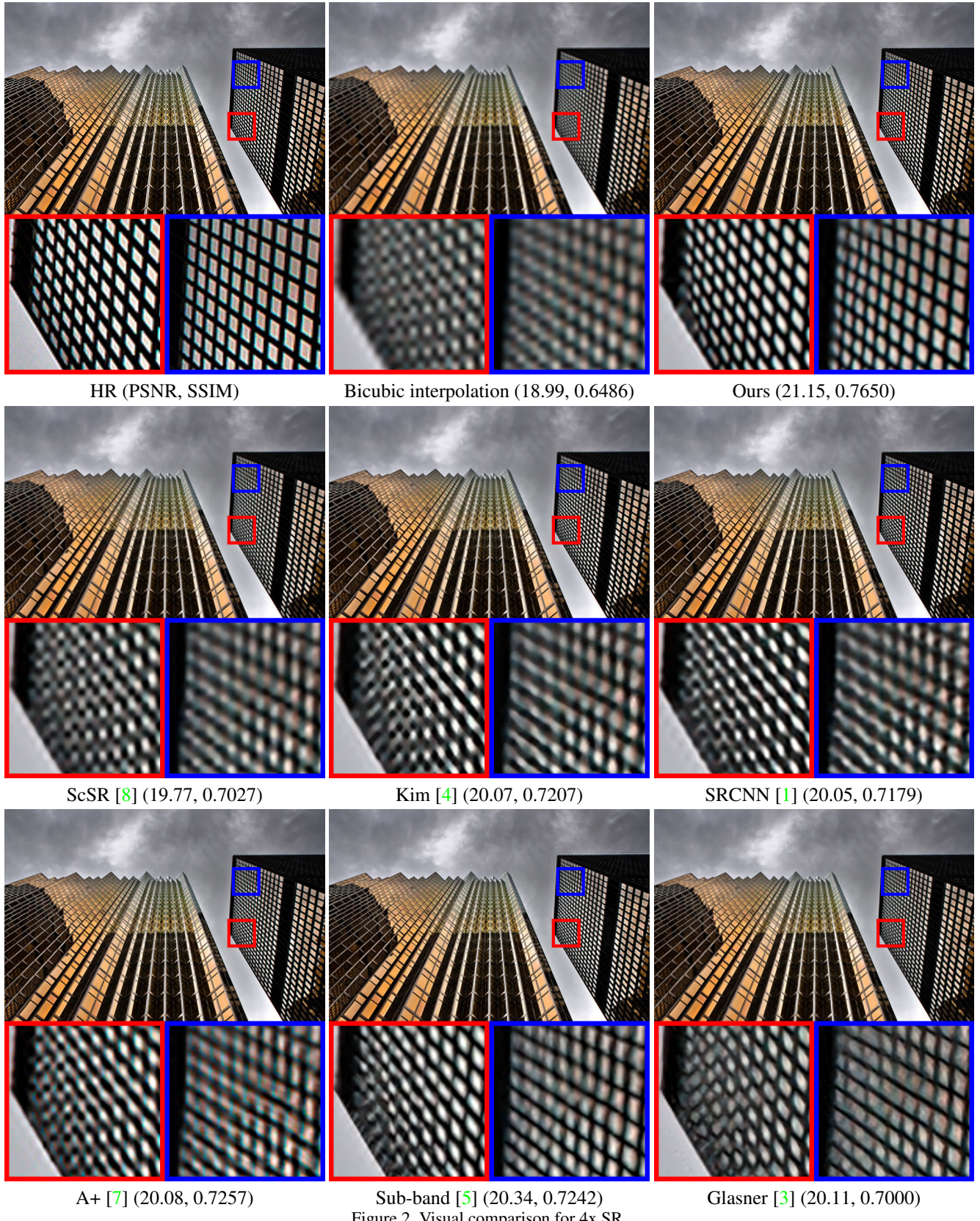


Figure 2. Visual comparison for 4x SR.

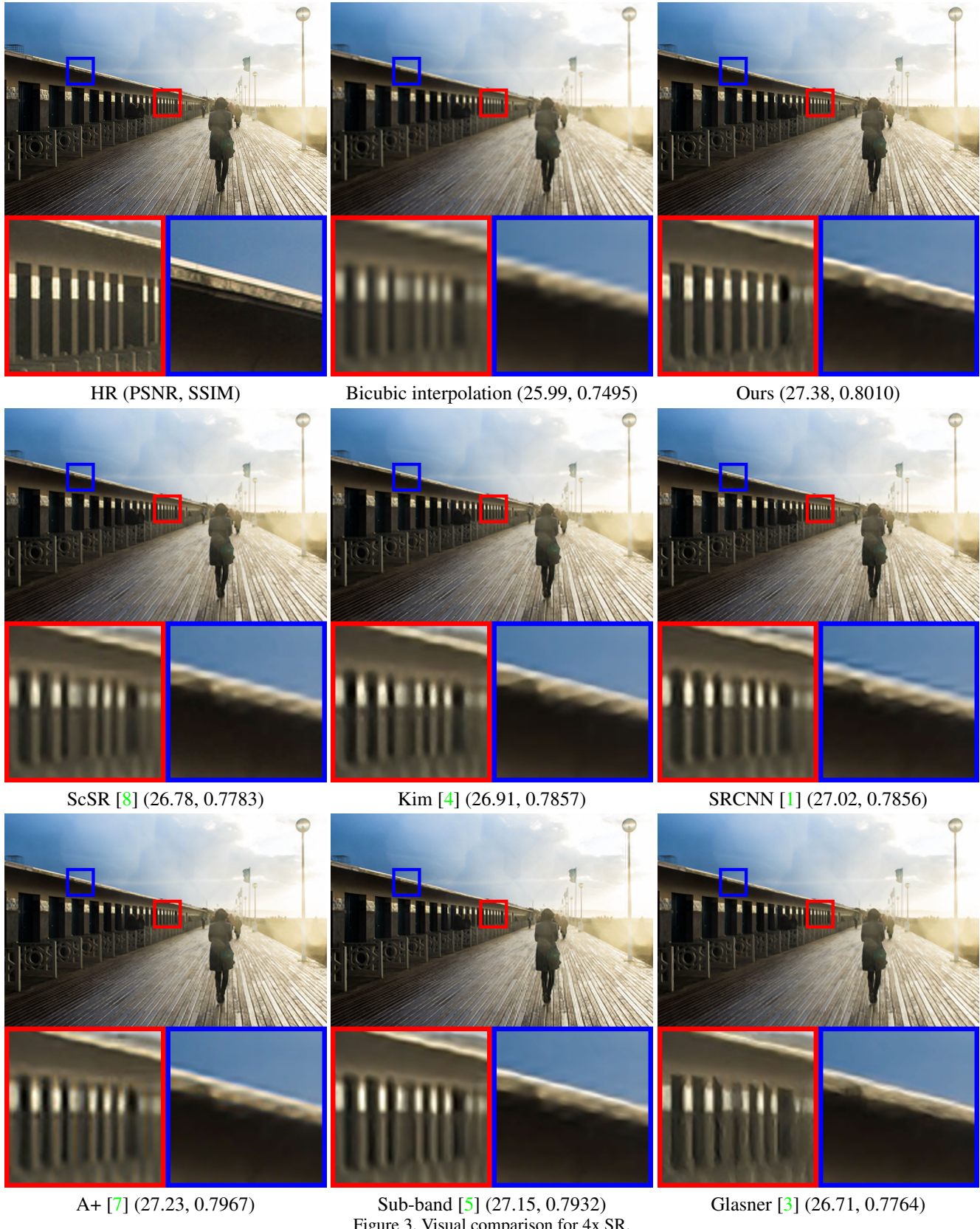


Figure 3. Visual comparison for 4x SR.



Figure 4. Visual comparison for 4x SR.

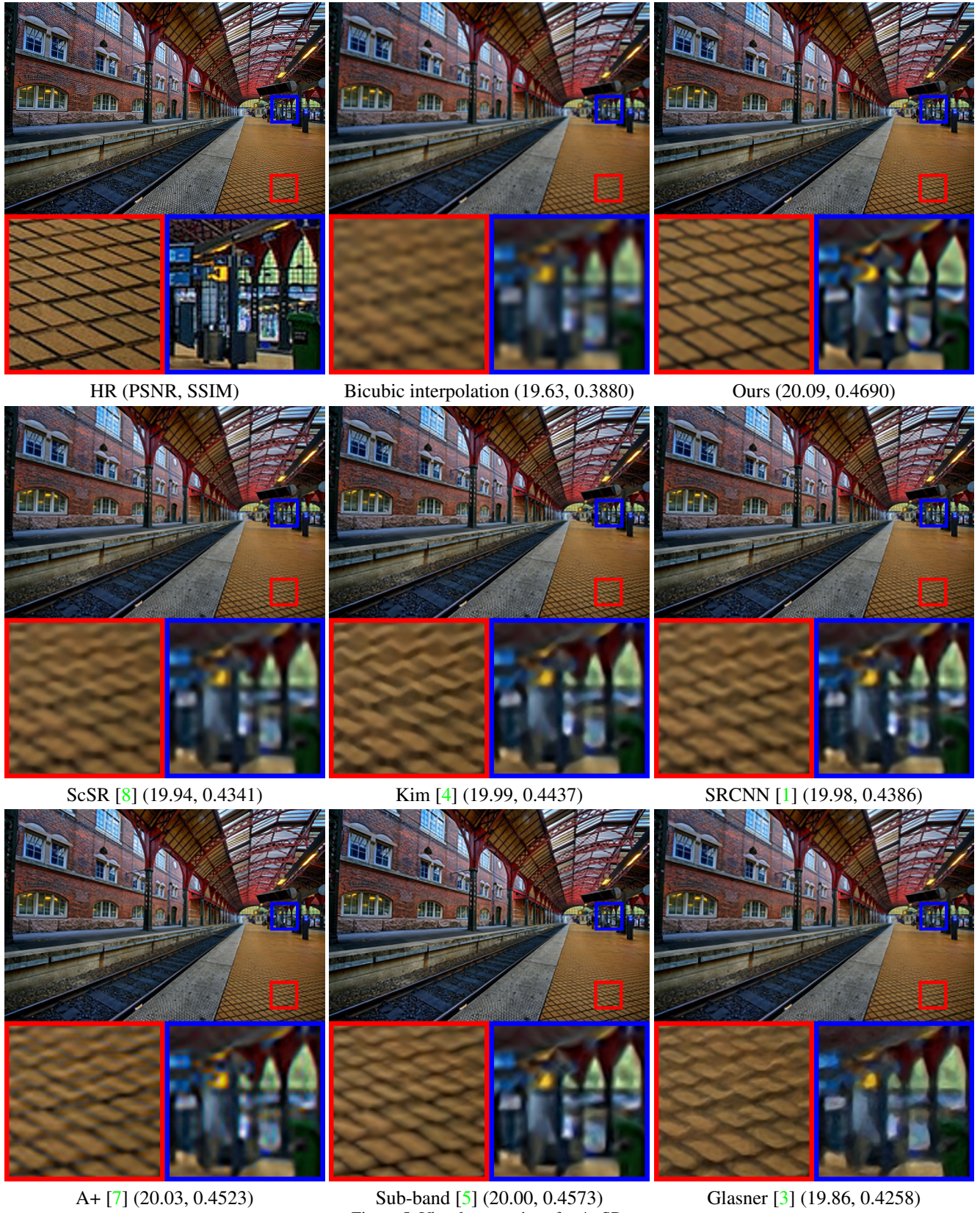


Figure 5. Visual comparison for 4x SR.

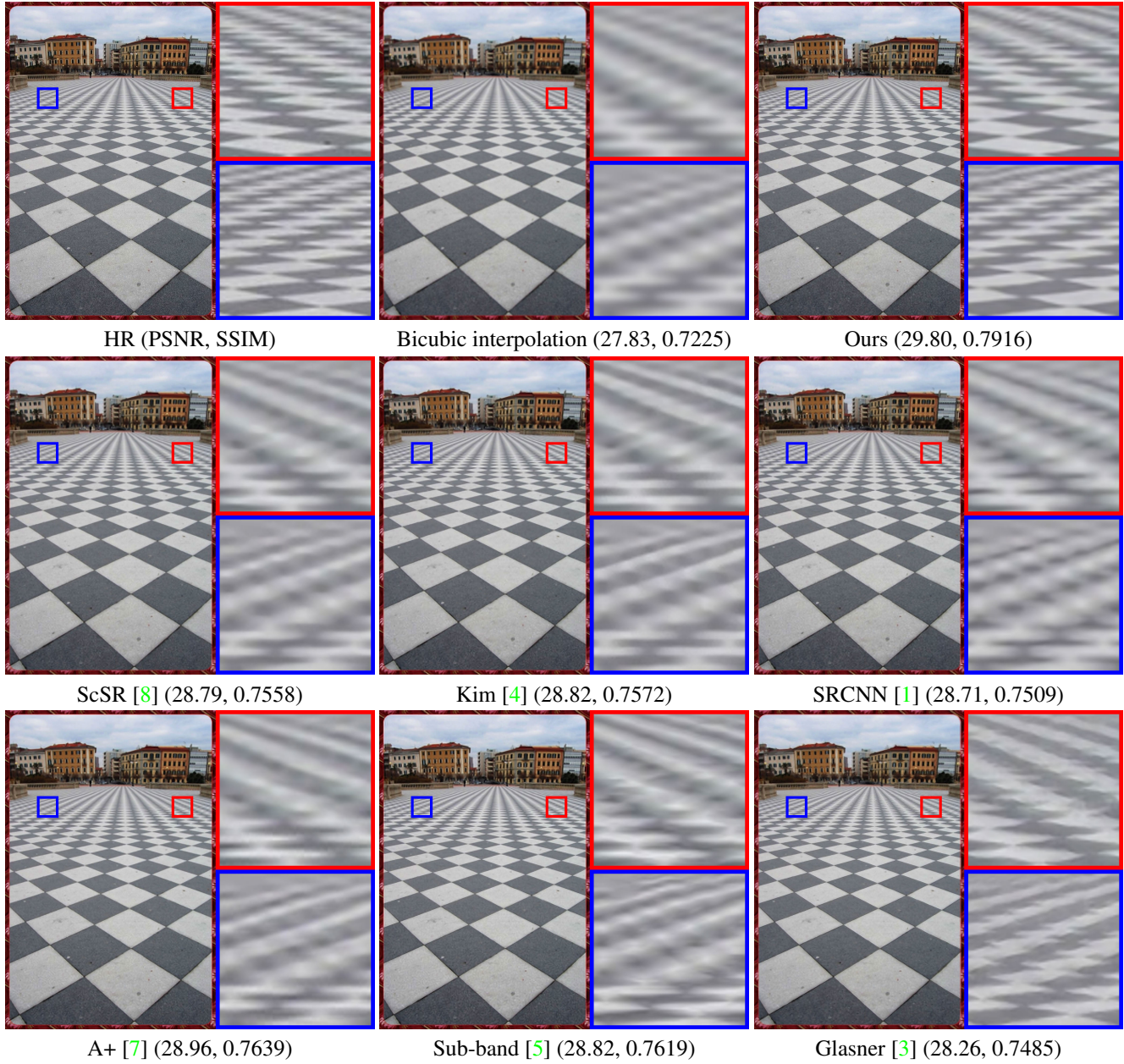


Figure 6. Visual comparison for 4x SR.

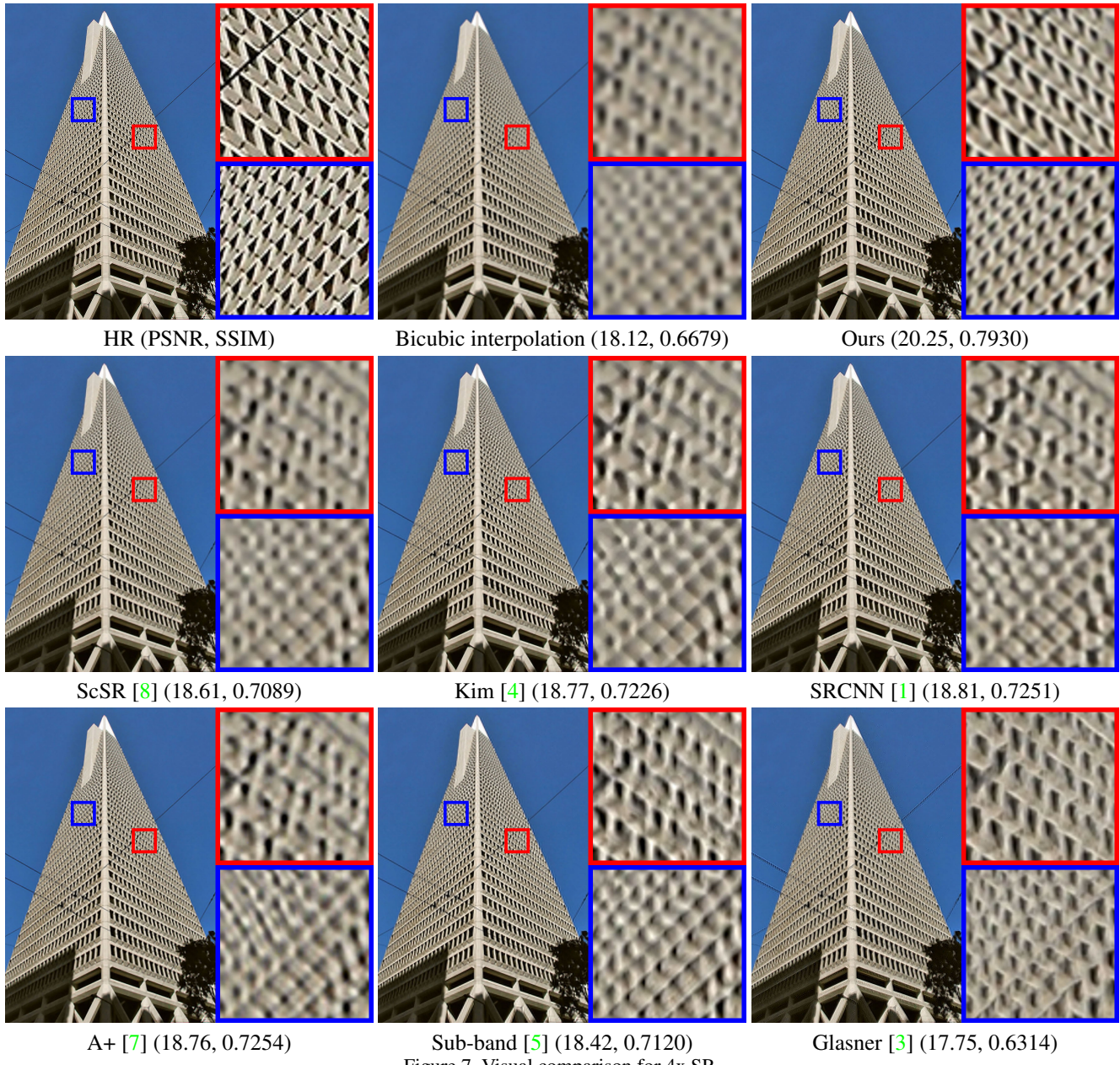


Figure 7. Visual comparison for 4x SR.

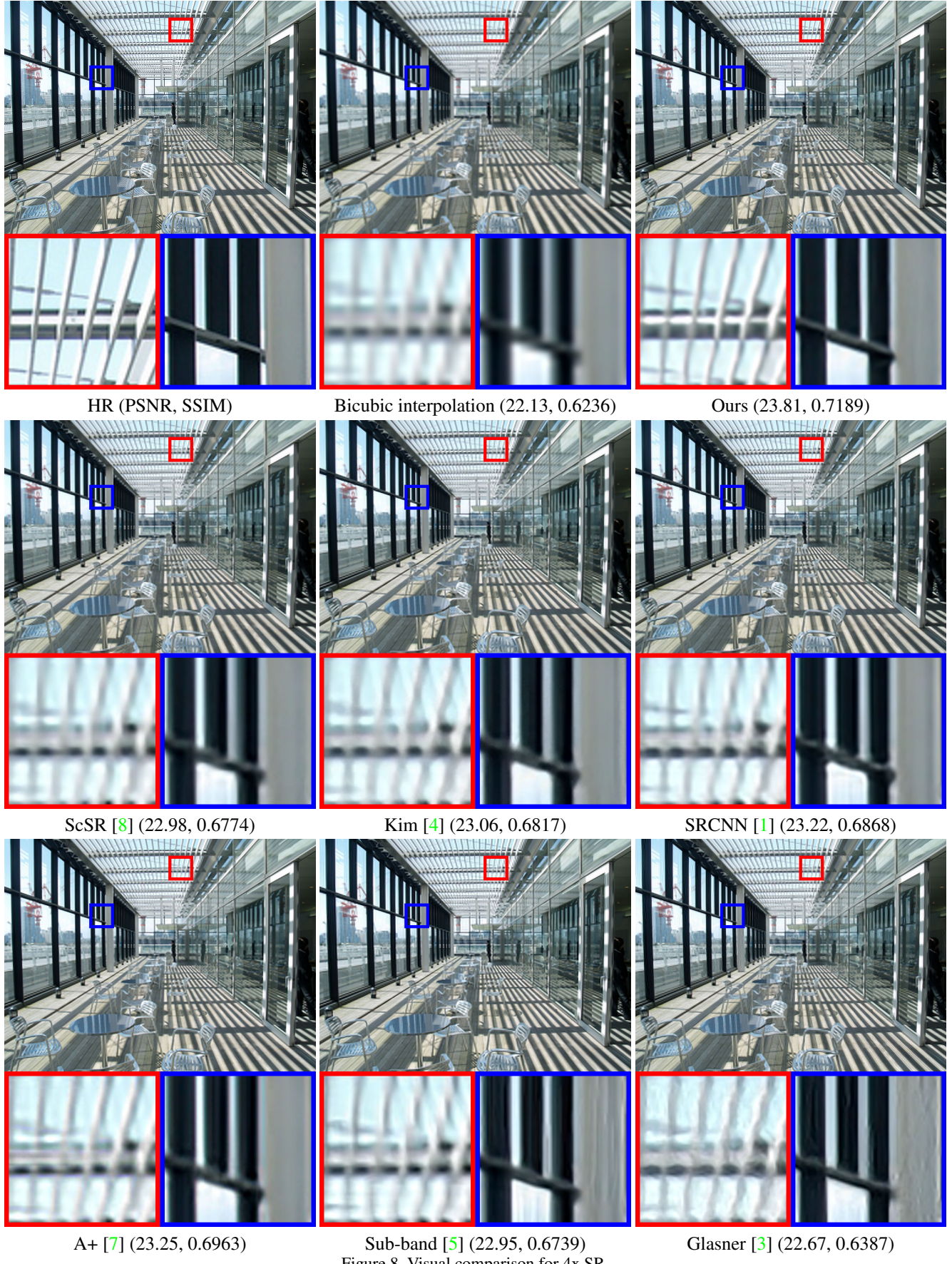


Figure 8. Visual comparison for 4x SR.

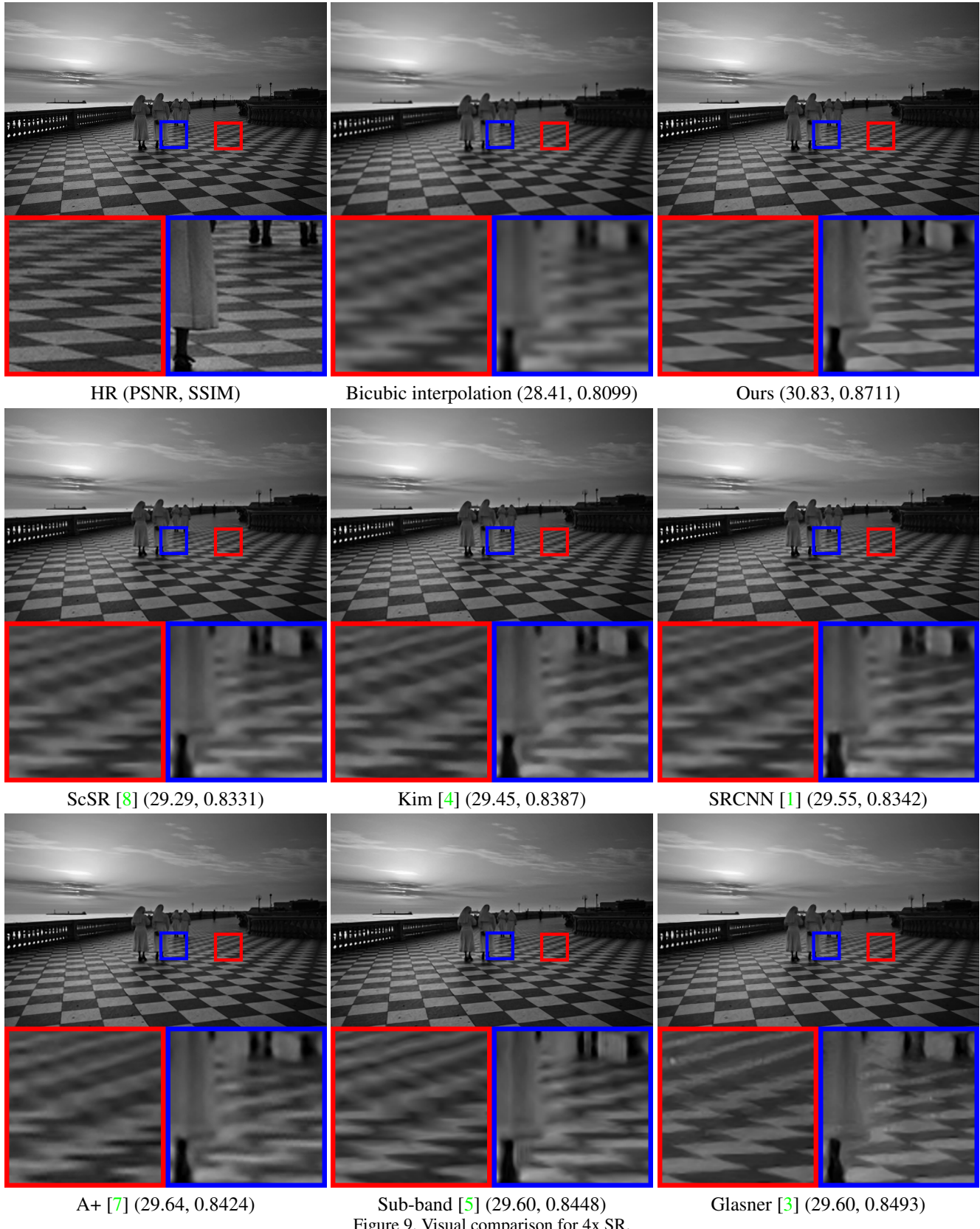


Figure 9. Visual comparison for 4x SR.

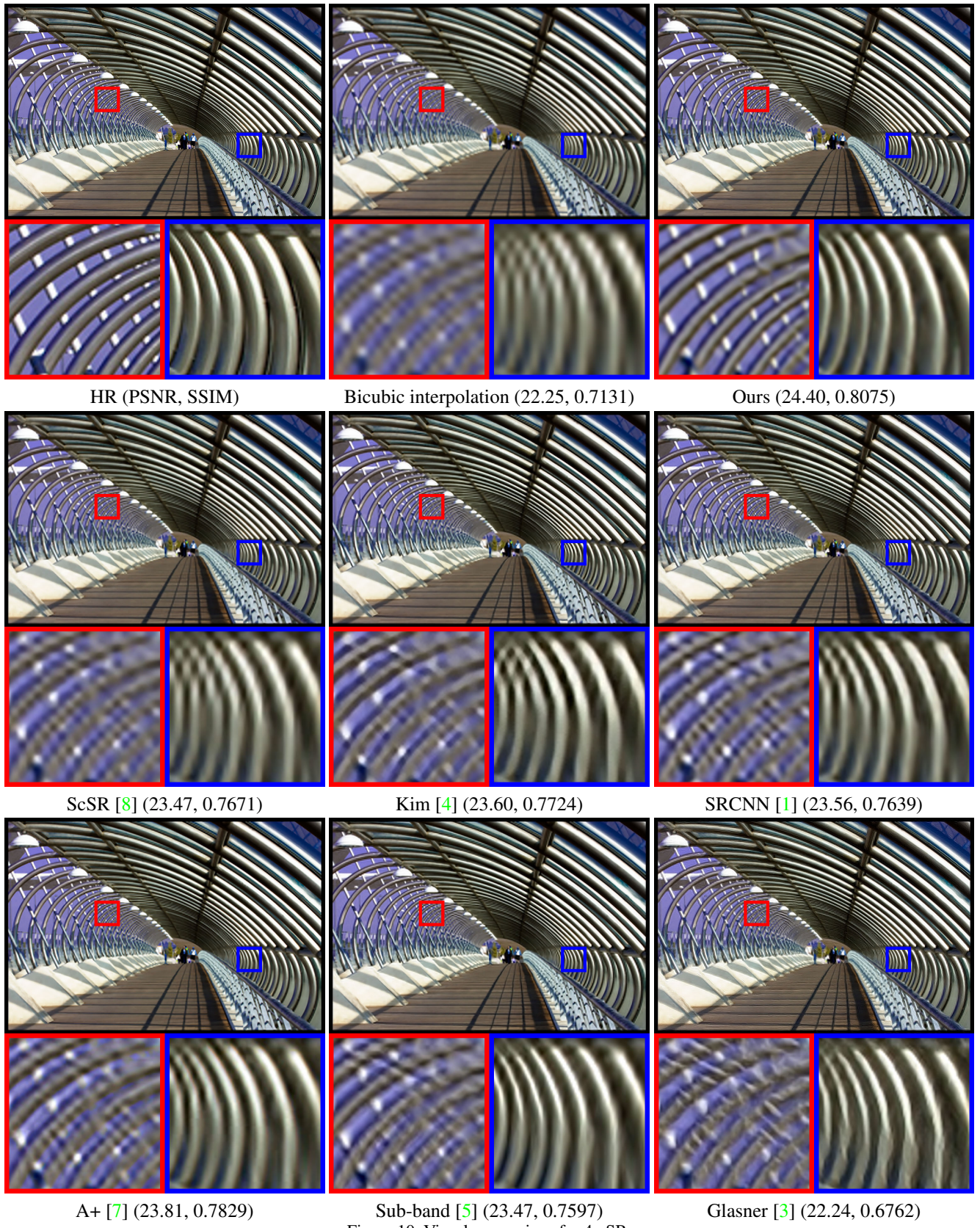


Figure 10. Visual comparison for 4x SR.

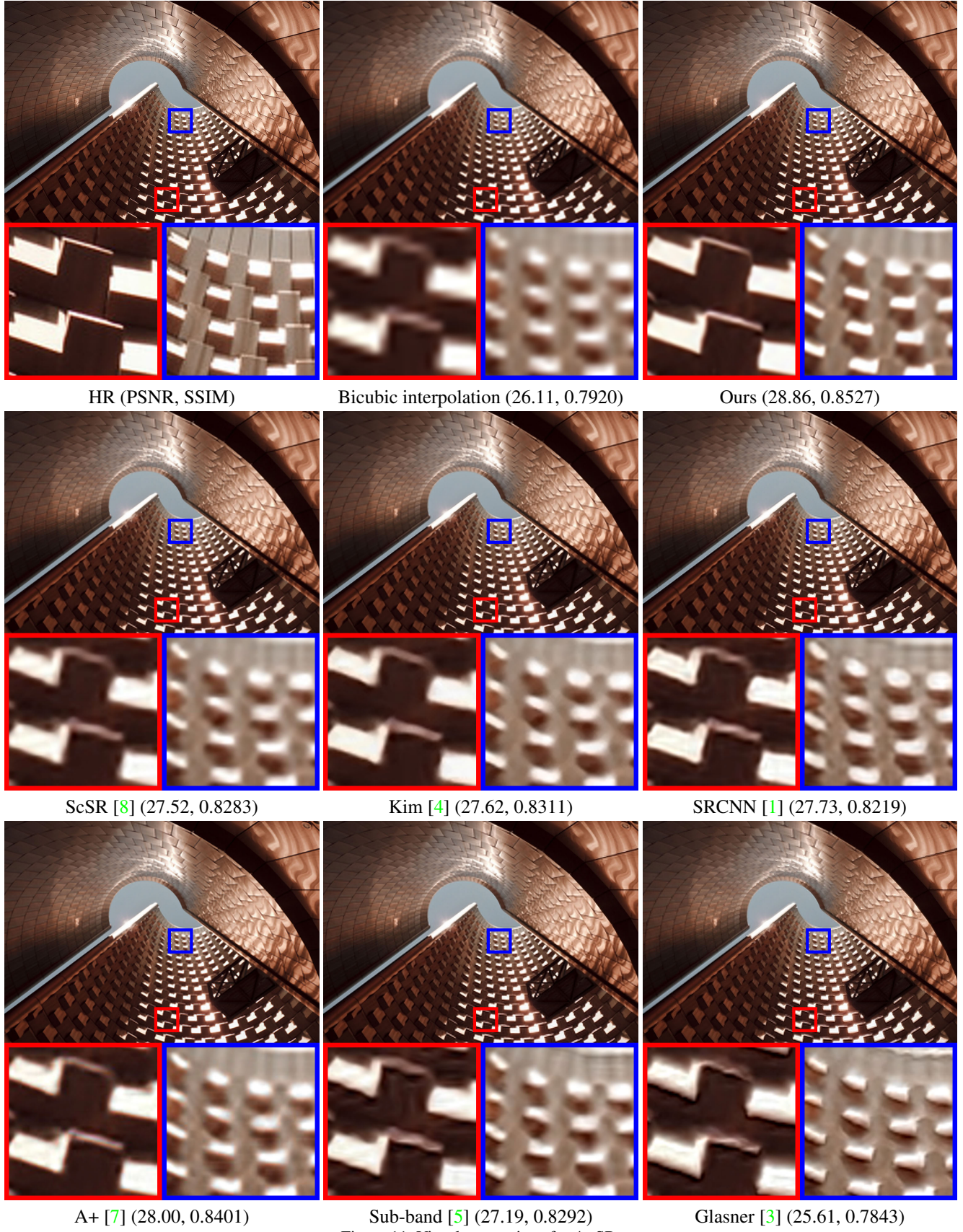


Figure 11. Visual comparison for 4x SR.

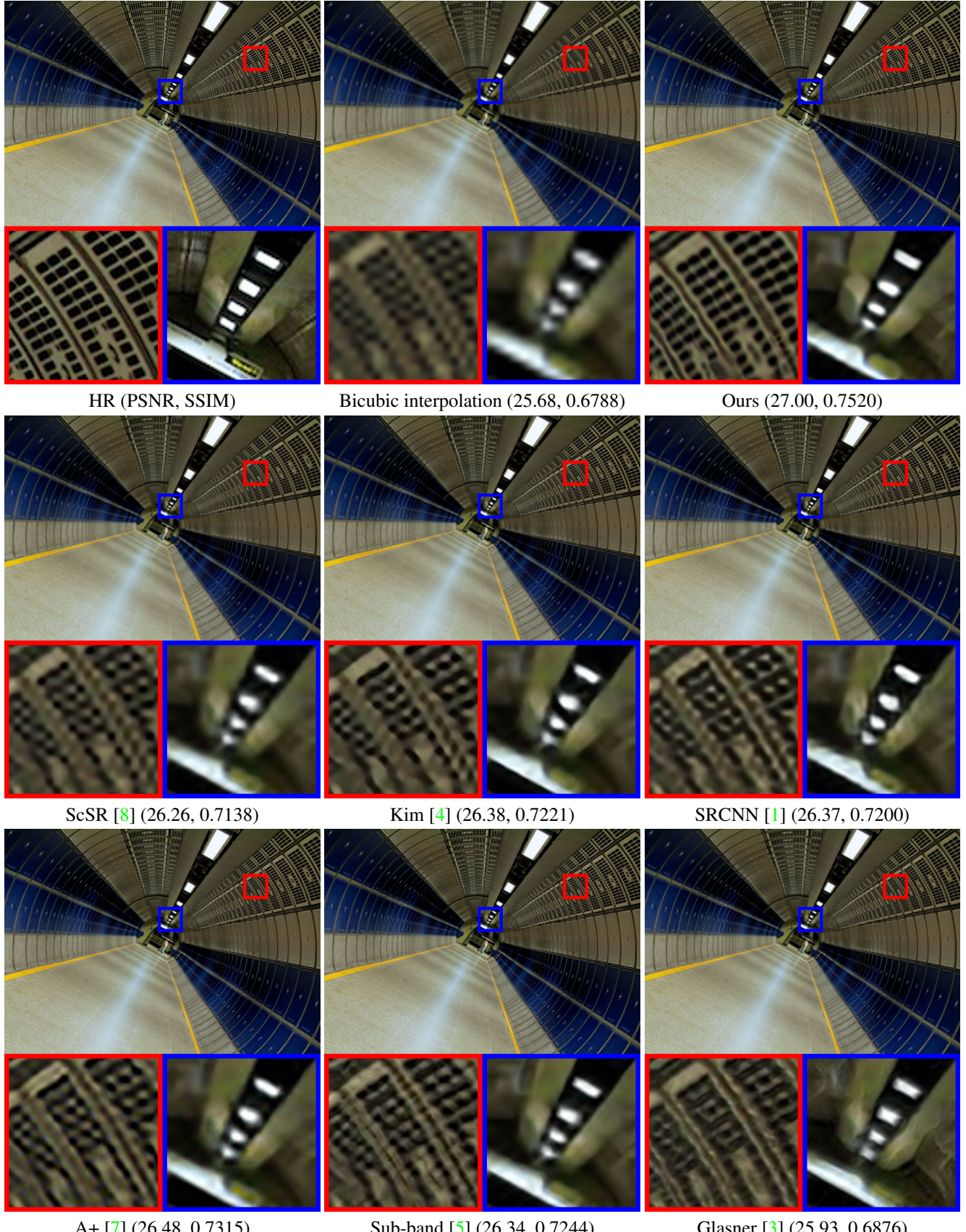


Figure 12. Visual comparison for 4x SR.

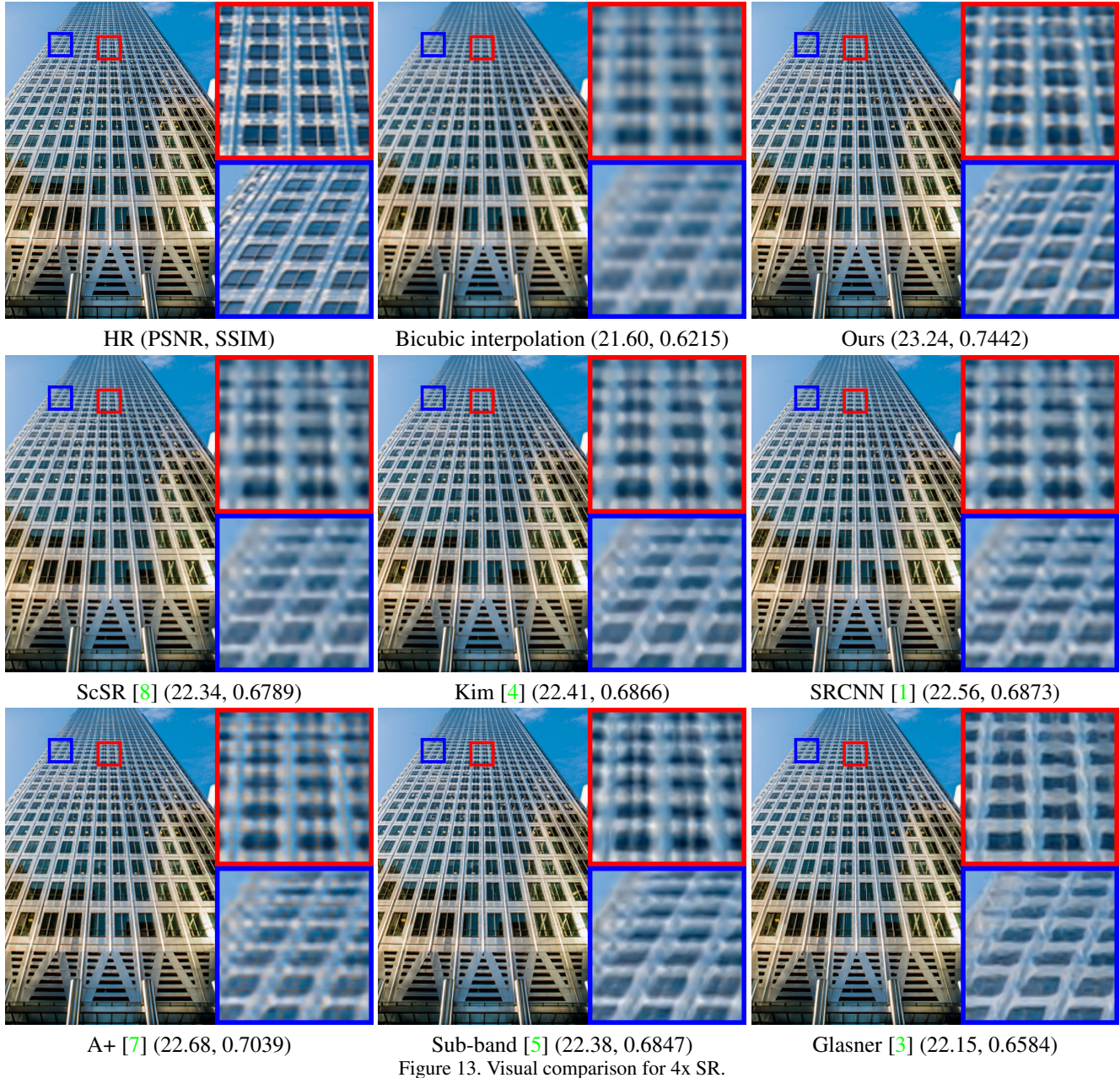


Figure 13. Visual comparison for 4x SR.

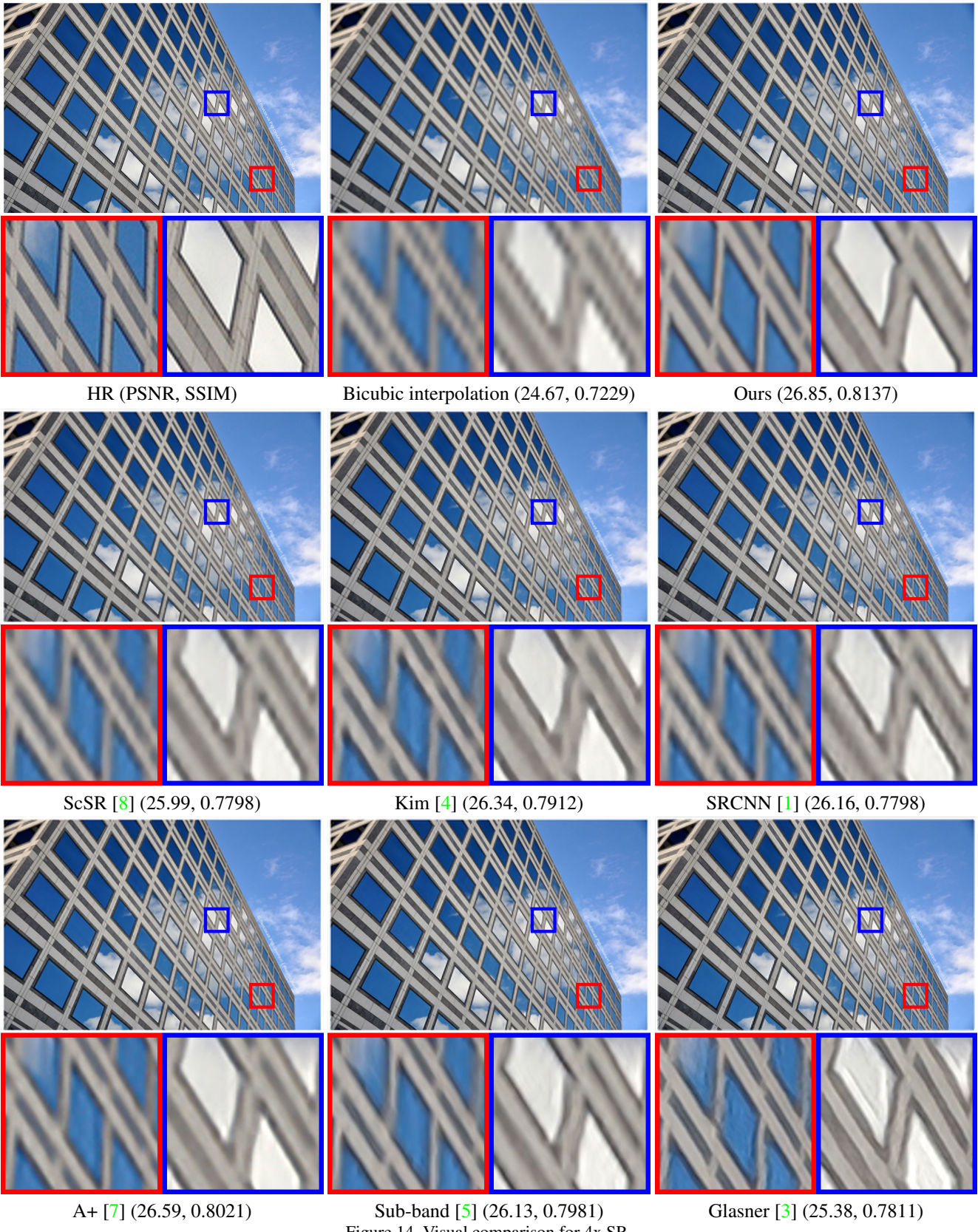


Figure 14. Visual comparison for 4x SR.

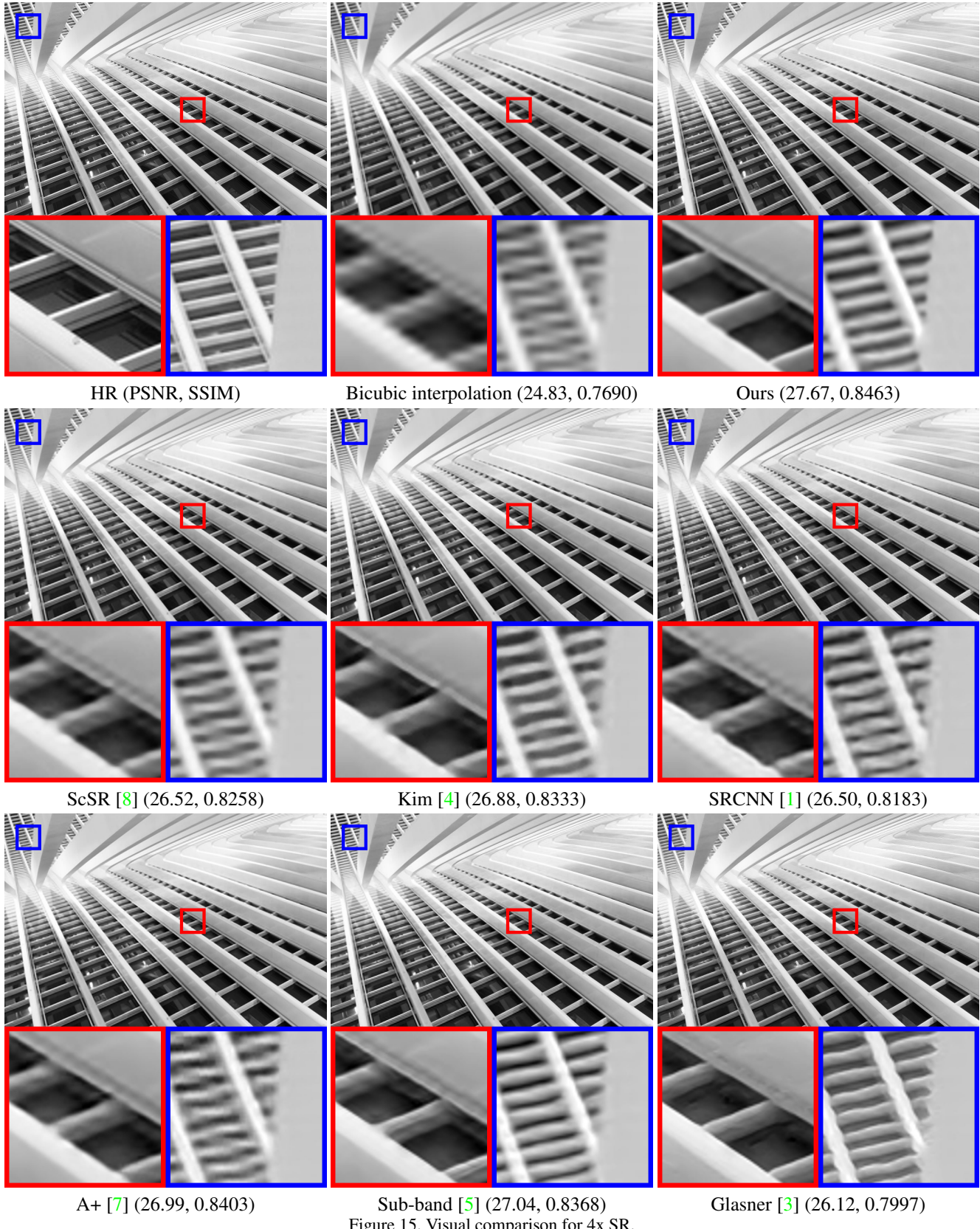


Figure 15. Visual comparison for 4x SR.

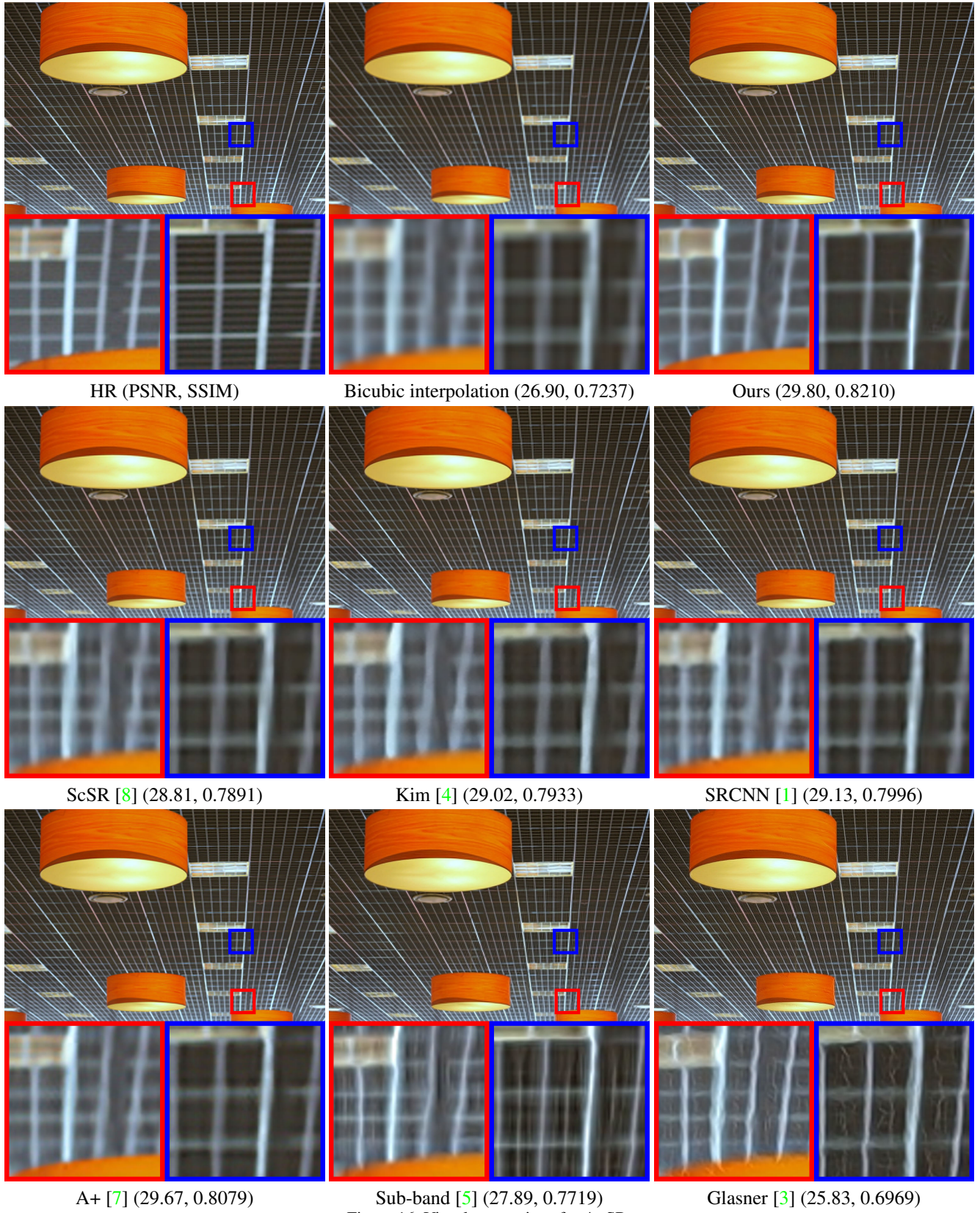


Figure 16. Visual comparison for 4x SR.



Figure 17. Visual comparison for 4x SR.

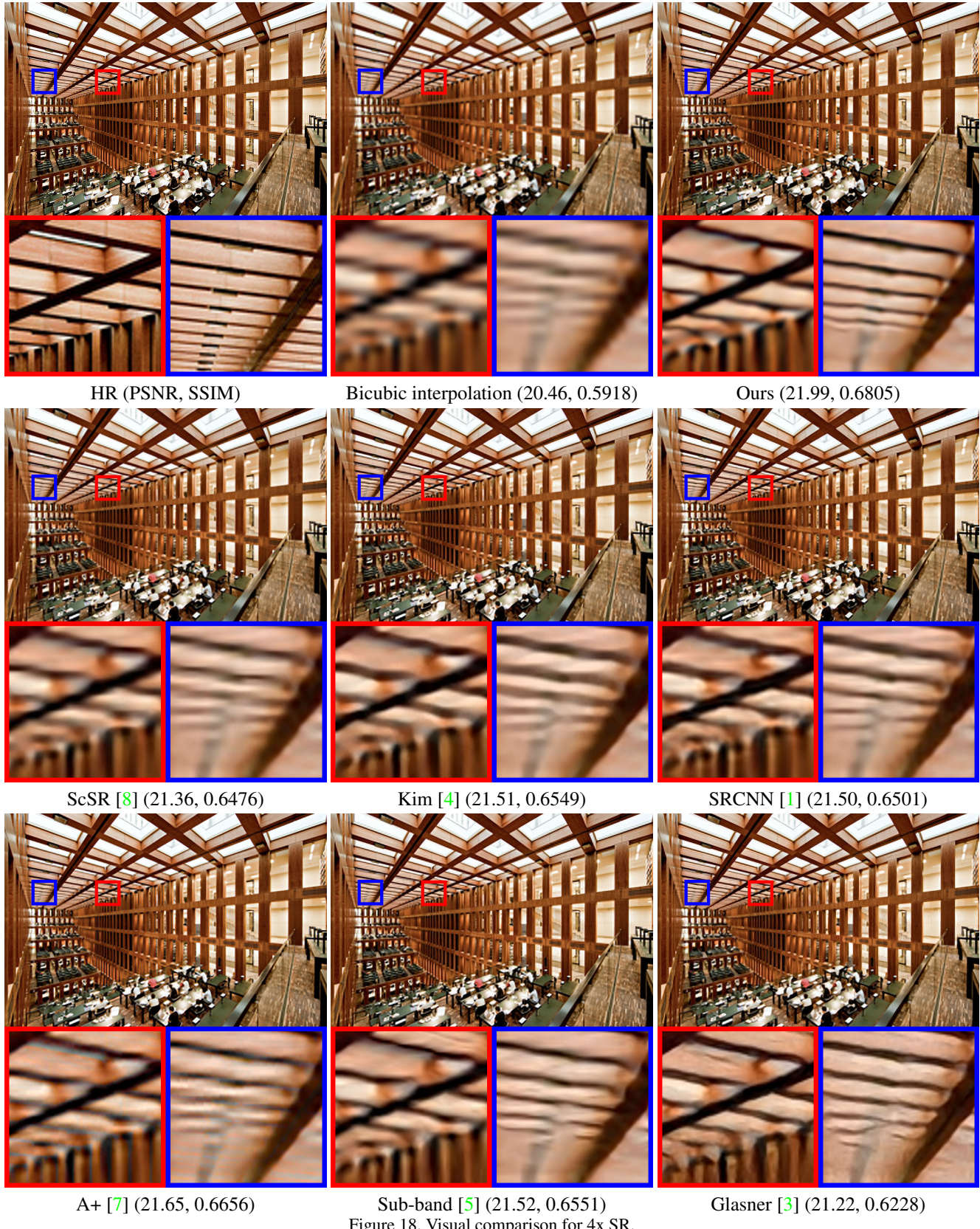


Figure 18. Visual comparison for 4x SR.

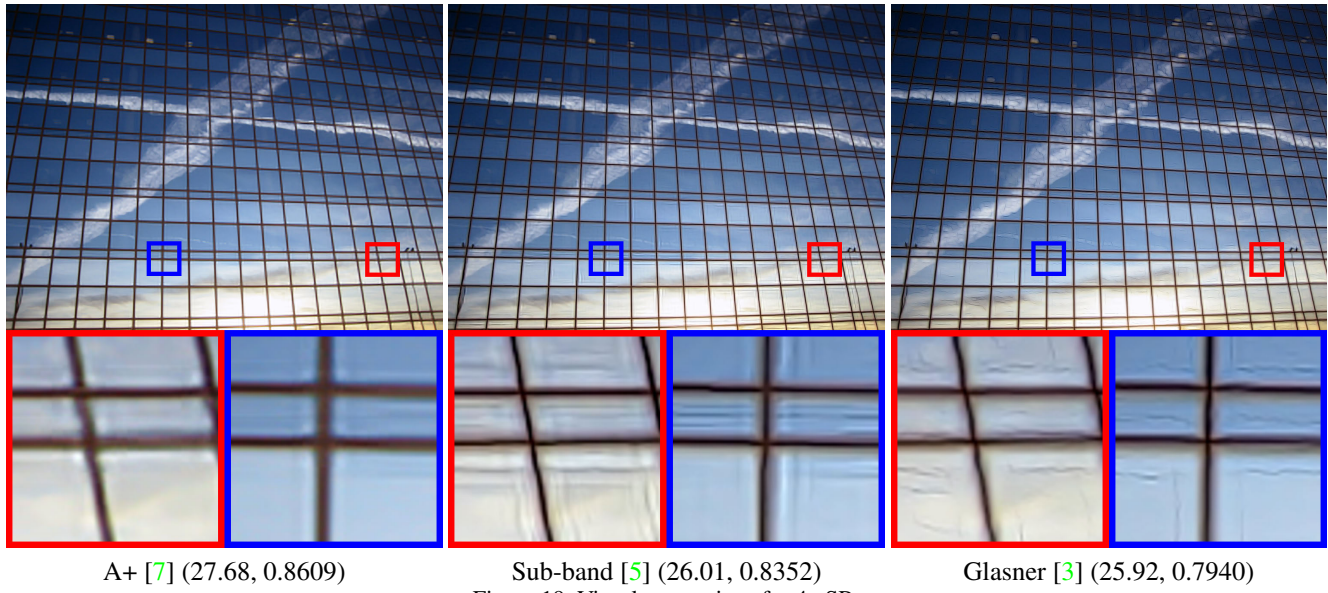
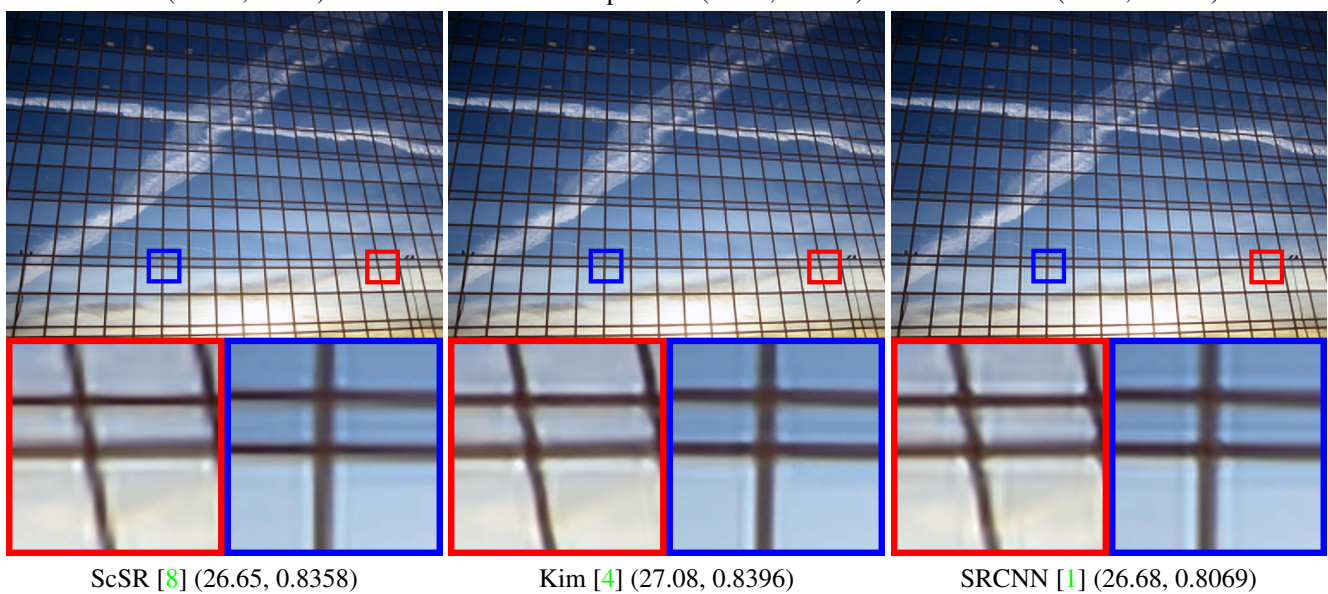
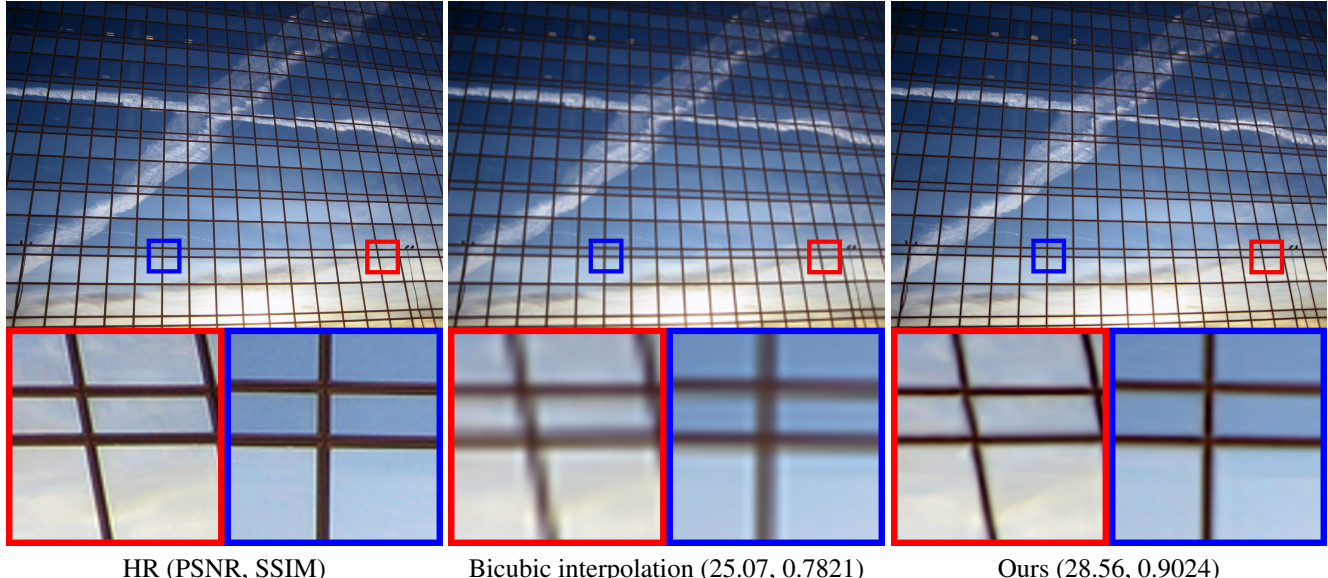


Figure 19. Visual comparison for 4x SR.

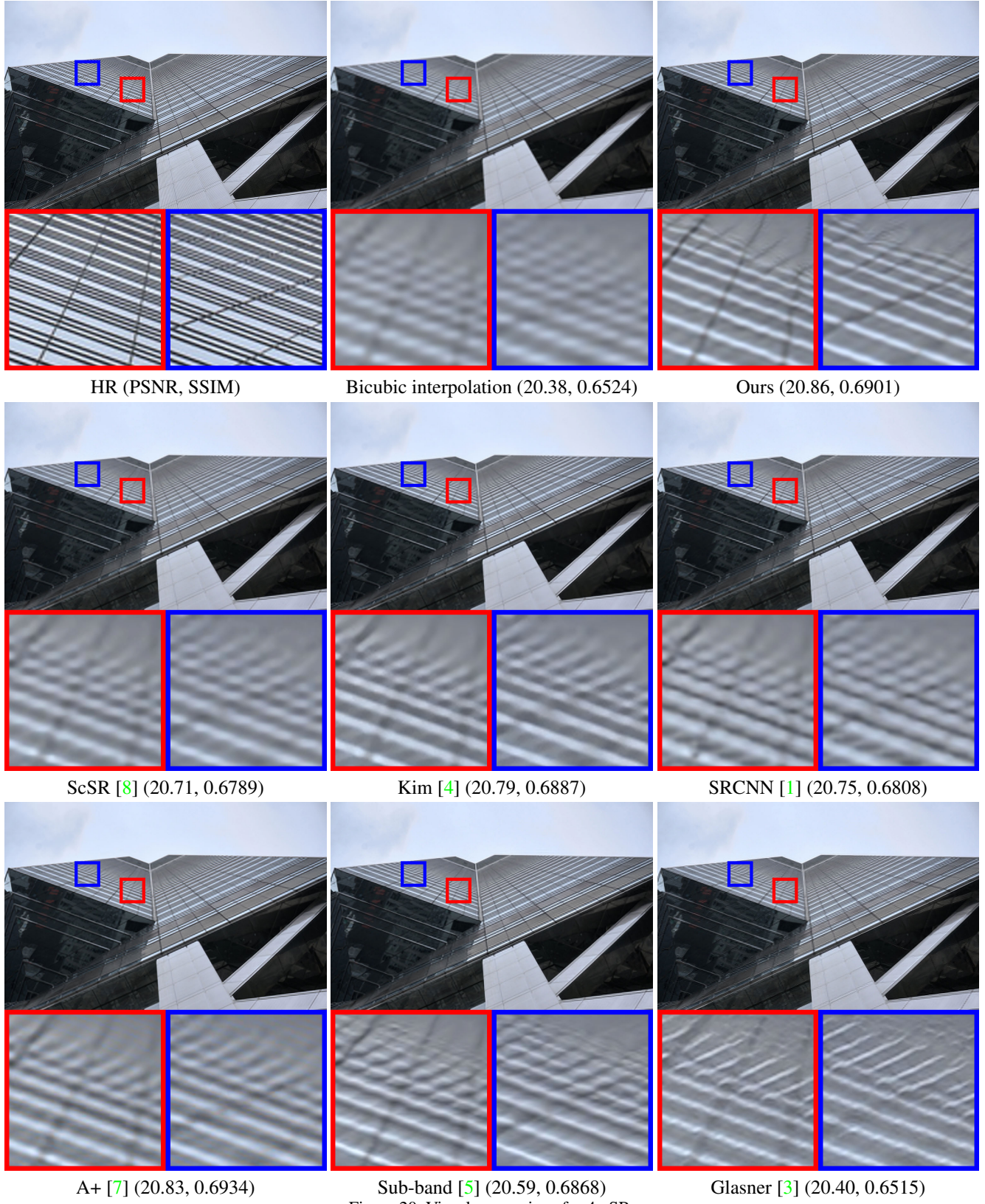


Figure 20. Visual comparison for 4x SR.

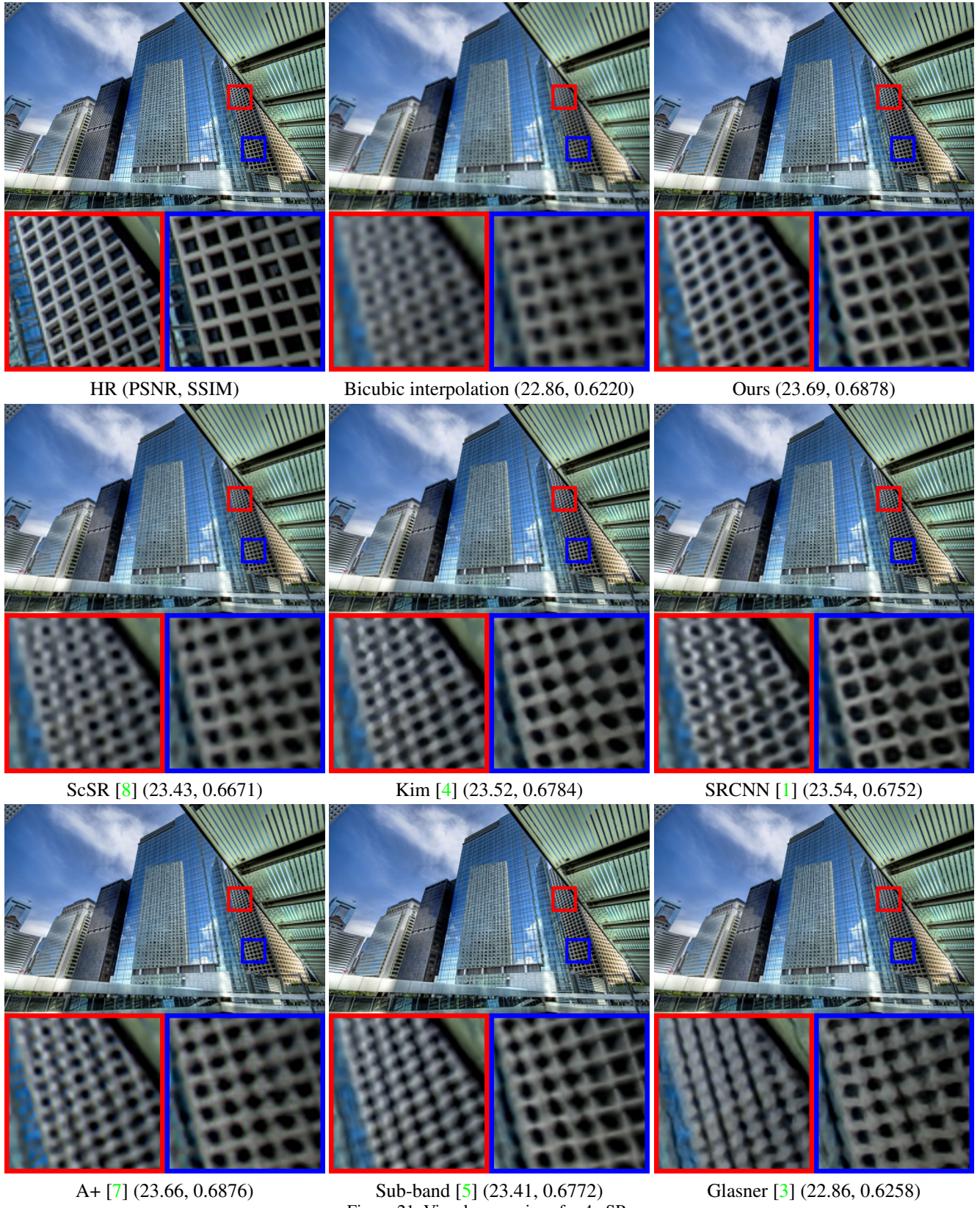
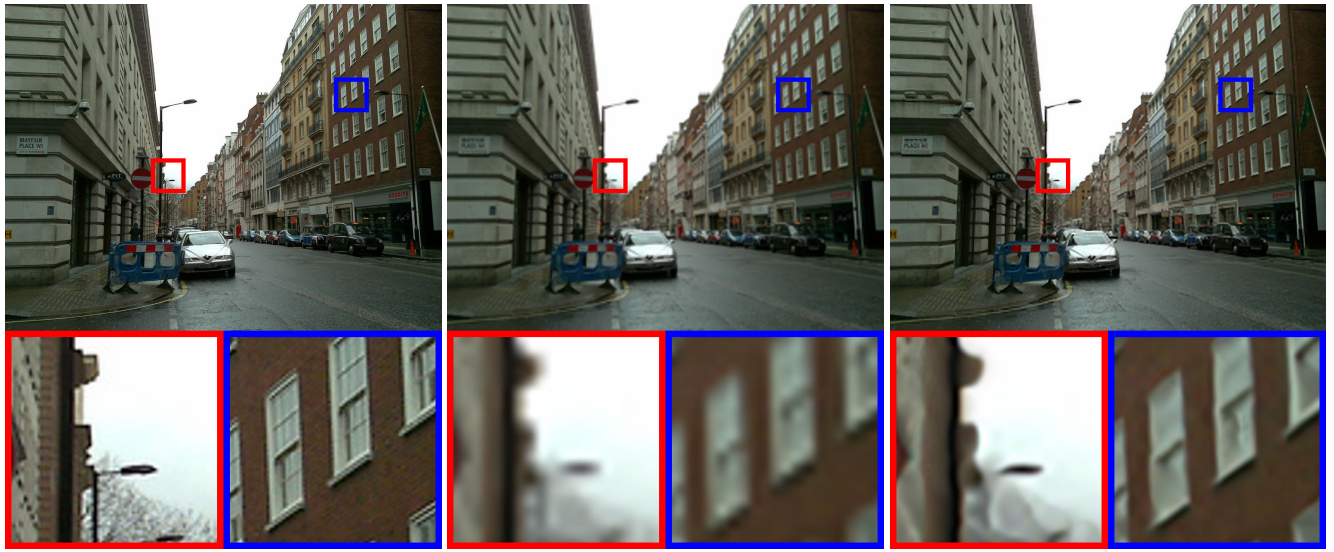


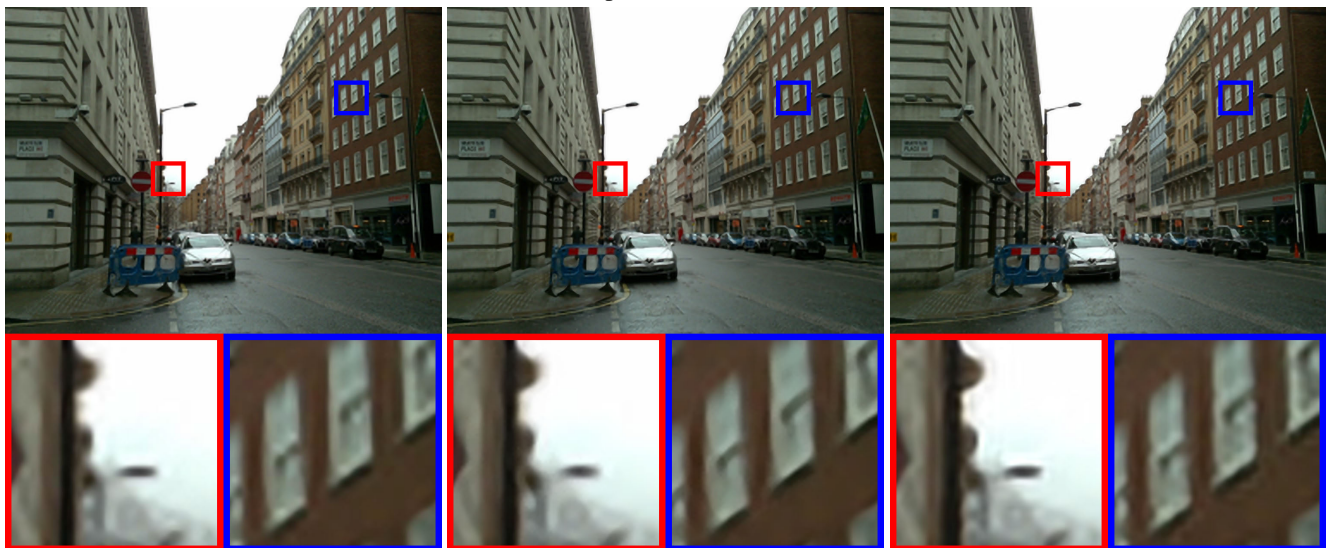
Figure 21. Visual comparison for 4x SR.



HR (PSNR, SSIM)

Bicubic interpolation (25.31, 0.7010)

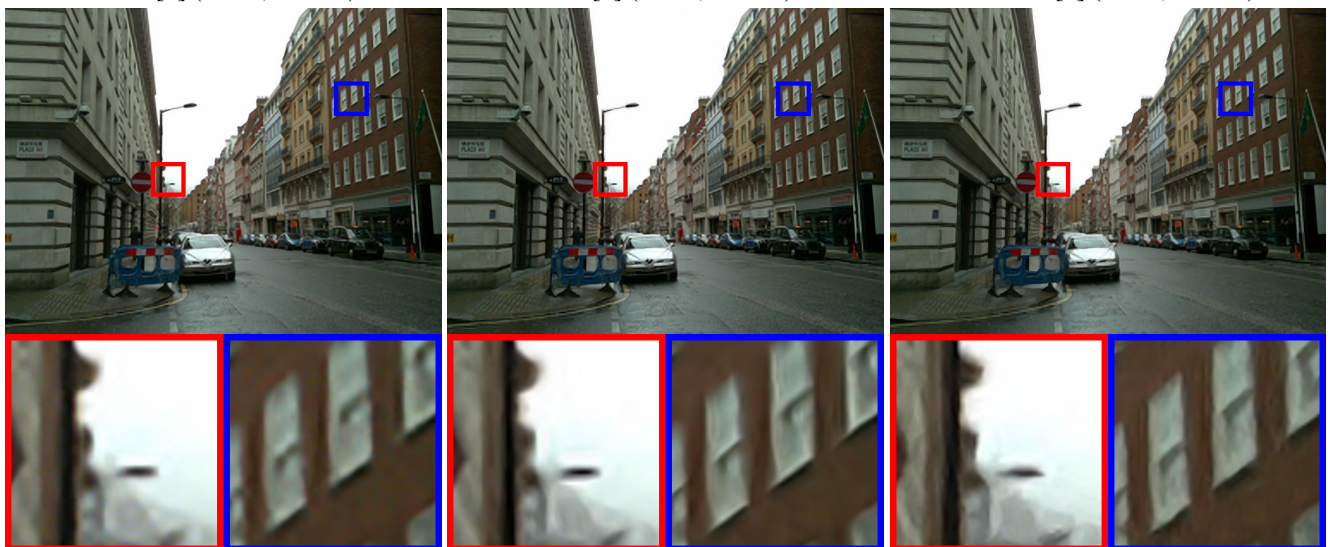
Ours (26.18, 0.7438)



ScSR [8] (25.91, 0.7312)

Kim [4] (25.97, 0.7347)

SRCNN [1] (26.00, 0.7325)



A+ [7] (26.12, 0.7429)

Sub-band [5] (25.92, 0.7332)

Glasner [3] (25.74, 0.7189)

Figure 22. Visual comparison for 4x SR.

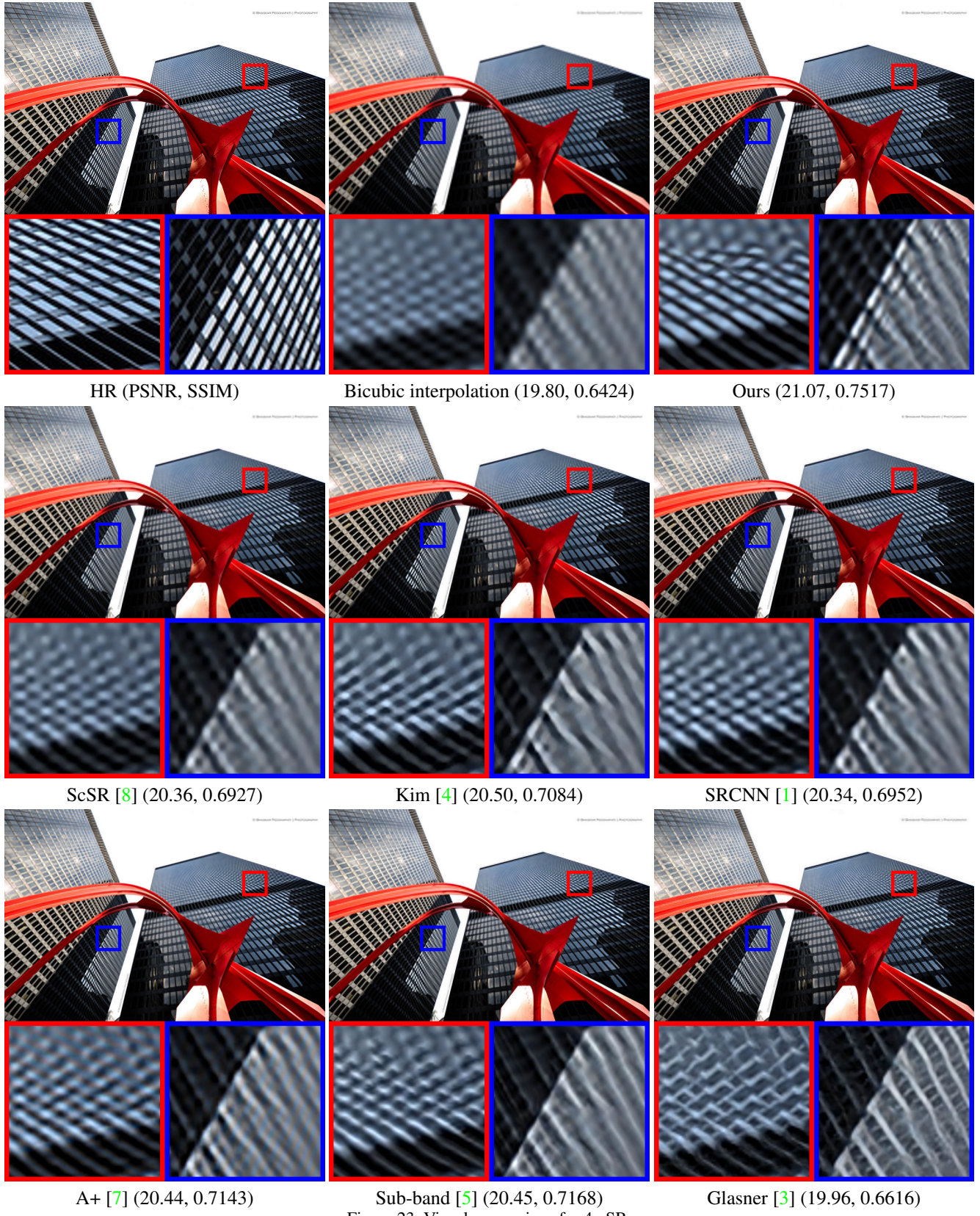


Figure 23. Visual comparison for 4x SR.

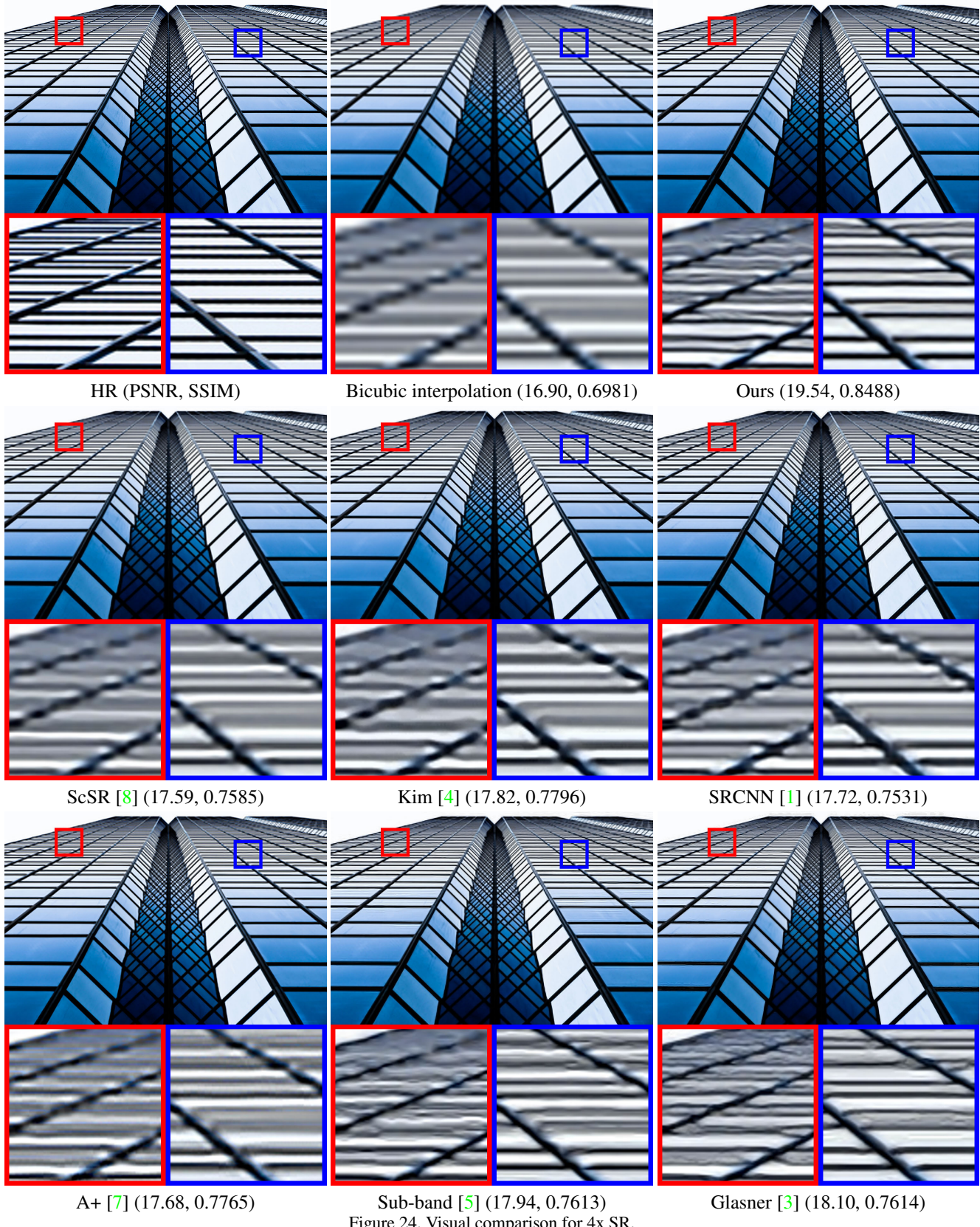


Figure 24. Visual comparison for 4x SR.

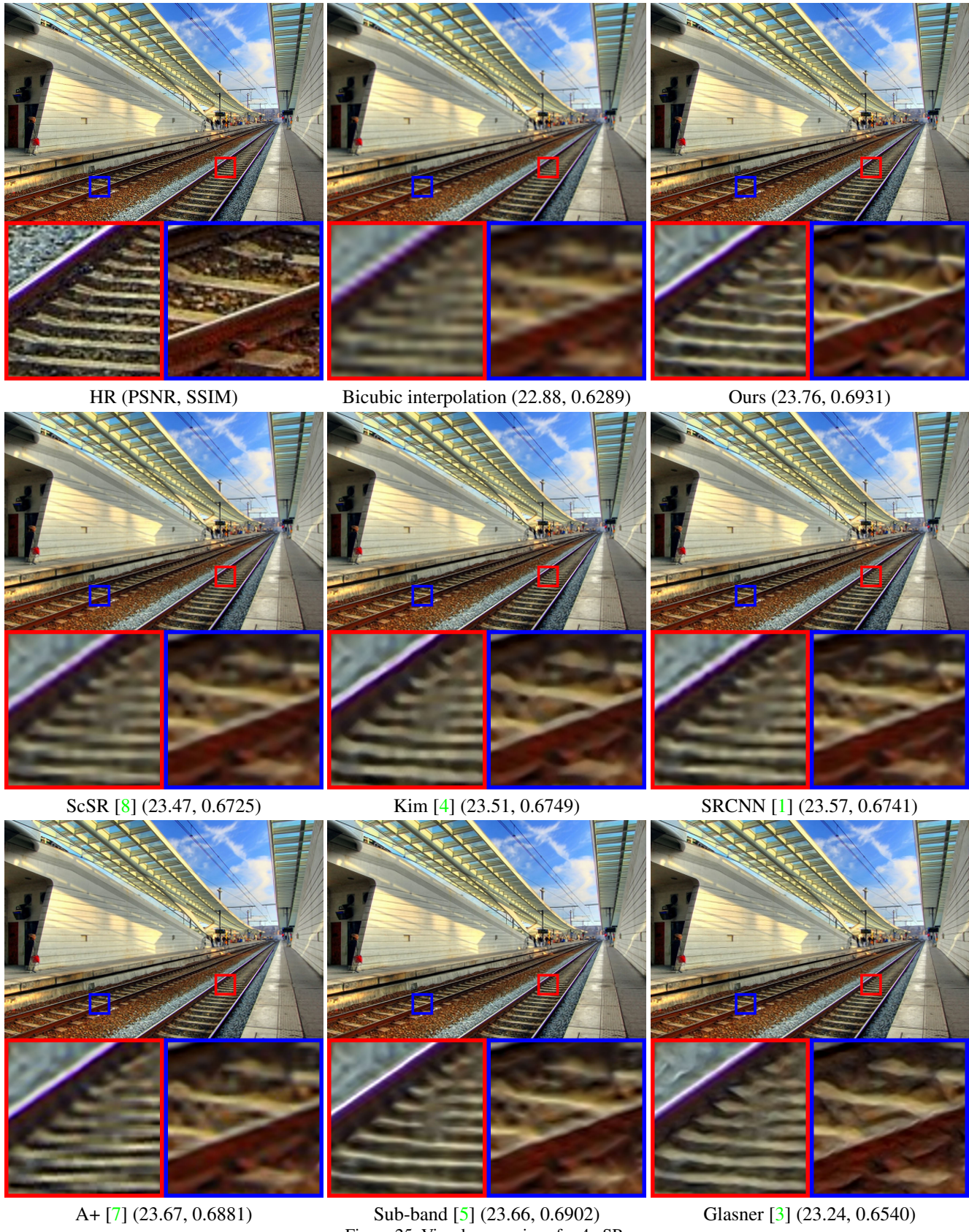
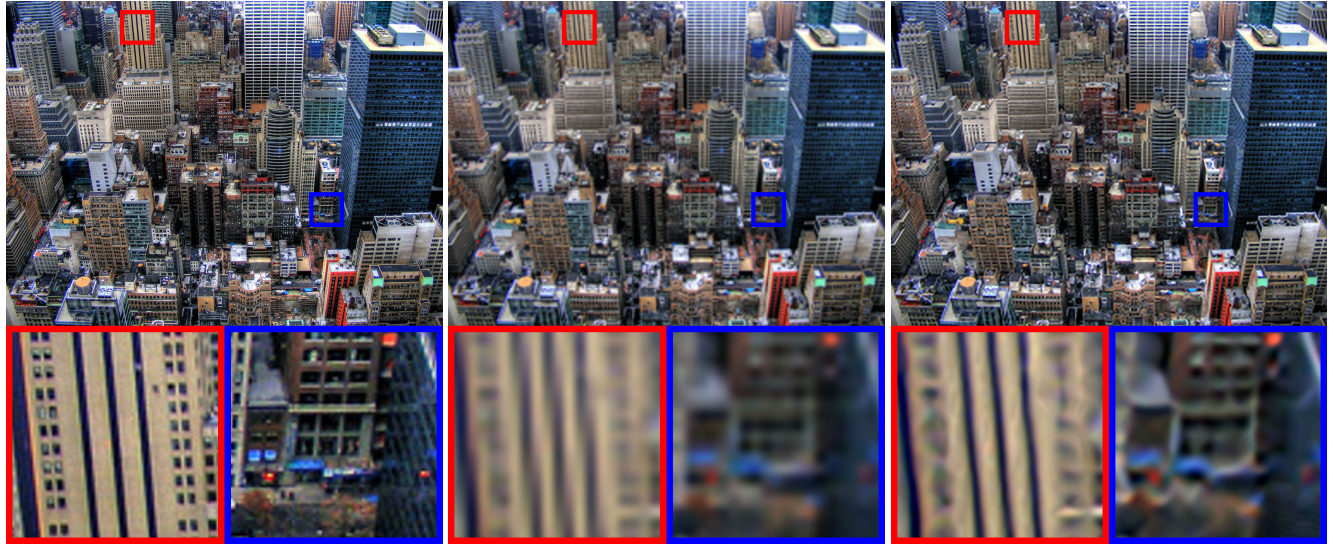


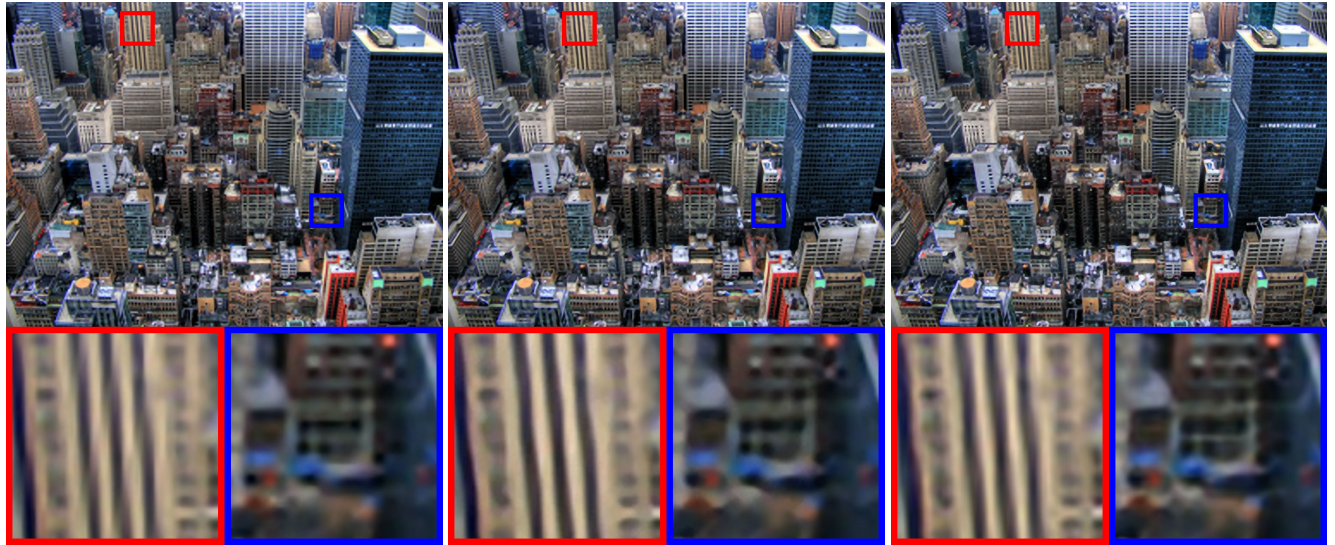
Figure 25. Visual comparison for 4x SR.



HR (PSNR, SSIM)

Bicubic interpolation (19.46, 0.4363)

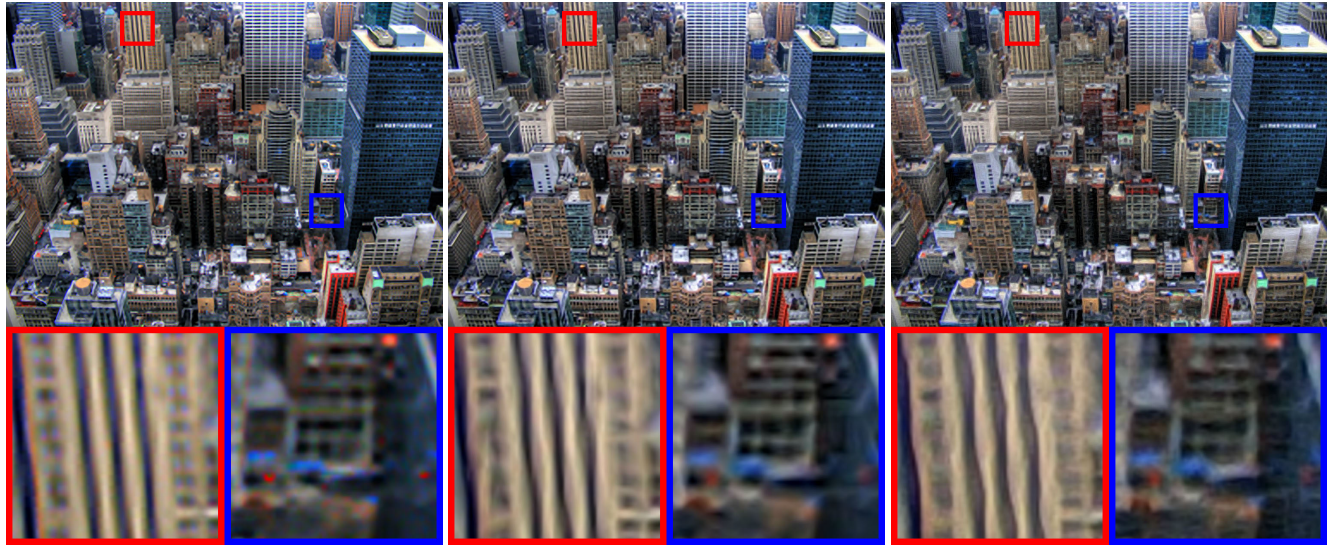
Ours (19.80, 0.5048)



ScSR [8] (19.78, 0.4861)

Kim [4] (19.80, 0.4943)

SRCNN [1] (19.84, 0.4970)



A+ [7] (19.92, 0.5050)

Sub-band [5] (19.46, 0.4911)

Glasner [3] (19.28, 0.4491)

Figure 26. Visual comparison for 4x SR.

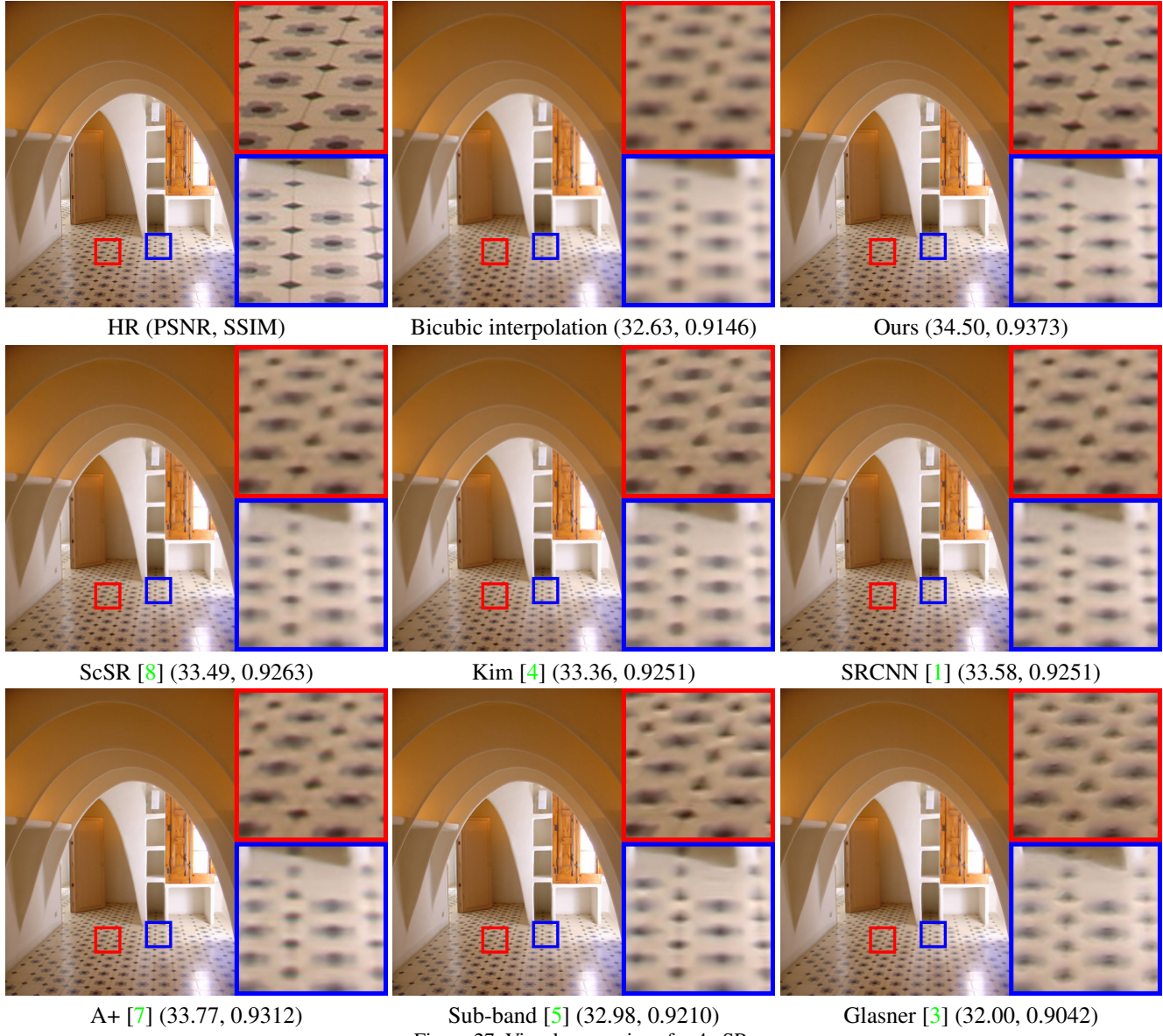


Figure 27. Visual comparison for 4x SR.

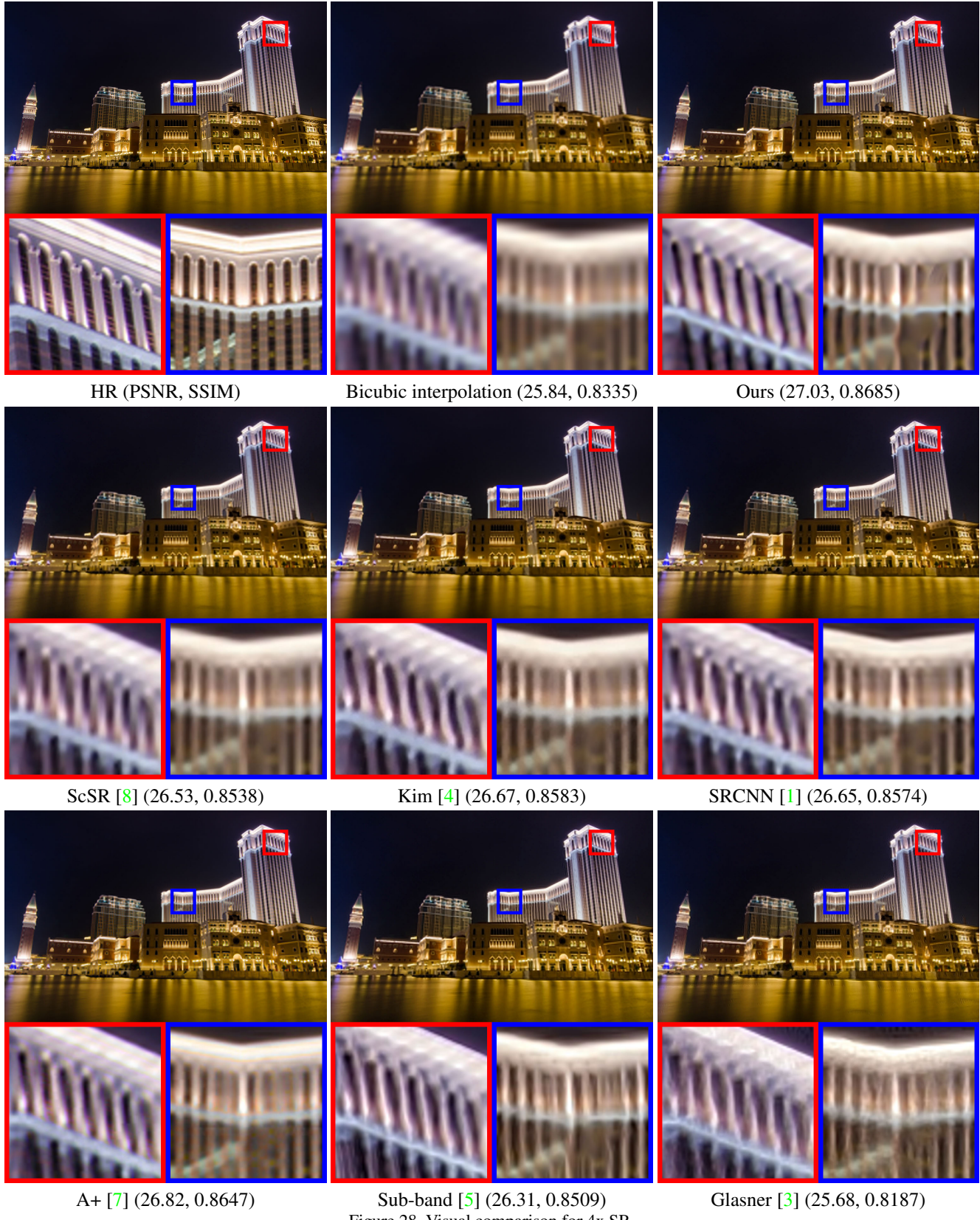
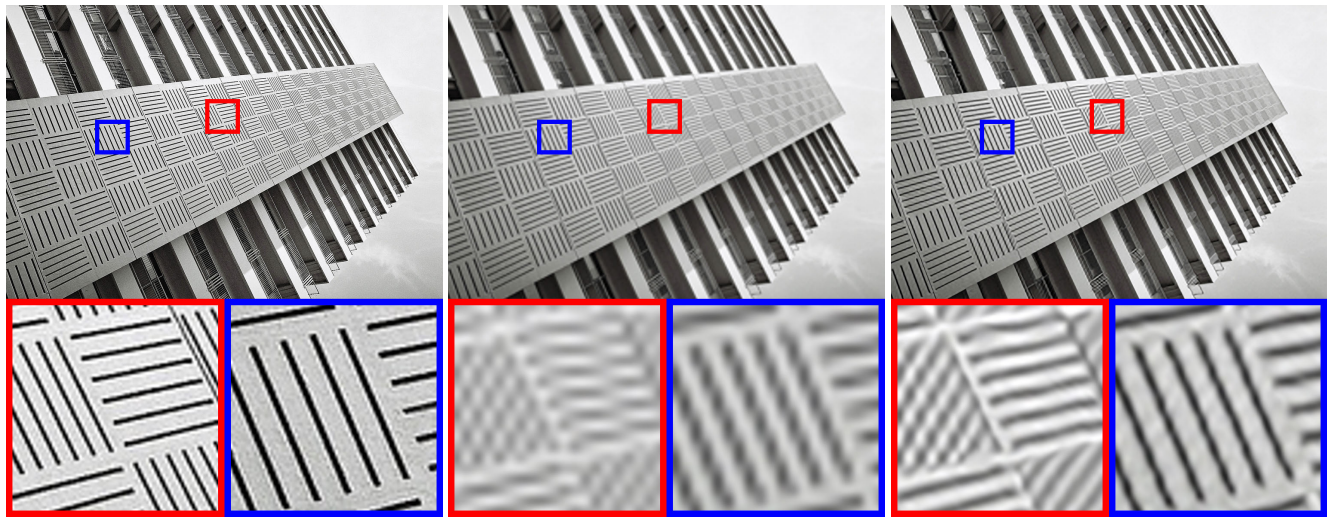


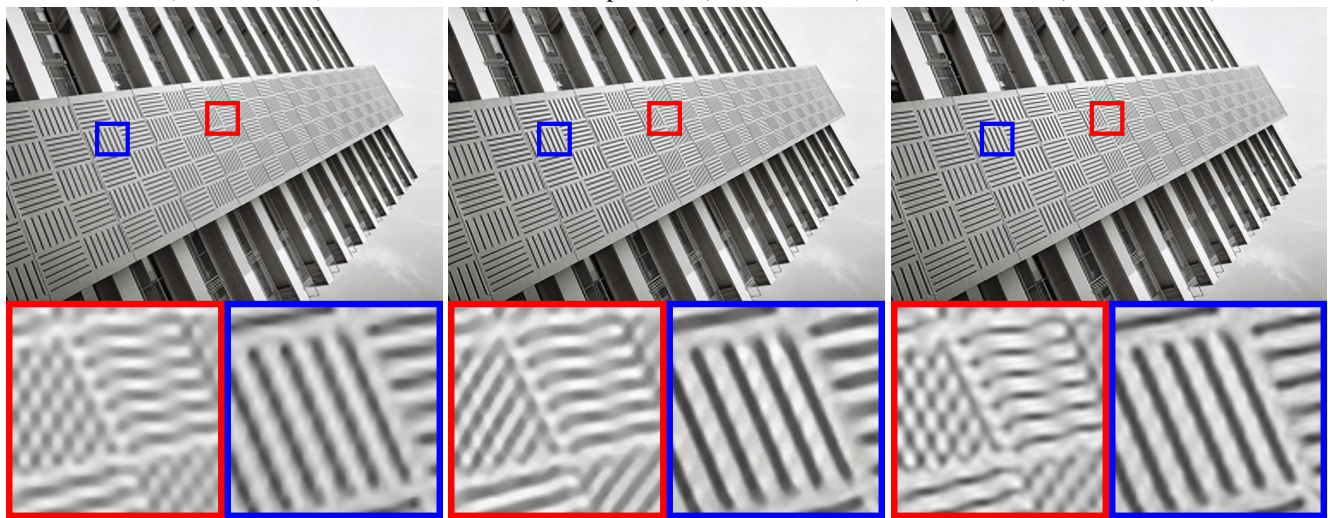
Figure 28. Visual comparison for 4x SR.



HR (PSNR, SSIM)

Bicubic interpolation (16.53, 0.4338)

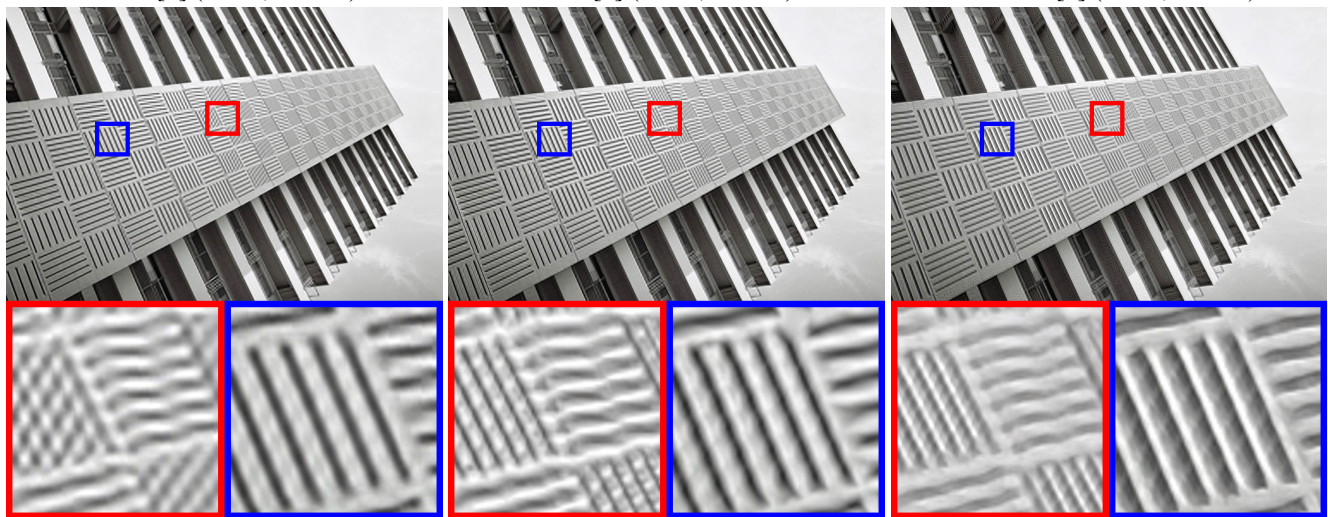
Ours (17.53, 0.5412)



ScSR [8] (17.03, 0.4921)

Kim [4] (17.00, 0.5025)

SRCNN [1] (17.30, 0.5160)

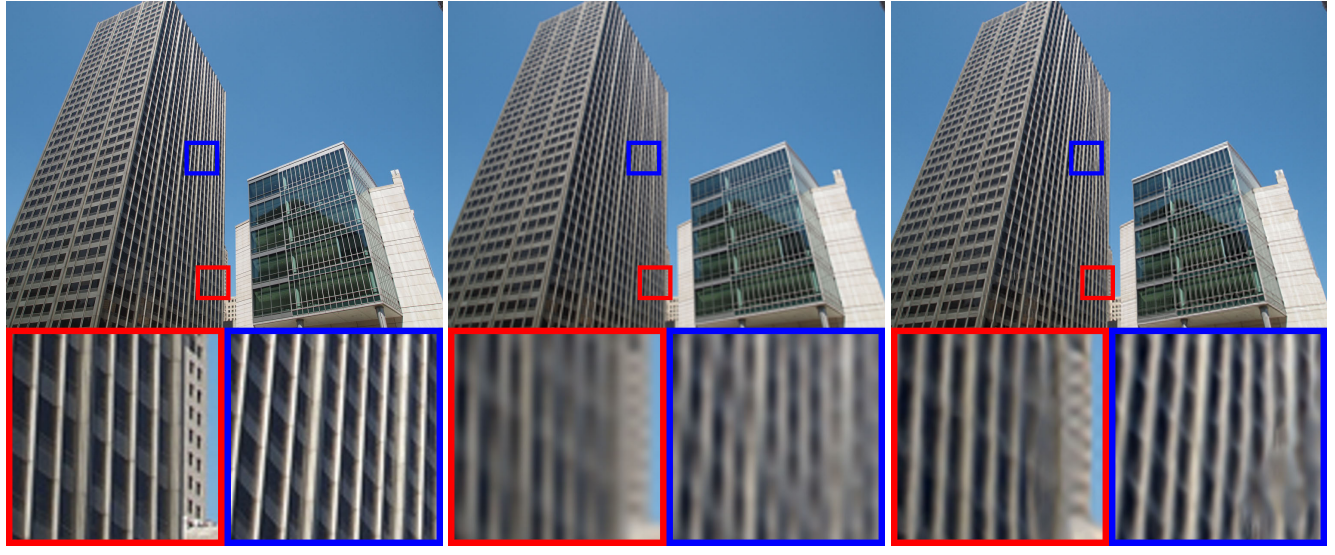


A+ [7] (17.28, 0.5202)

Sub-band [5] (17.24, 0.5115)

Glasner [3] (16.60, 0.4311)

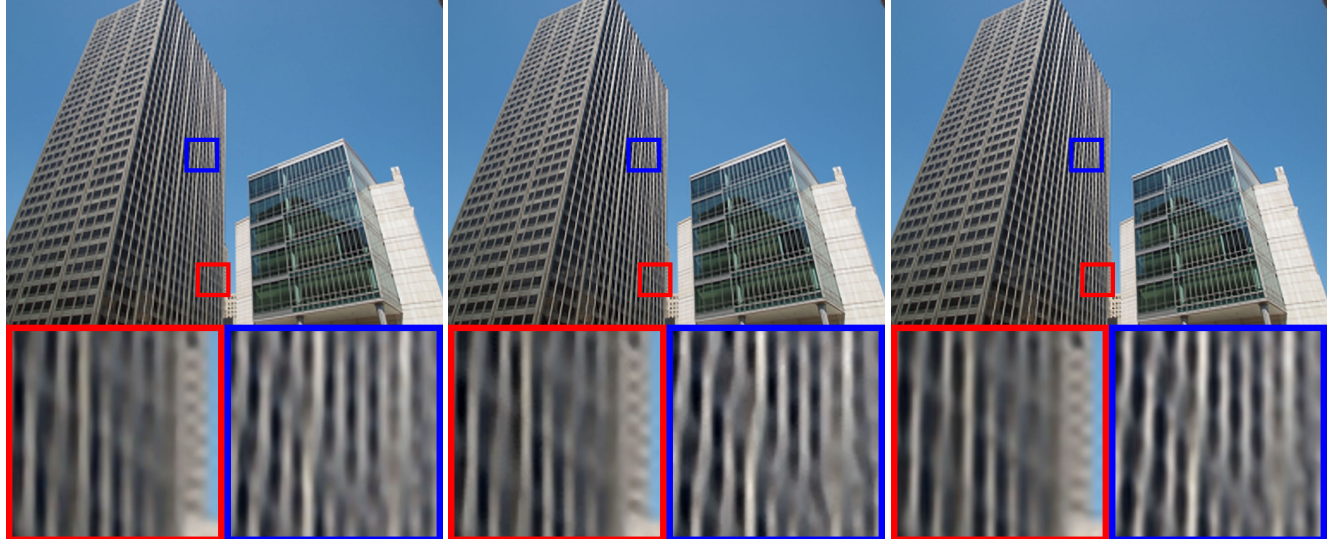
Figure 29. Visual comparison for 4x SR.



HR (PSNR, SSIM)

Bicubic interpolation (21.26, 0.6815)

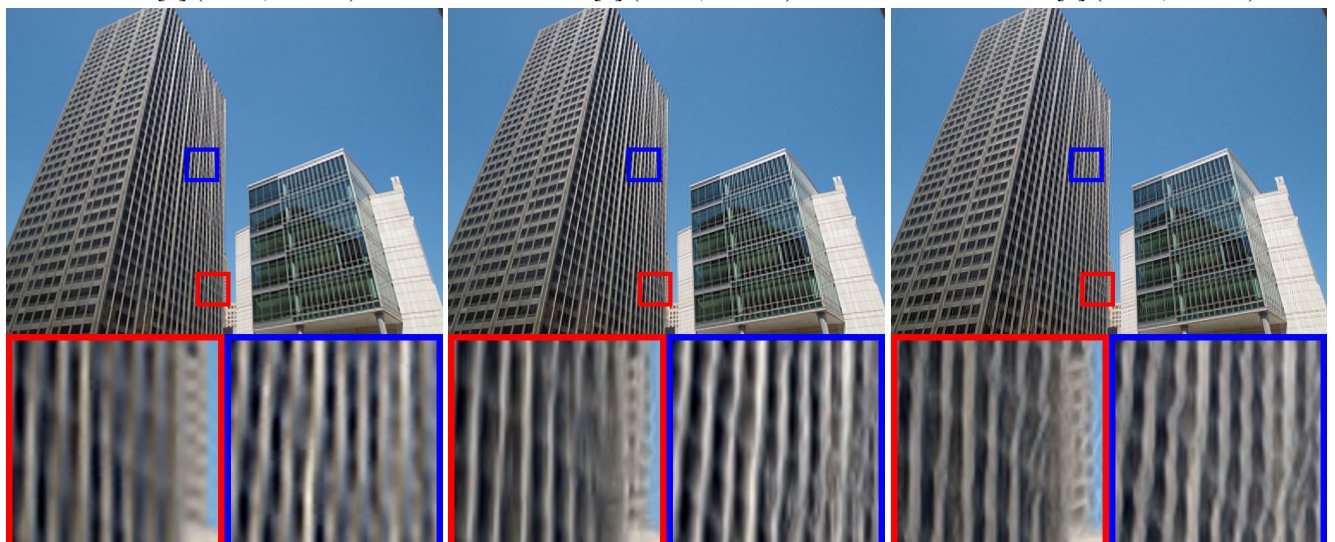
Ours (22.52, 0.7573)



ScSR [8] (21.72, 0.7166)

Kim [4] (21.71, 0.7248)

SRCNN [1] (22.13, 0.7344)



A+ [7] (22.00, 0.7383)

Sub-band [5] (22.59, 0.7531)

Glasner [3] (21.60, 0.6981)

Figure 30. Visual comparison for 4x SR.

3. Sample comparisons on *BSD 100* dataset

Here we show 30 sample comparisons from the *BSD 100* dataset. As a reference, we show two quantitative evaluation metrics: PSNR and SSIM (computed using the luminance channel) for each method.

Below we show results with SR factor 3x and compare our method with ScSR [8], Kim [4], SRCNN [1], A+ [7], Sub-band [5], and Glasner [3].

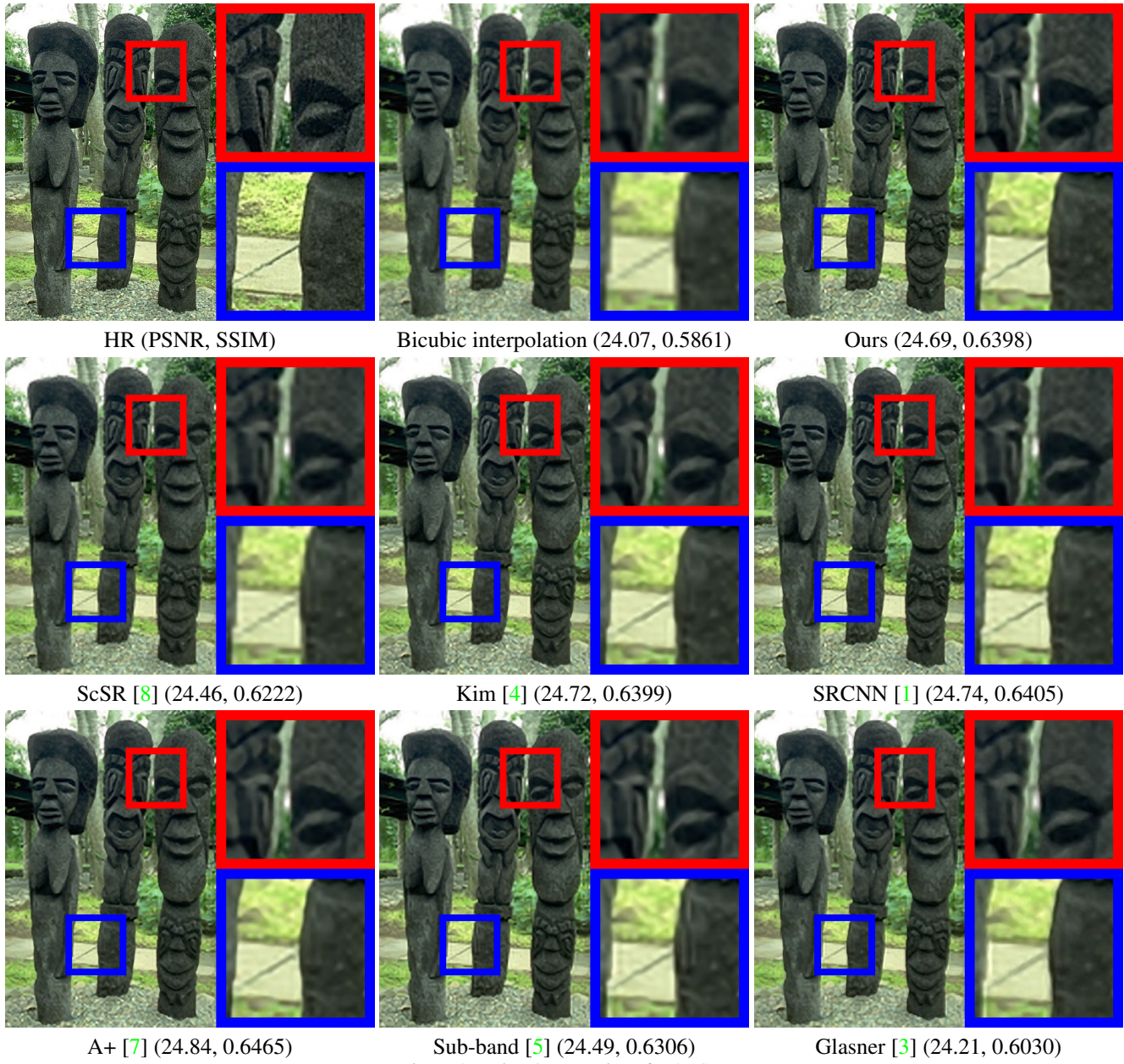


Figure 31. Visual comparison for 3x SR.

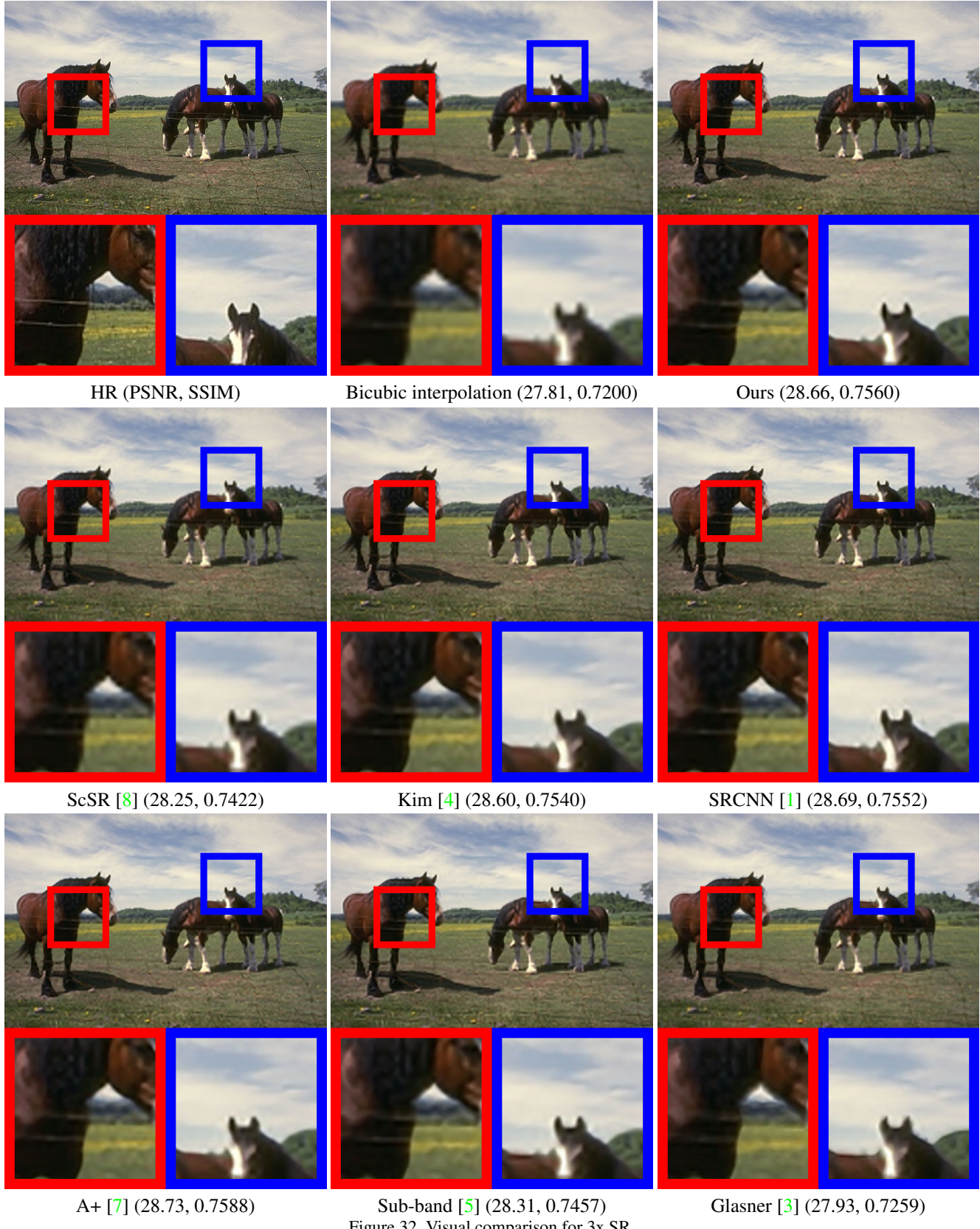


Figure 32. Visual comparison for 3x SR.



Figure 33. Visual comparison for 3x SR.



Figure 34. Visual comparison for 3x SR.

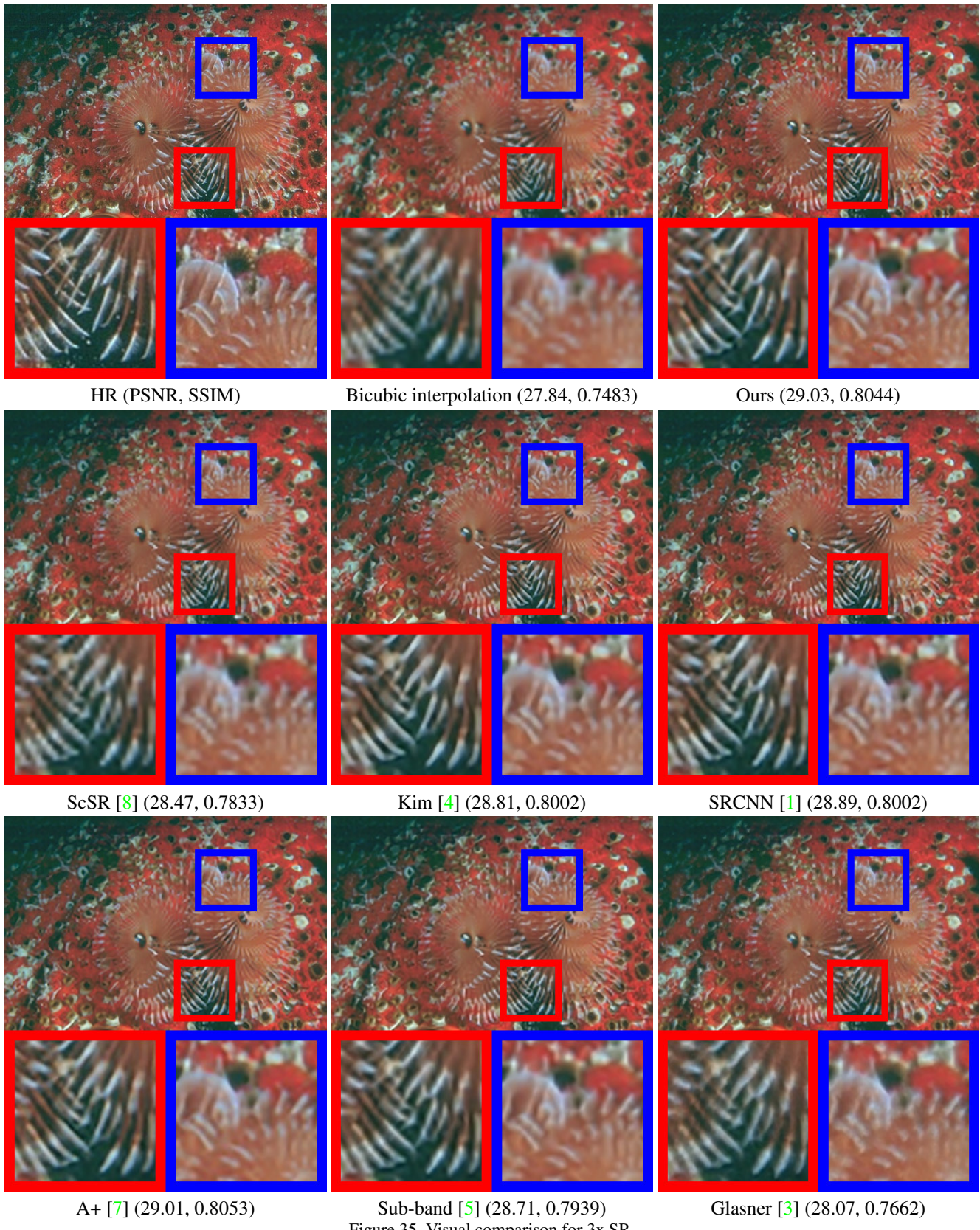


Figure 35. Visual comparison for 3x SR.



Figure 36. Visual comparison for 3x SR.

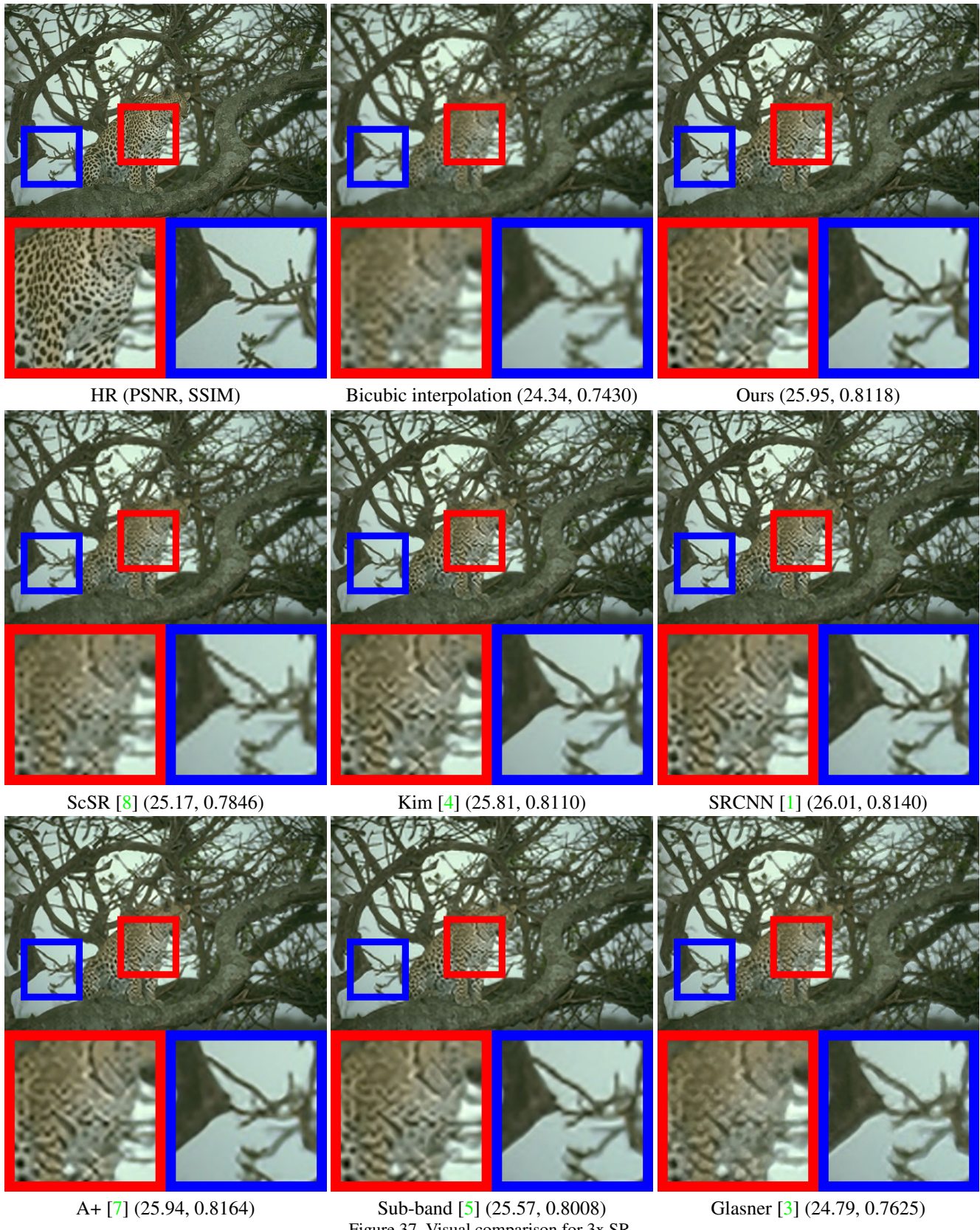


Figure 37. Visual comparison for 3x SR.

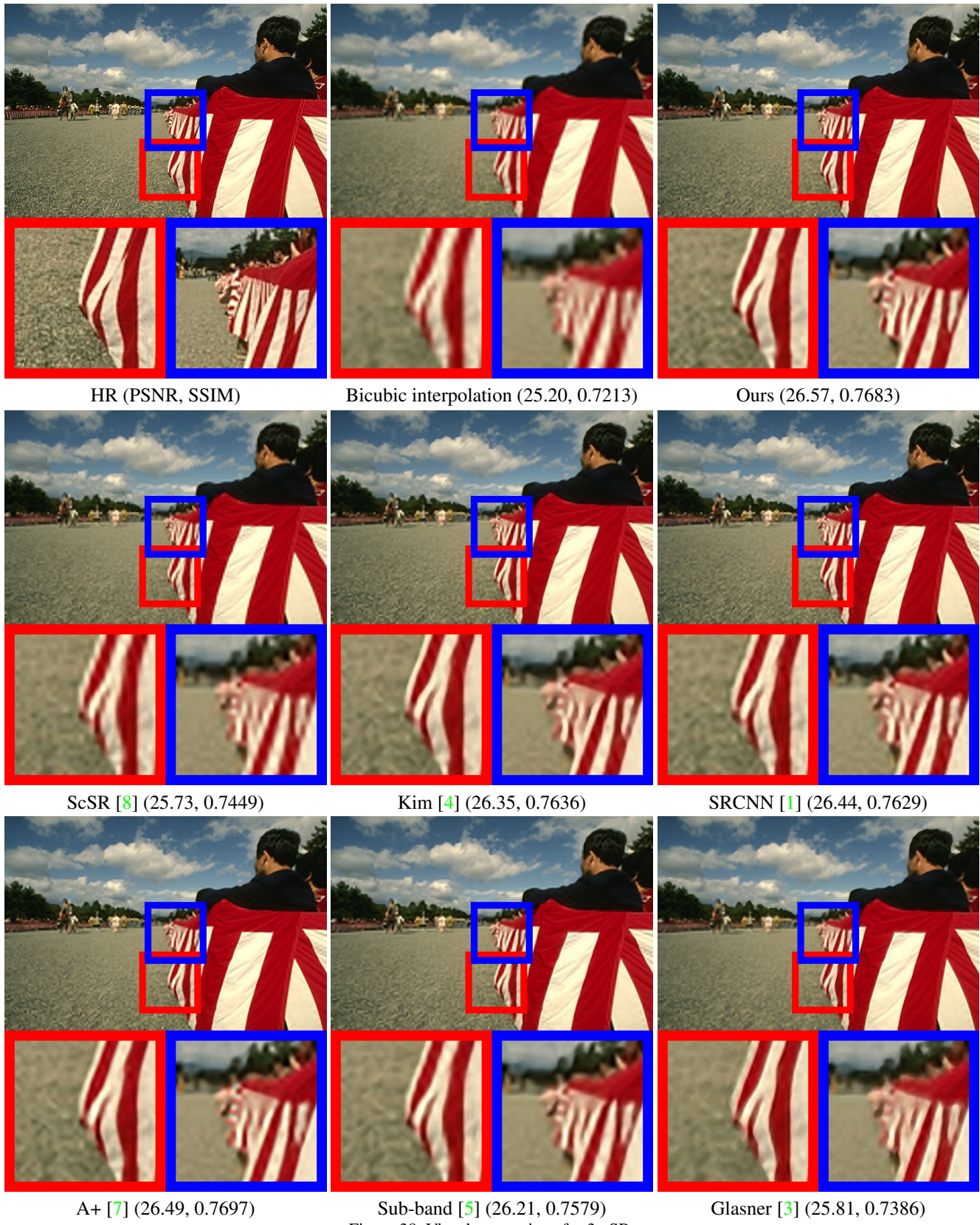


Figure 38. Visual comparison for 3x SR.

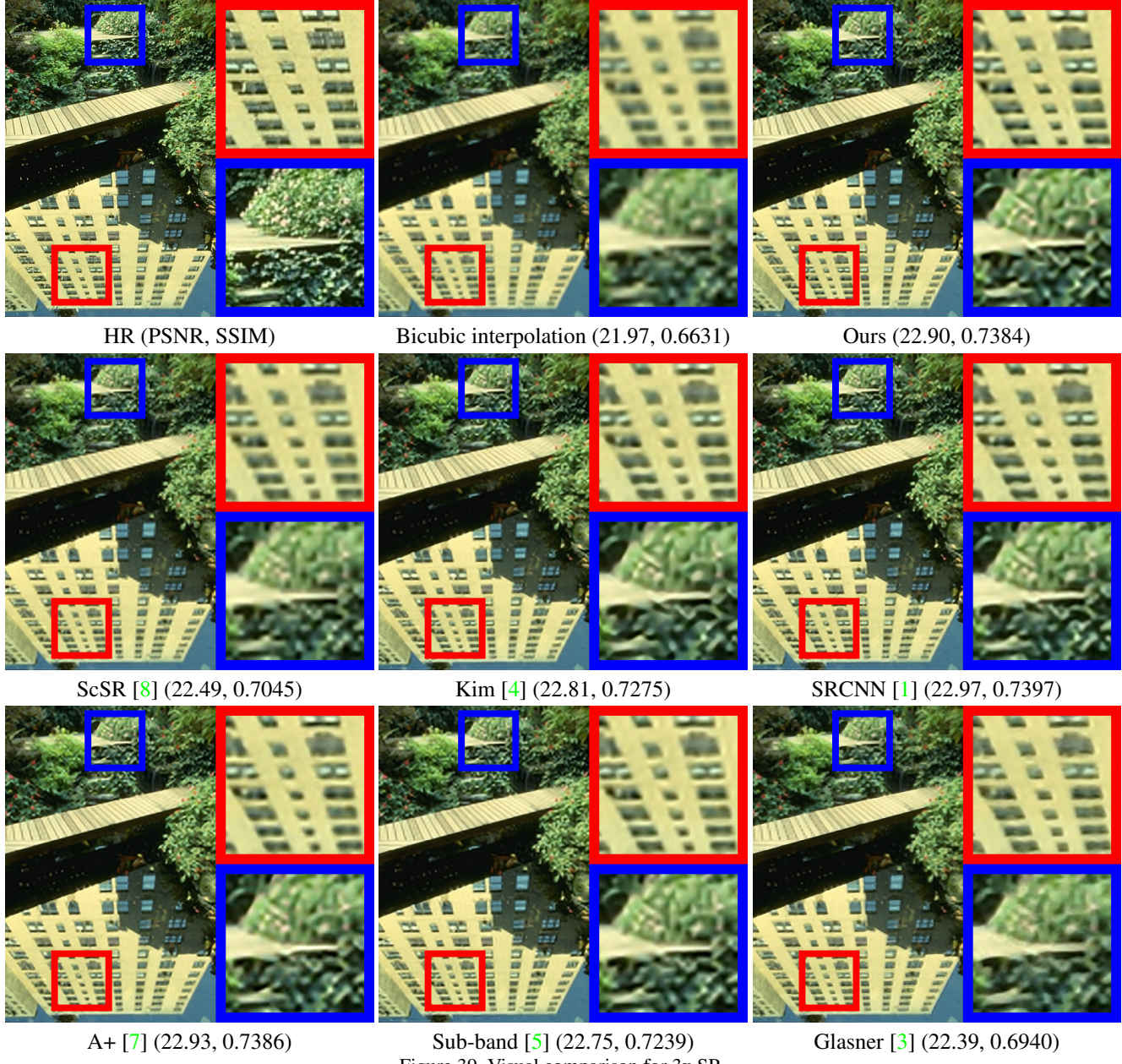


Figure 39. Visual comparison for 3x SR.

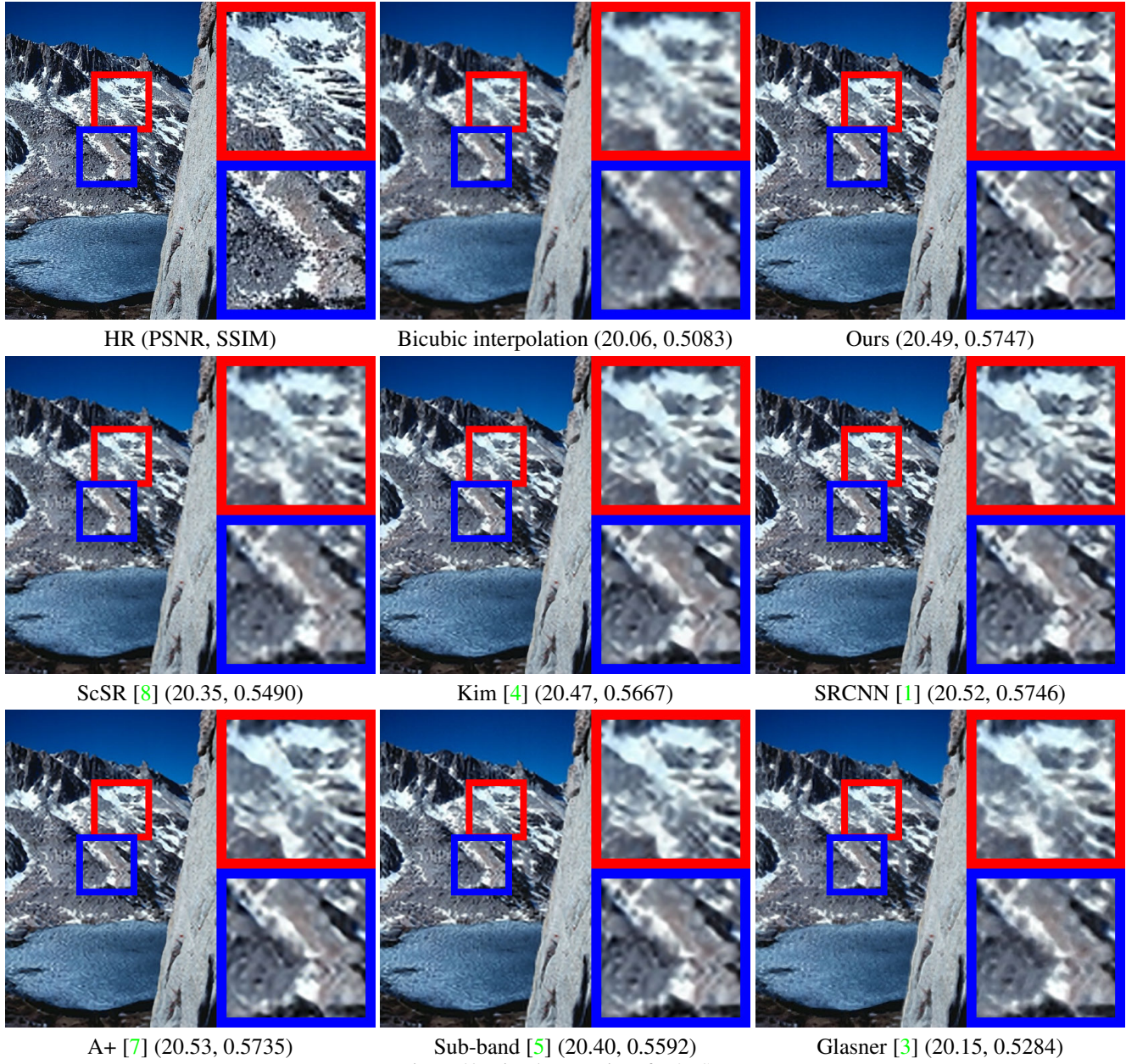


Figure 40. Visual comparison for 3x SR.

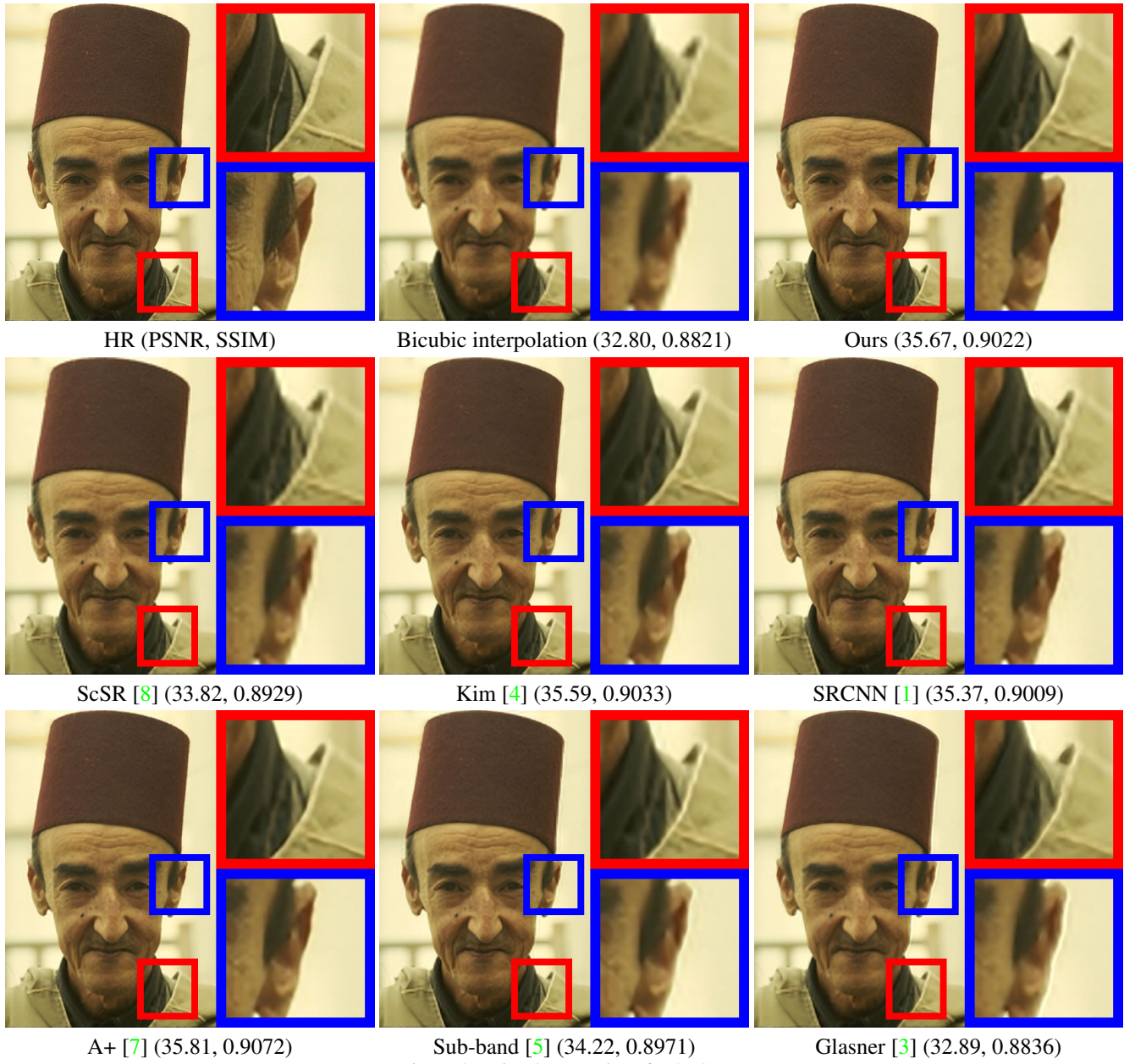


Figure 41. Visual comparison for 3x SR.

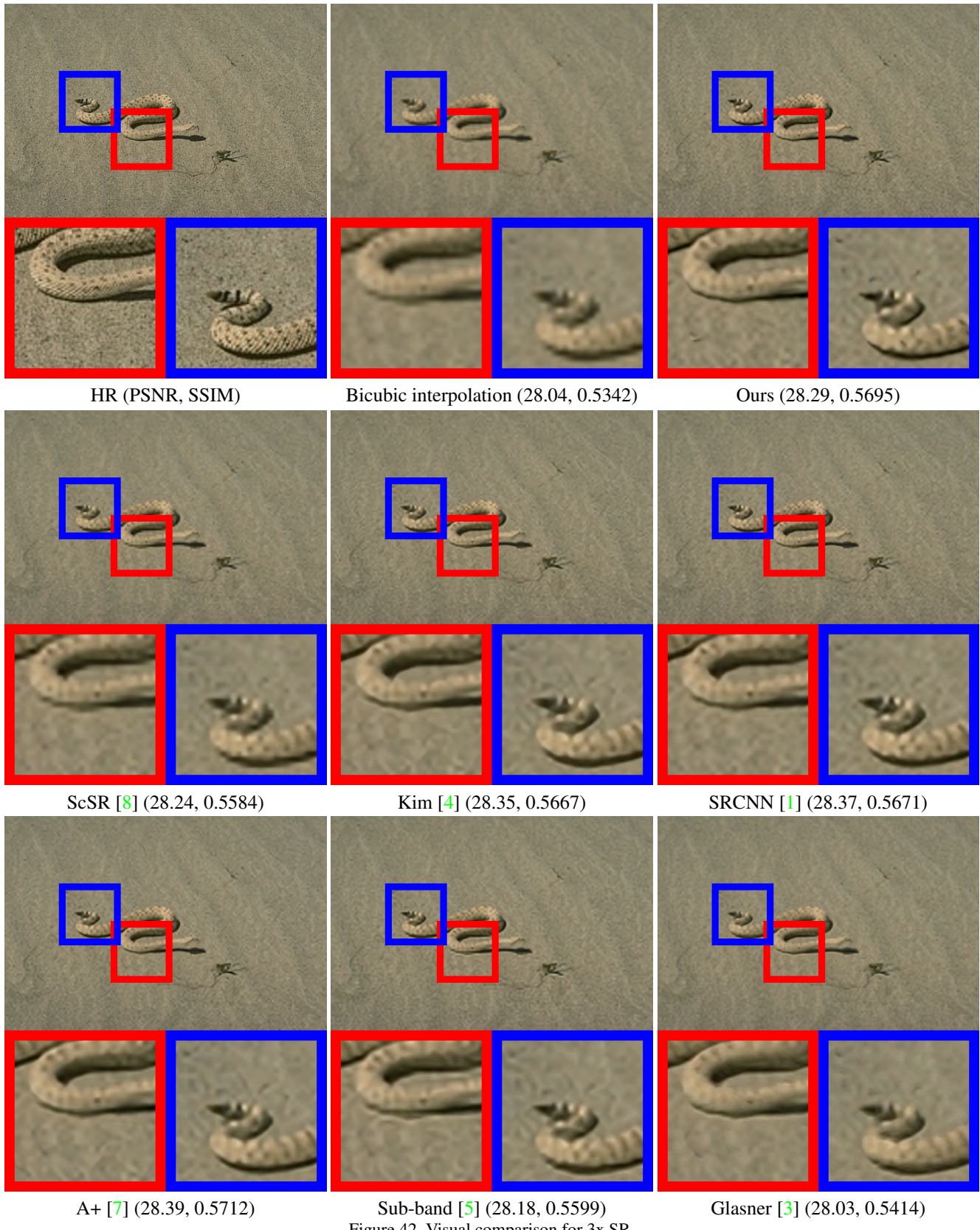


Figure 42. Visual comparison for 3x SR.

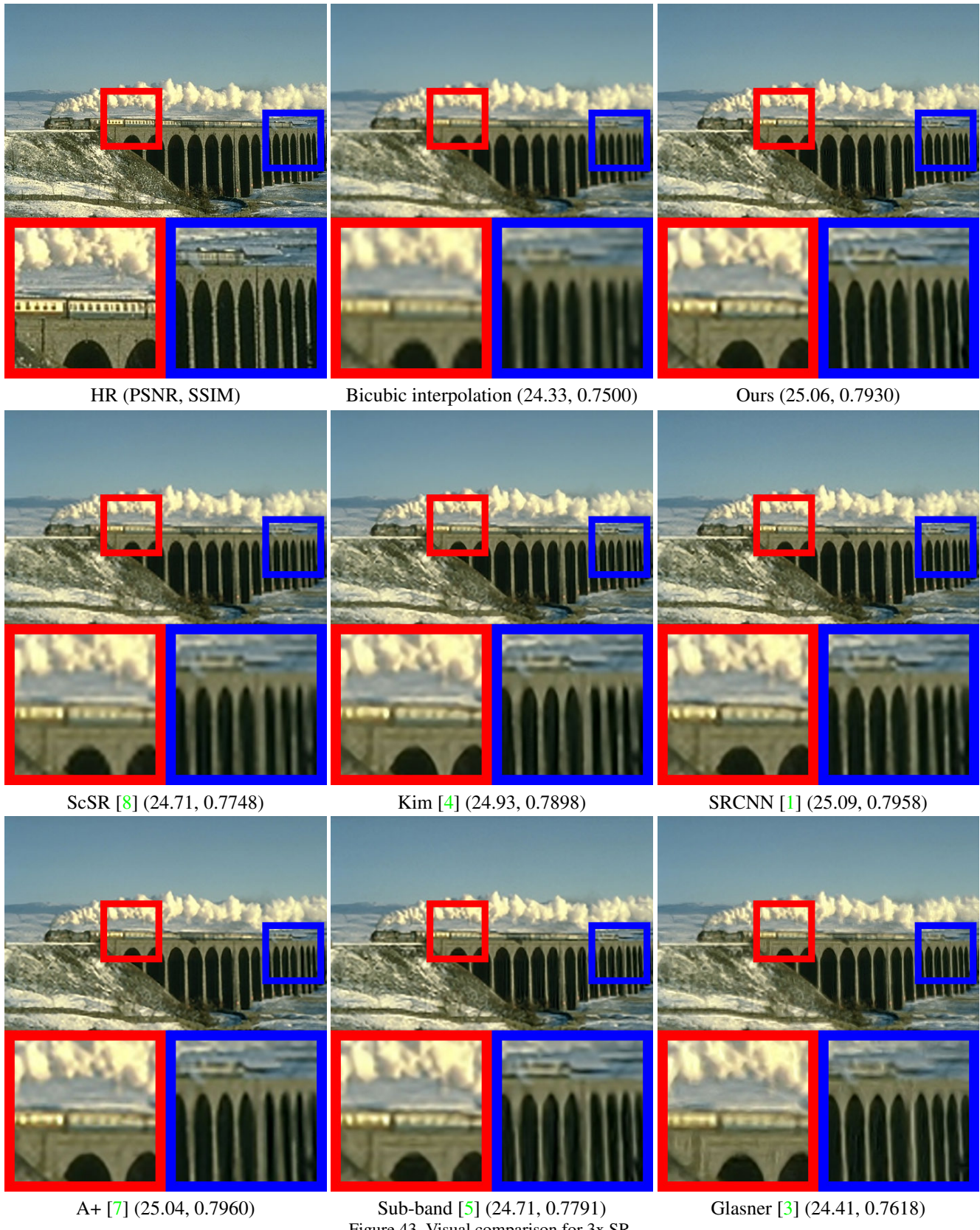


Figure 43. Visual comparison for 3x SR.

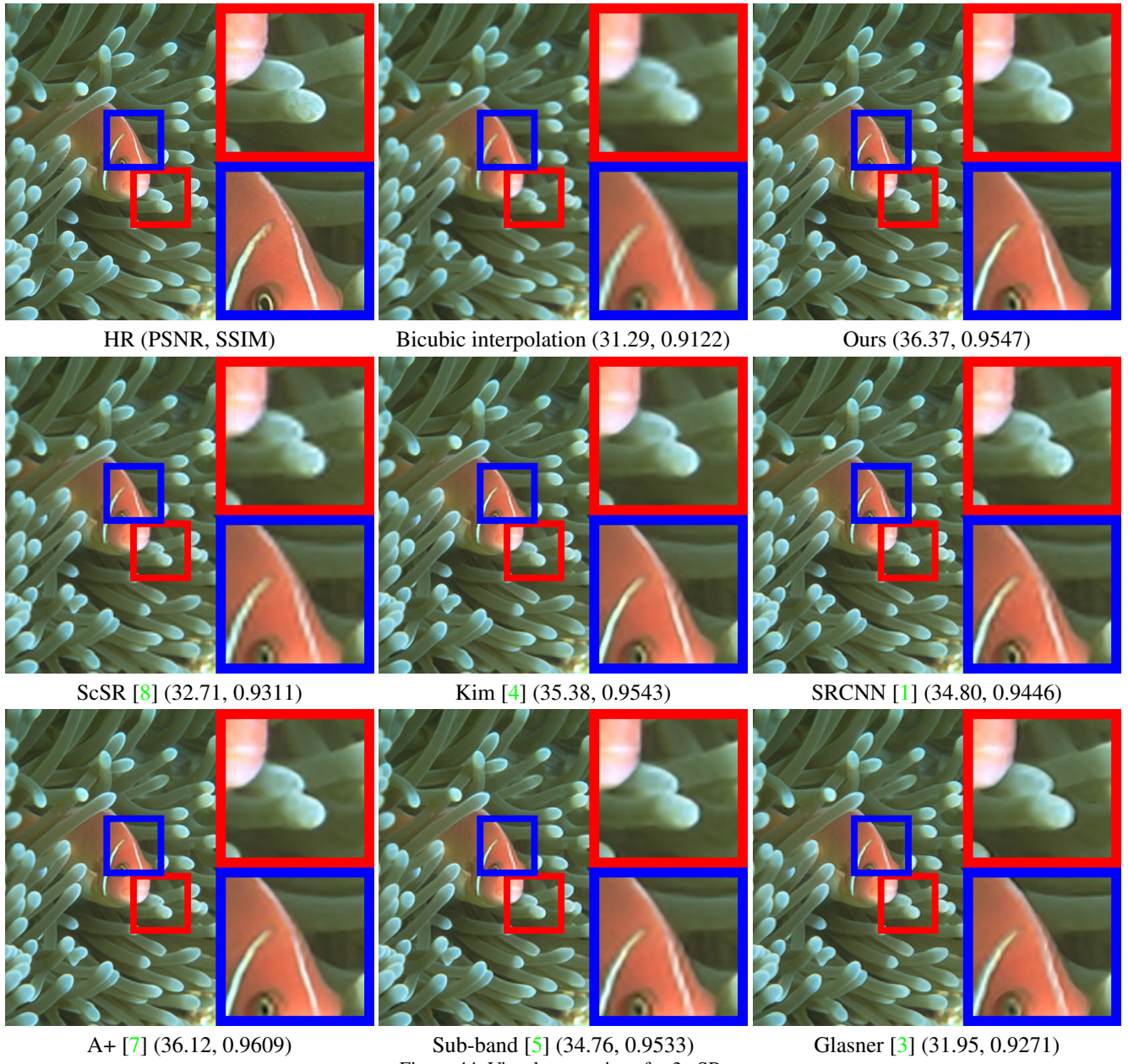


Figure 44. Visual comparison for 3x SR.

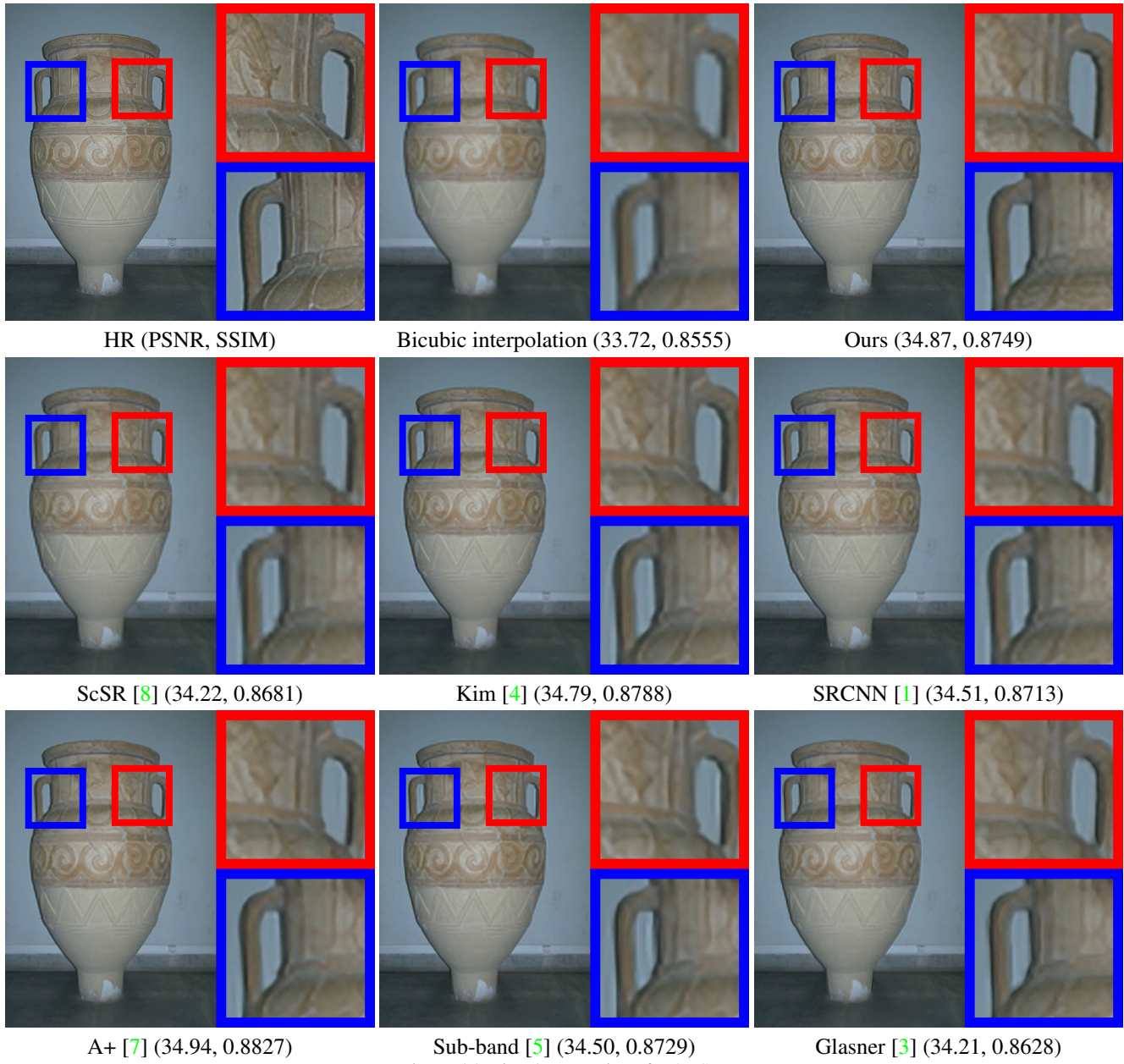


Figure 45. Visual comparison for 3x SR.

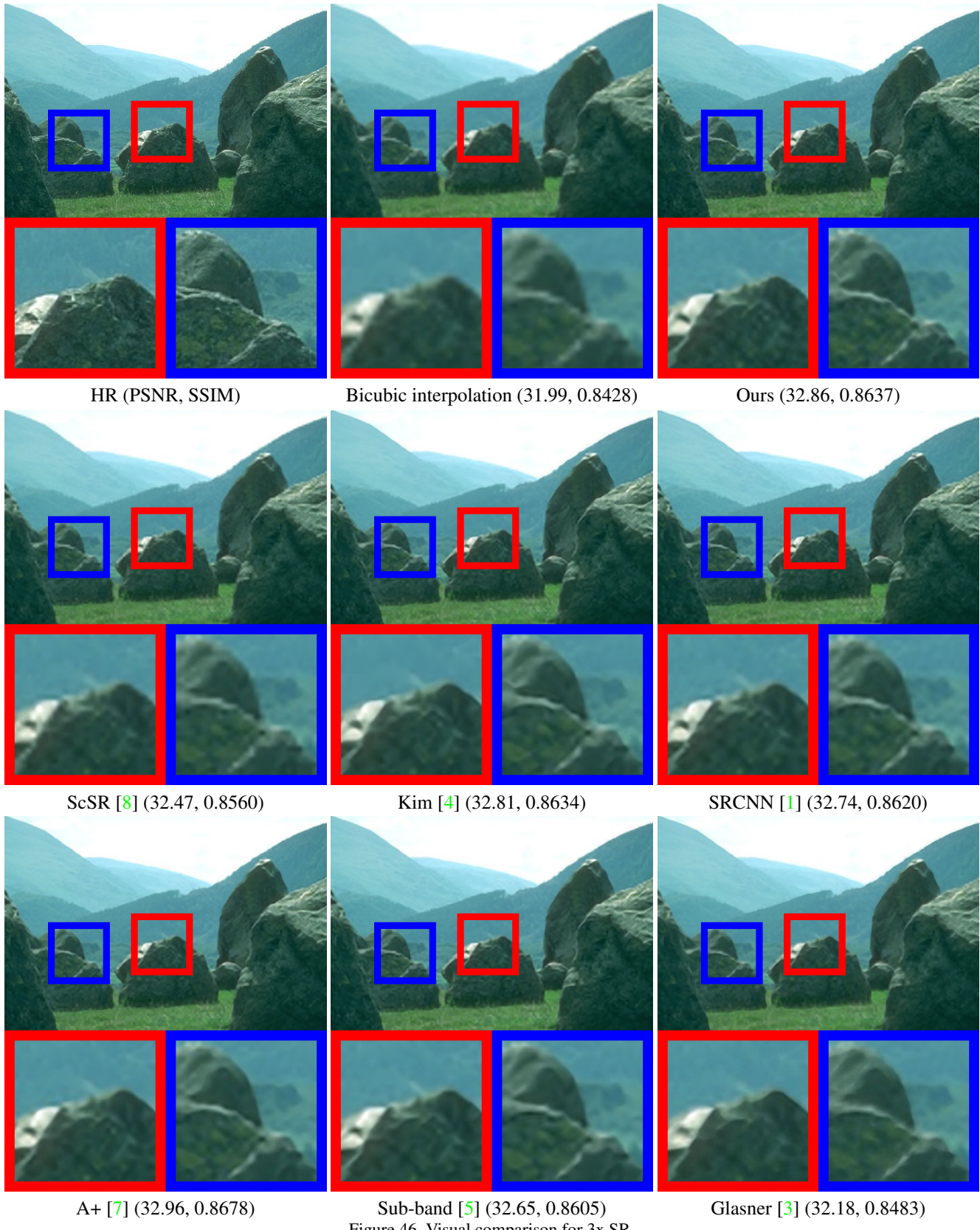


Figure 46. Visual comparison for 3x SR.

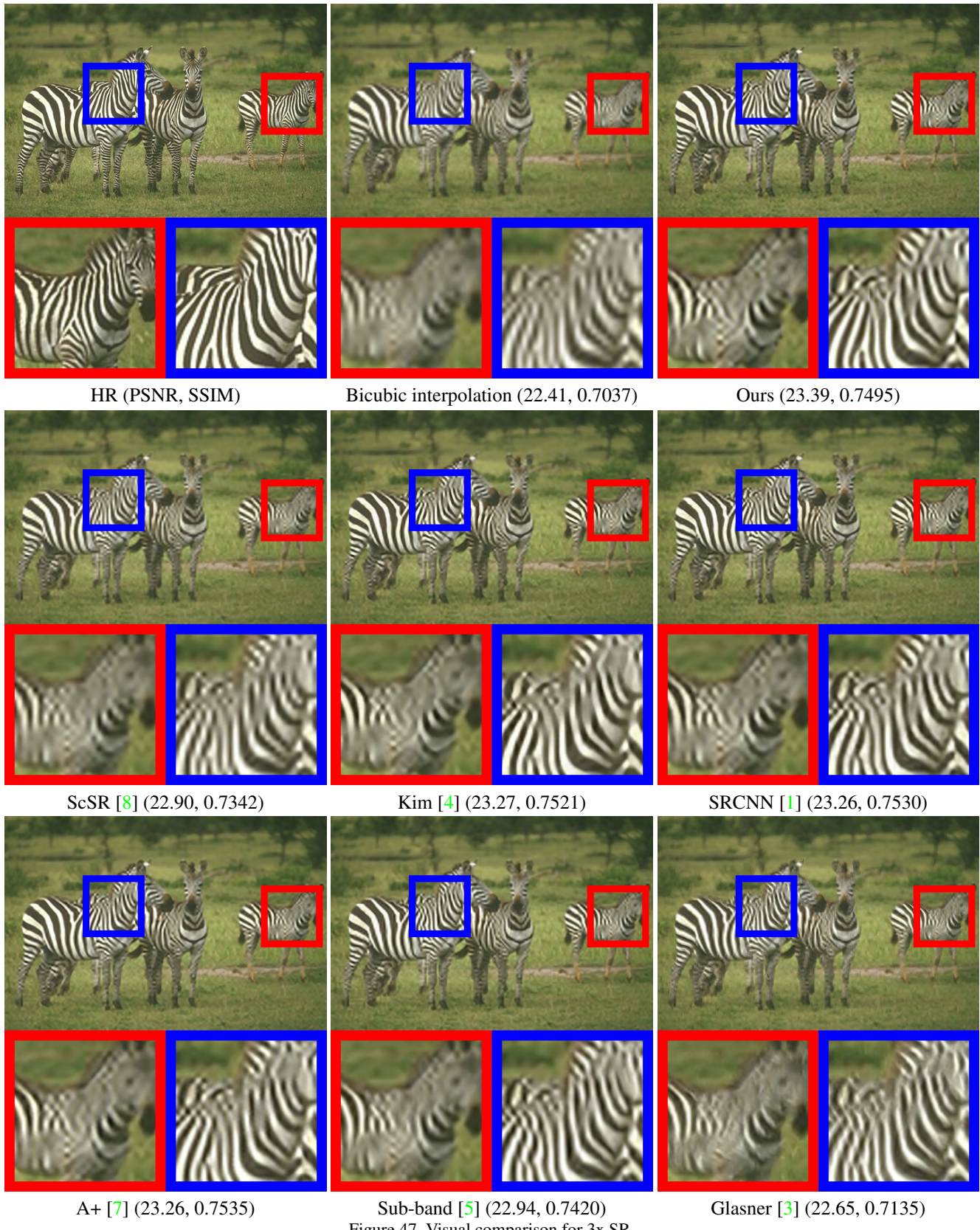


Figure 47. Visual comparison for 3x SR.

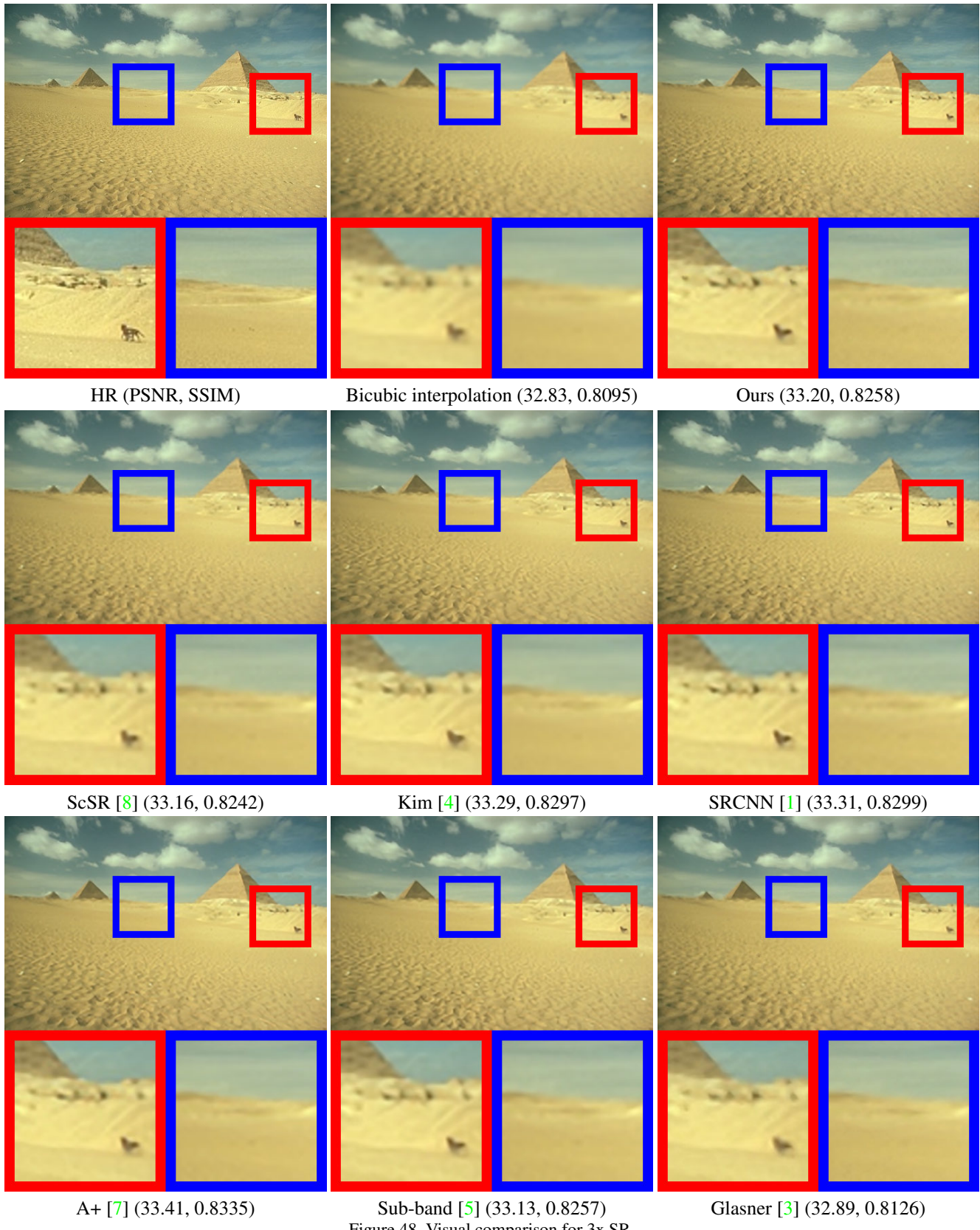


Figure 48. Visual comparison for 3x SR.



Figure 49. Visual comparison for 3x SR.

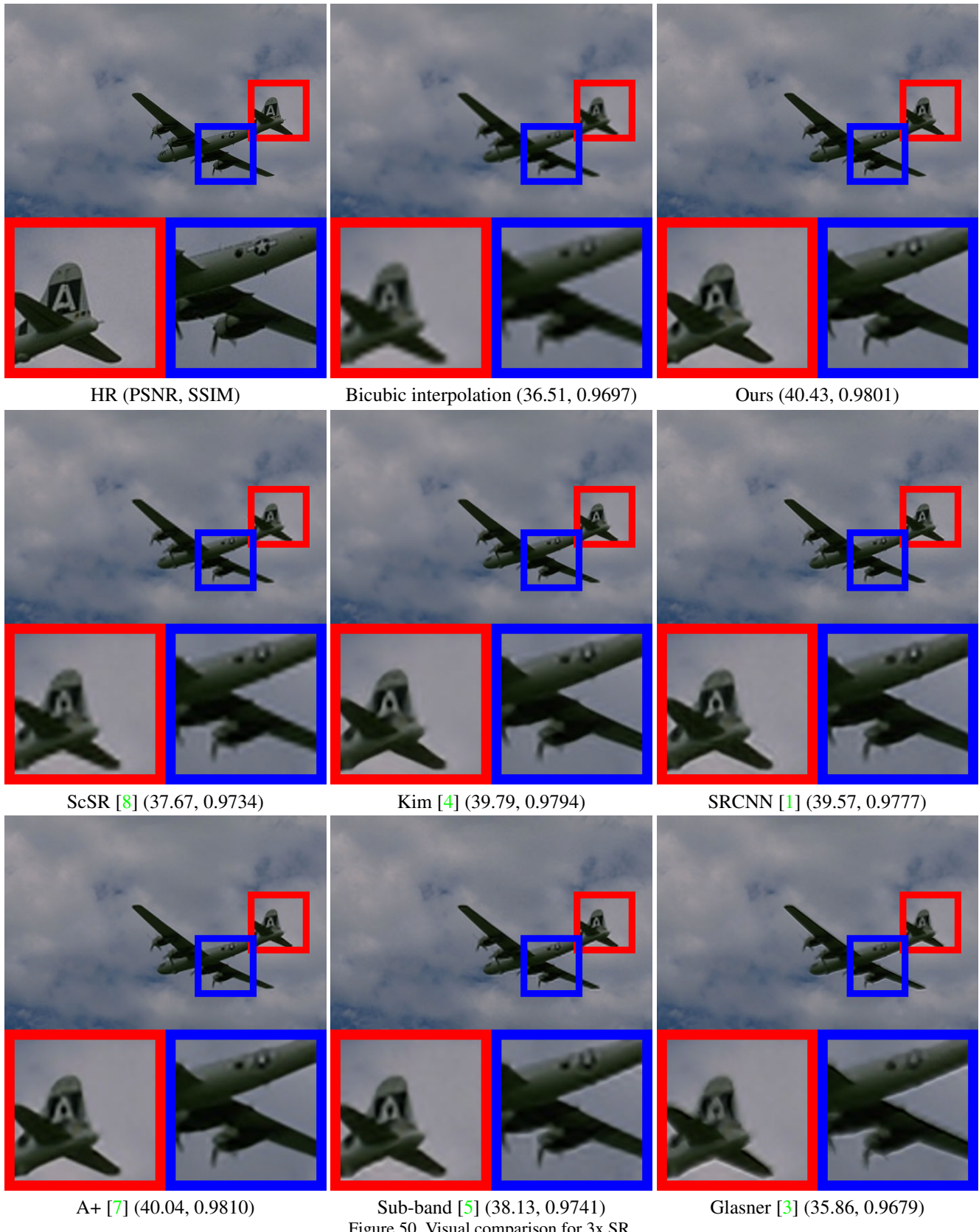


Figure 50. Visual comparison for 3x SR.



Figure 51. Visual comparison for 3x SR.



Figure 52. Visual comparison for 3x SR.

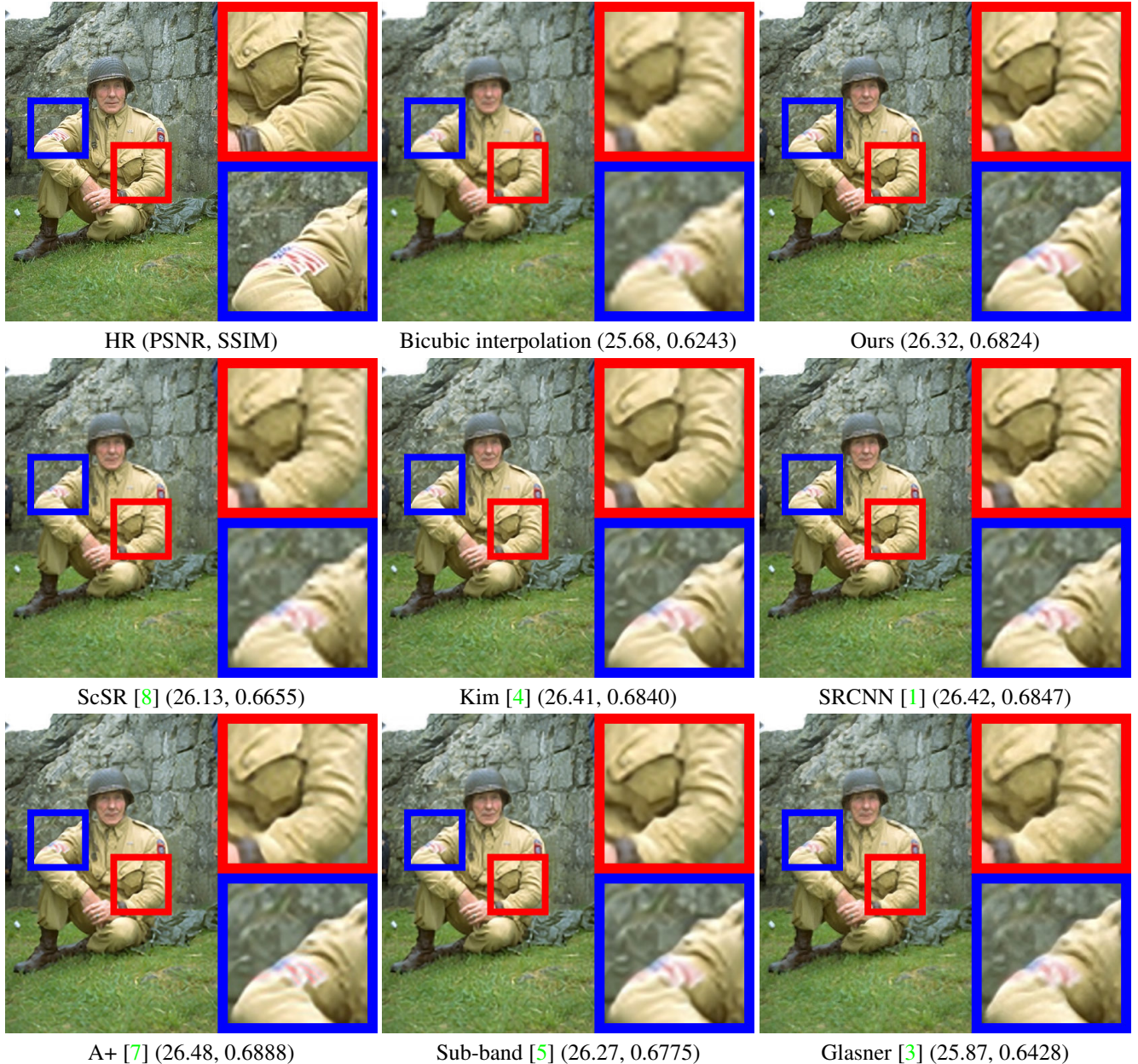


Figure 53. Visual comparison for 3x SR.

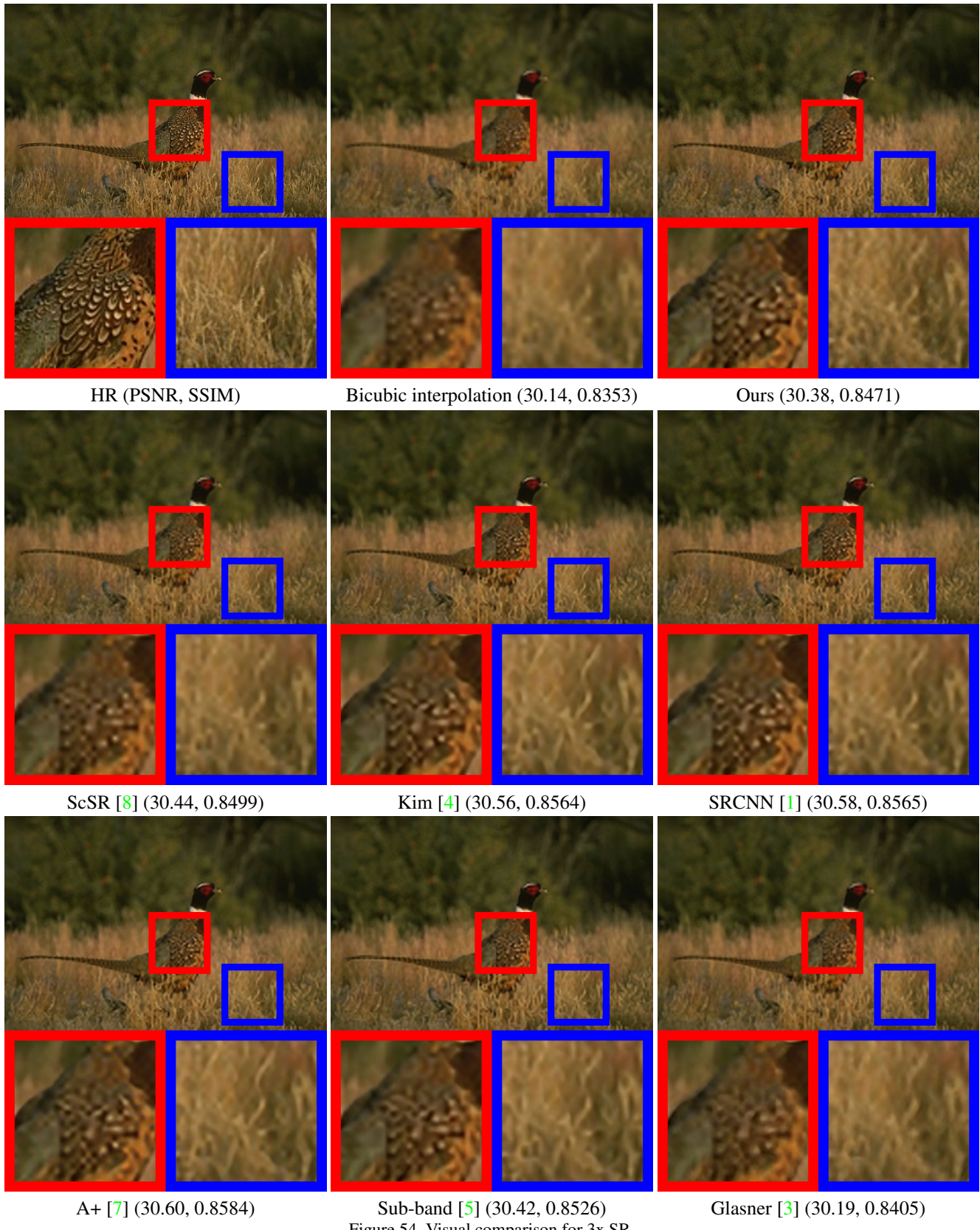


Figure 54. Visual comparison for 3x SR.



Figure 55. Visual comparison for 3x SR.

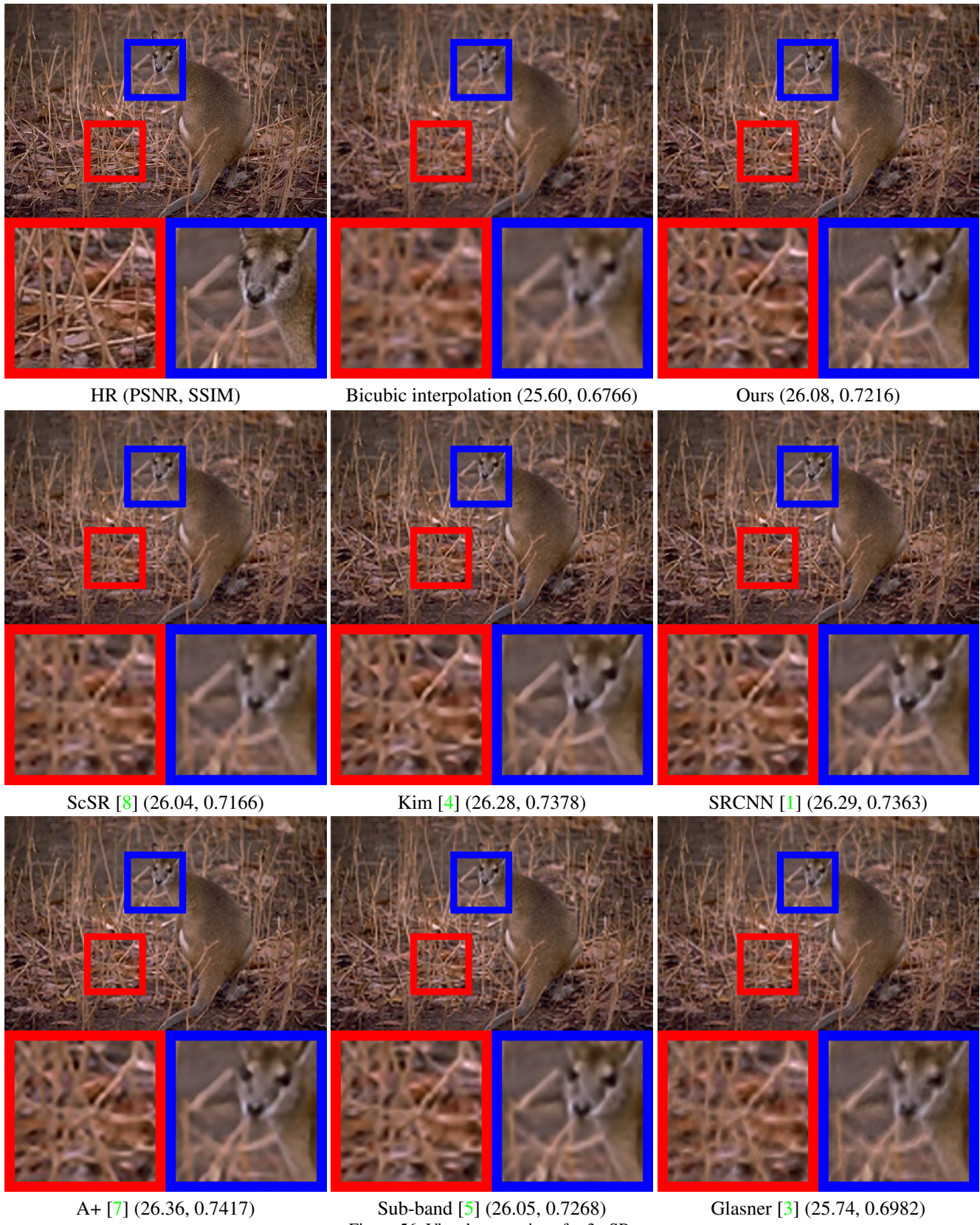


Figure 56. Visual comparison for 3x SR.

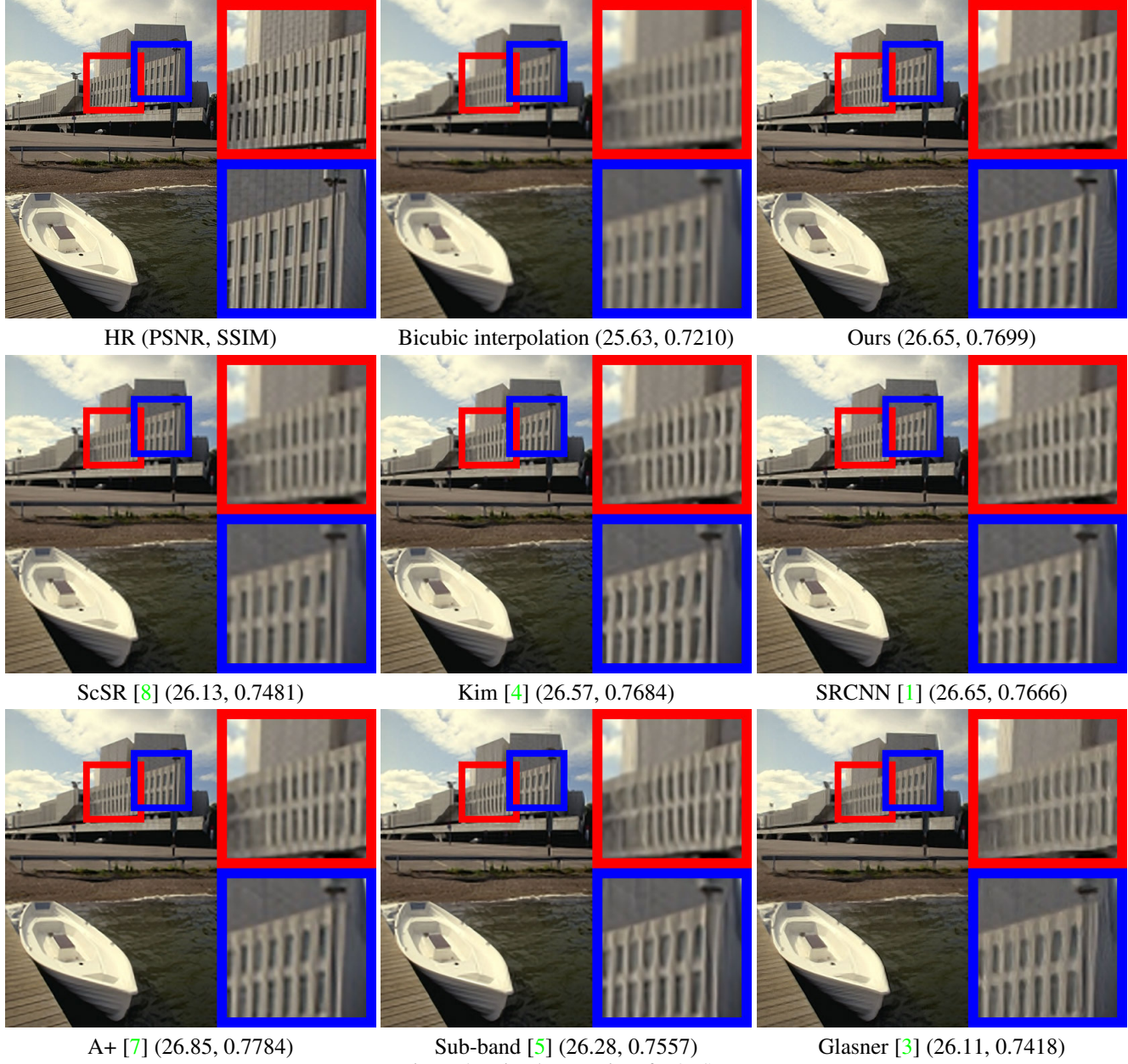


Figure 57. Visual comparison for 3x SR.

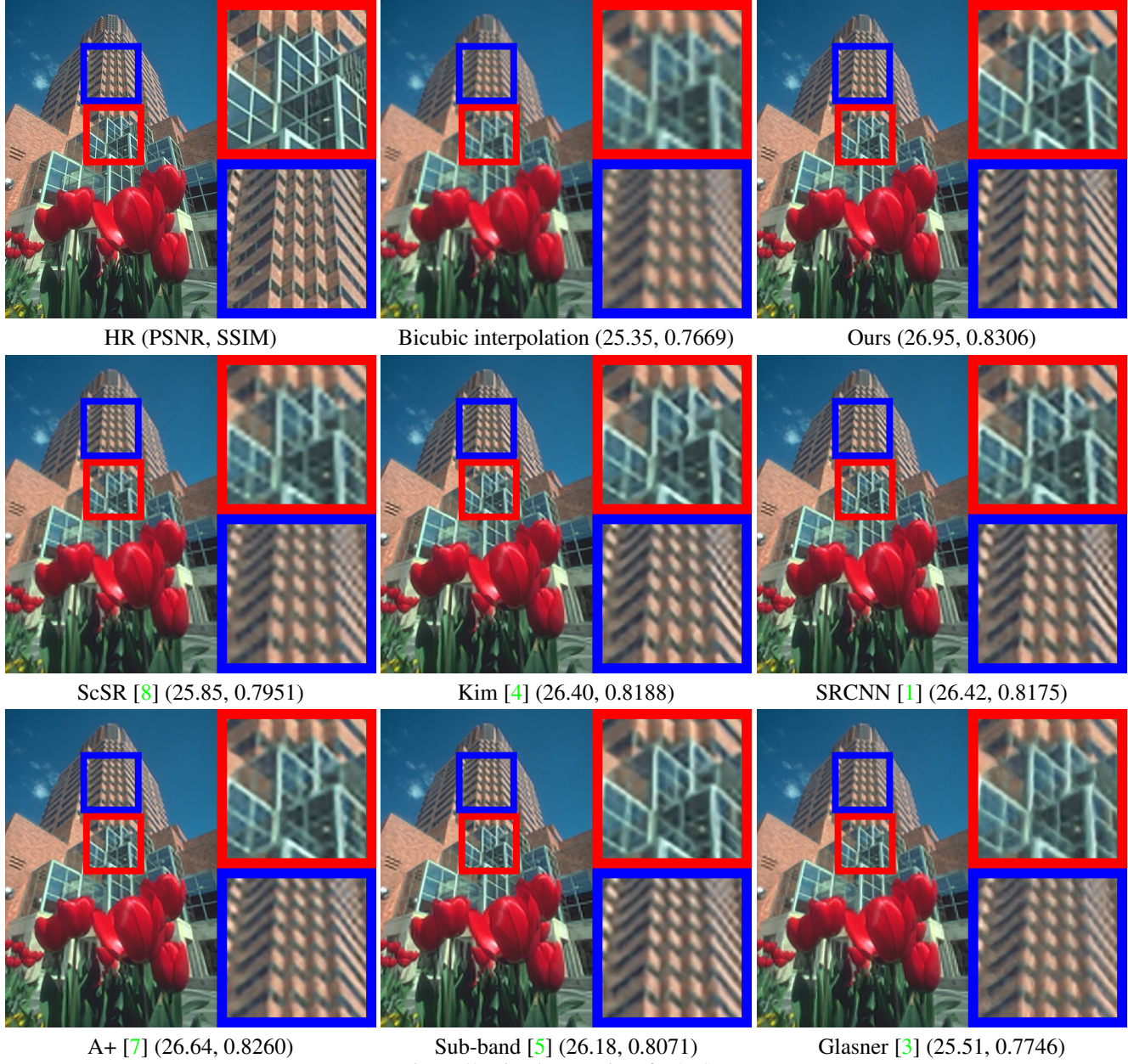


Figure 58. Visual comparison for 3x SR.

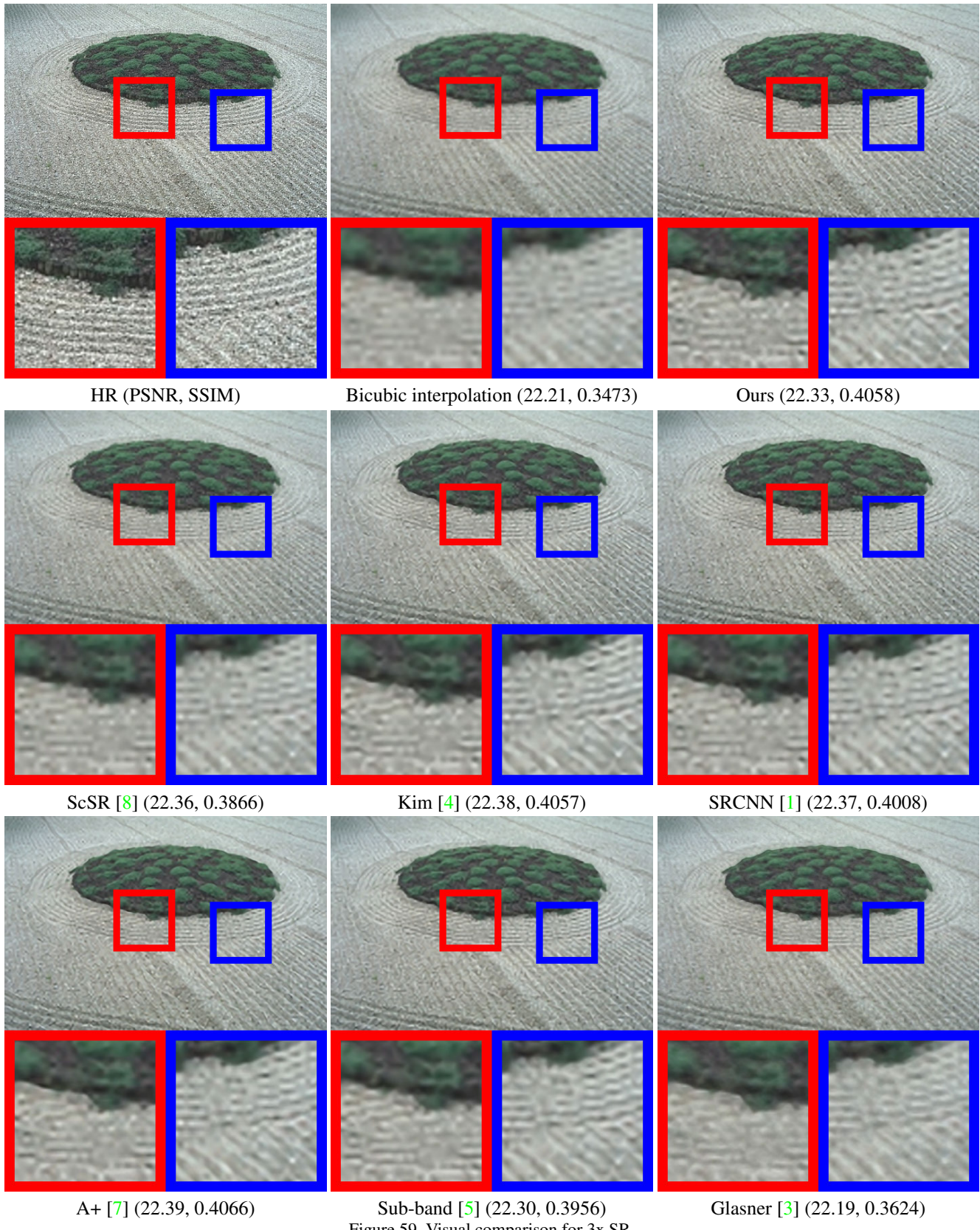


Figure 59. Visual comparison for 3x SR.

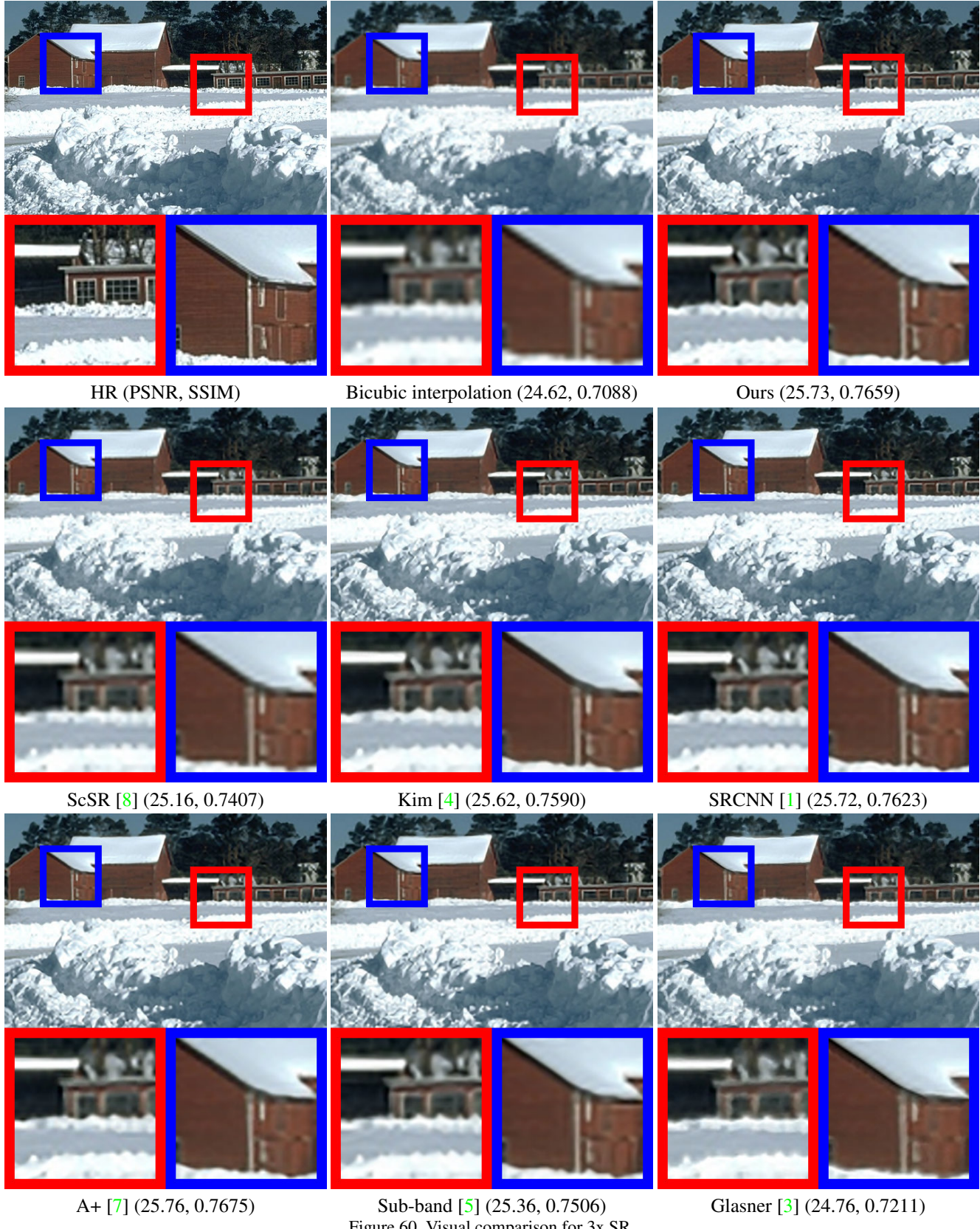


Figure 60. Visual comparison for 3x SR.

4. Sample comparisons on Sun-Hays 80 dataset

We compare our algorithm with Sun and Hays [6] using their dataset, which contains 80 natural images. We refer the dataset as *Sun-Hays 80*.

Below we show 30 sample comparisons on this dataset. We follow the experimental settings in [6] and show 8x SR results. Under such a large SR factor, the quantitative evaluation such as PSNR or SSIM may not correlate well with the perceived quality, we thus show the qualitative results only. For the first 10 images, the results from Sun and Hays [6] are available on the authors' project page http://cs.brown.edu/~lbsun/SRproj2012/SR_iccp2012.html. As the results from [6] for the rest 20 images are not available, for those images, we compare our method with Kim and Kwon [4] instead. We also show results from ScSR [8] and SRCNN [1] as two strong baselines.

For methods Kim [4], ScSR [8] and SRCNN [1], there are no trained models for SR factor 8x. We thus iteratively apply the SR factor 2x three times to achieve the SR factor 8x.



HR



Bicubic interpolation



Sun and Hays [6]



Ours



ScSR [8]



SRCNN [1]

Figure 61. Visual comparison for 8x SR.



HR



Bicubic interpolation



Sun and Hays [6]



Ours



ScSR [8]



SRCNN [1]

Figure 62. Visual comparison for 8x SR.



HR



Bicubic interpolation



Sun and Hays [6]



Ours



ScSR [8]



SRCCNN [1]

Figure 63. Visual comparison for 8x SR.



HR



Bicubic interpolation



Sun and Hays [6]



Ours



ScSR [8]



SRCCNN [1]

Figure 64. Visual comparison for 8x SR.



HR



Bicubic interpolation



Sun and Hays [6]



Ours



ScSR [8]



SRCCNN [1]

Figure 65. Visual comparison for 8x SR.



HR



Bicubic interpolation



Sun and Hays [6]



Ours



ScSR [8]



SRCCNN [1]

Figure 66. Visual comparison for 8x SR.



HR



Bicubic interpolation



Sun and Hays [6]



Ours



ScSR [8]



SRCCNN [1]

Figure 67. Visual comparison for 8x SR.



HR



Bicubic interpolation



Sun and Hays [6]



Ours



ScSR [8]



SRCNN [1]

Figure 68. Visual comparison for 8x SR.



HR



Bicubic interpolation



Sun and Hays [6]



Ours



ScSR [8]



SRCCNN [1]

Figure 69. Visual comparison for 8x SR.



HR



Bicubic interpolation



Sun and Hays [6]



Ours



ScSR [8]



SRCCNN [1]

Figure 70. Visual comparison for 8x SR.



HR



Bicubic interpolation



Kim and Kwon [4]



Ours



ScSR [8]



SRCNN [1]

Figure 71. Visual comparison for 8x SR.



HR



Bicubic interpolation



Kim and Kwon [4]



Ours



ScSR [8]



SRCNN [1]

Figure 72. Visual comparison for 8x SR.



HR



Bicubic interpolation



Kim and Kwon [4]



Ours



ScSR [8]



SRCNN [1]

Figure 73. Visual comparison for 8x SR.



HR



Bicubic interpolation



Kim and Kwon [4]



Ours



ScSR [8]



SRCNN [1]

Figure 74. Visual comparison for 8x SR.



HR



Bicubic interpolation



Kim and Kwon [4]



Ours



ScSR [8]



SRCNN [1]

Figure 75. Visual comparison for 8x SR.



HR



Bicubic interpolation



Kim and Kwon [4]



Ours



ScSR [8]



SRCCNN [1]

Figure 76. Visual comparison for 8x SR.



HR



Bicubic interpolation



Kim and Kwon [4]



Ours



ScSR [8]



SRCNN [1]

Figure 77. Visual comparison for 8x SR.



HR



Bicubic interpolation



Kim and Kwon [4]



Ours



ScSR [8]



SRCNN [1]

Figure 78. Visual comparison for 8x SR.



HR



Bicubic interpolation



Kim and Kwon [4]



Ours



ScSR [8]



SRCNN [1]

Figure 79. Visual comparison for 8x SR.



HR



Bicubic interpolation



Kim and Kwon [4]



Ours



ScSR [8]



SRCNN [1]

Figure 80. Visual comparison for 8x SR.



HR



Bicubic interpolation



Kim and Kwon [4]



Ours



ScSR [8]



SRCNN [1]

Figure 81. Visual comparison for 8x SR.



HR



Bicubic interpolation



Kim and Kwon [4]



Ours



ScSR [8]



SRCNN [1]

Figure 82. Visual comparison for 8x SR.



HR



Bicubic interpolation



Kim and Kwon [4]



Ours



ScSR [8]



SRCNN [1]

Figure 83. Visual comparison for 8x SR.



HR



Bicubic interpolation



Kim and Kwon [4]



Ours



ScSR [8]



SRCNN [1]

Figure 84. Visual comparison for 8x SR.



HR



Bicubic interpolation



Kim and Kwon [4]



Ours



ScSR [8]



SRCNN [1]

Figure 85. Visual comparison for 8x SR.



HR



Bicubic interpolation



Kim and Kwon [4]



Ours



ScSR [8]



SRCNN [1]

Figure 86. Visual comparison for 8x SR.



HR



Bicubic interpolation



Kim and Kwon [4]



Ours



ScSR [8]



SRCNN [1]

Figure 87. Visual comparison for 8x SR.



HR



Bicubic interpolation



Kim and Kwon [4]



Ours



ScSR [8]



SRCNN [1]

Figure 88. Visual comparison for 8x SR.



HR



Bicubic interpolation



Kim and Kwon [4]



Ours



ScSR [8]



SRCNN [1]

Figure 89. Visual comparison for 8x SR.



HR



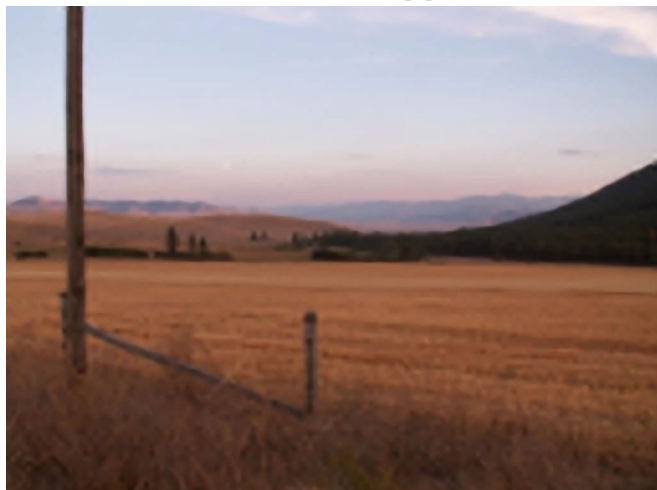
Bicubic interpolation



Kim and Kwon [4]



Ours



ScSR [8]



SRCCNN [1]

Figure 90. Visual comparison for 8x SR.

5. Comparison with TI-DTV [2]

We compare our algorithm with Fernandez-Granda and Cands [2] using the 8 test images provided in [2]. We show 22 additional comparisons using those test images from Urban 100 with only single plane in the scene.

Below we show results of SR factor 4x.

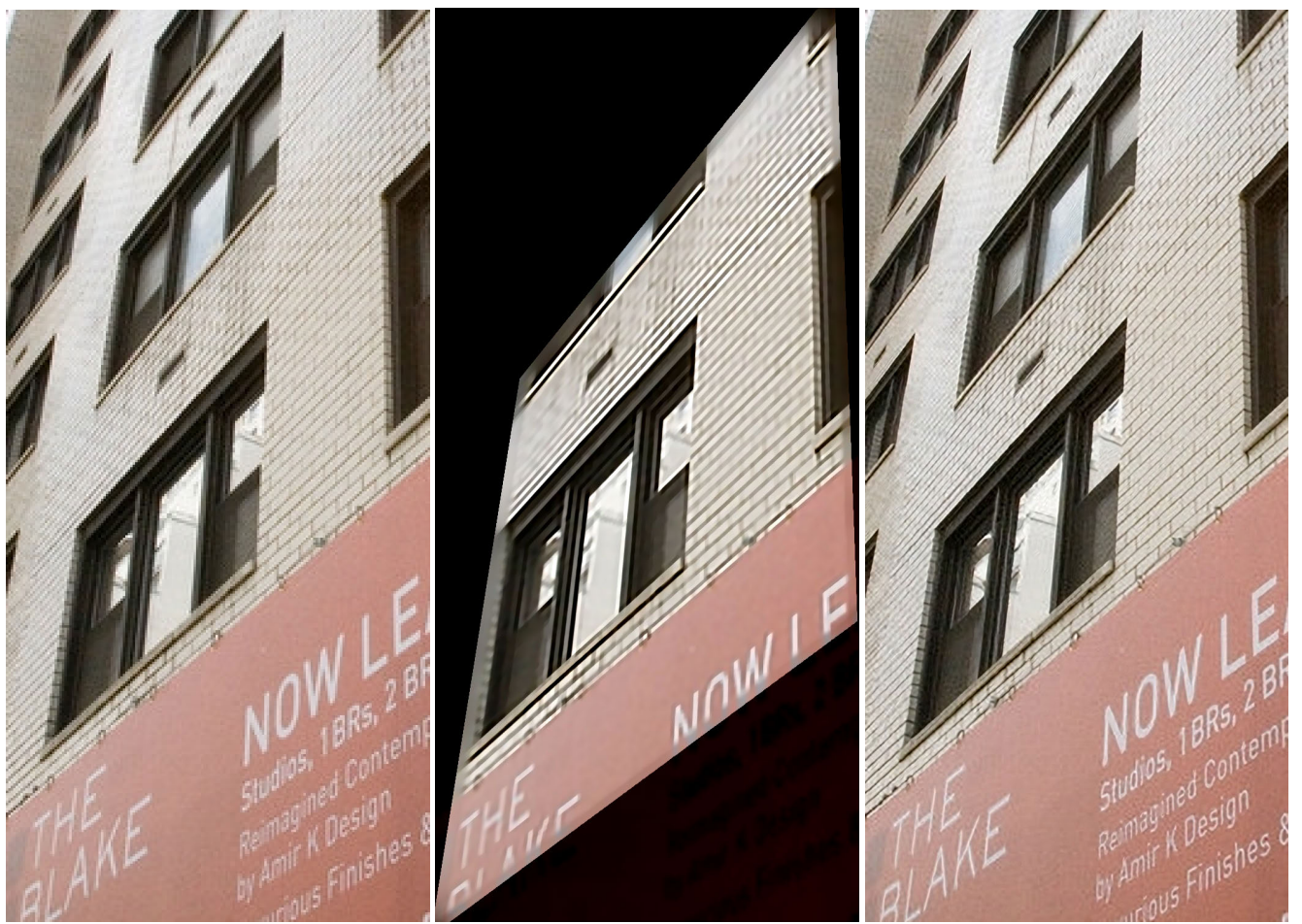


LR (NN interpolation)

TI-DTV [2]

Ours

Figure 91. Visual comparison for 4x SR.



LR (NN interpolation)

TI-DTV [2]

Ours

Figure 92. Visual comparison for 4x SR.



LR (NN interpolation)



TI-DTV [2]
Figure 93. Visual comparison for 4x SR.



Ours



LR (NN interpolation)



TI-DTV [2]
Figure 94. Visual comparison for 4x SR.



Ours



LR (NN interpolation)



TI-DTV [2]
Figure 95. Visual comparison for 4x SR.



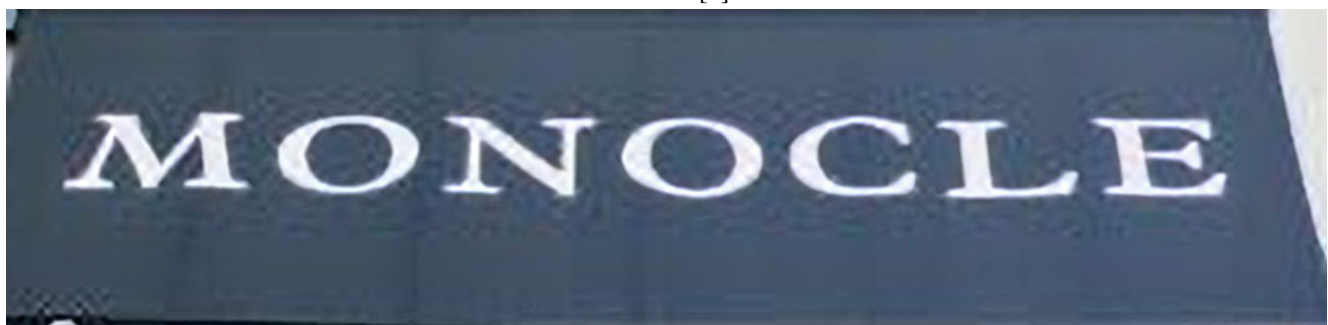
Ours



LR (NN intepolation)



TI-DTV [2]



Ours

Figure 96. Visual comparison for 4x SR.



LR (NN interpolation)



TI-DTV [2]



Ours

Figure 97. Visual comparison for 4x SR.



Figure 98. Visual comparison for 4x SR.



Figure 99. Visual comparison for 4x SR.

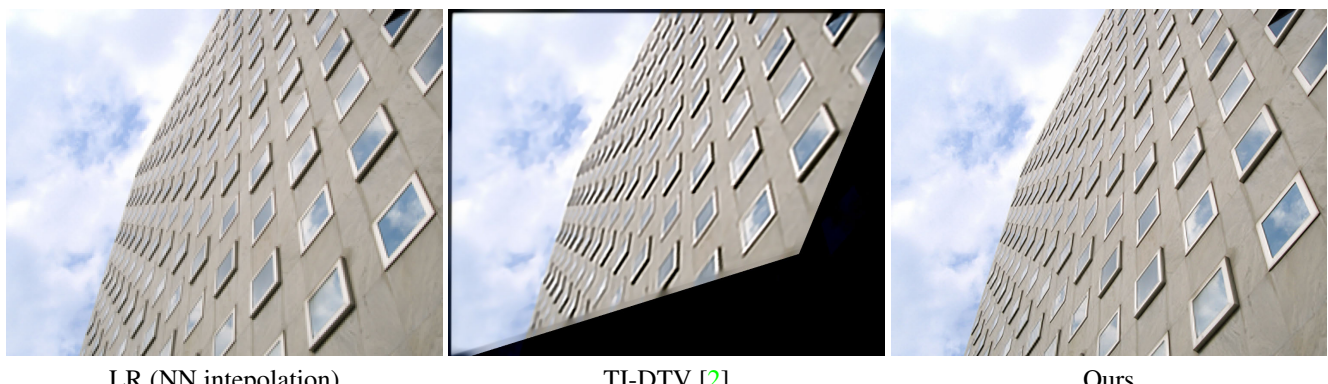


Figure 100. Visual comparison for 4x SR.



LR (NN interpolation)

TI-DTV [2]

Ours

Figure 101. Visual comparison for 4x SR.



LR (NN interpolation)

TI-DTV [2]

Ours

Figure 102. Visual comparison for 4x SR.



LR (NN interpolation)

TI-DTV [2]

Ours

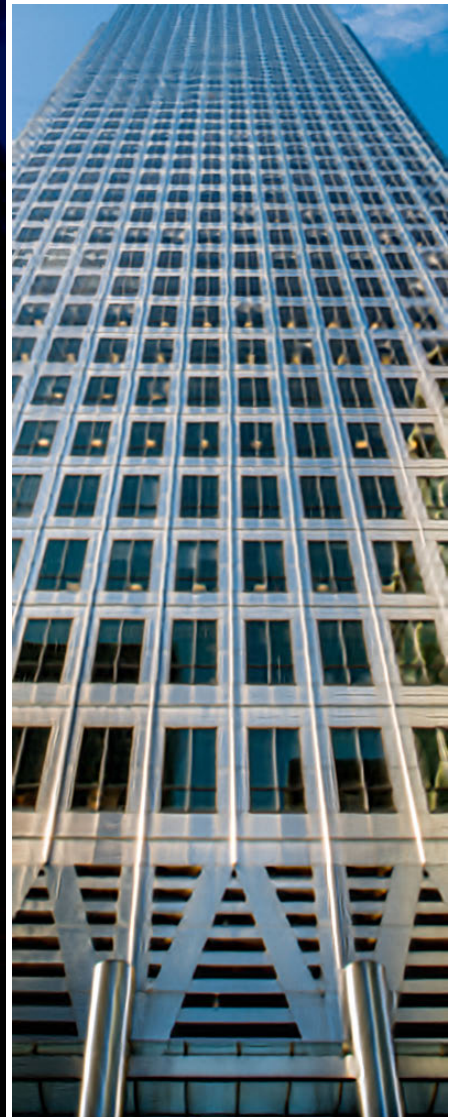
Figure 103. Visual comparison for 4x SR.



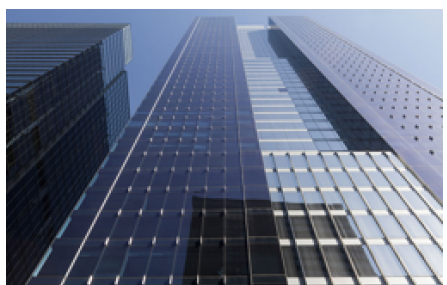
LR (NN interpolation)



TI-DTV [2]
Figure 104. Visual comparison for 4x SR.



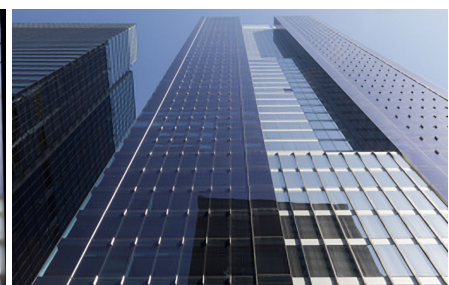
Ours



LR (NN interpolation)



TI-DTV [2]
Figure 105. Visual comparison for 4x SR.



Ours



LR (NN interpolation)



TI-DTV [2]

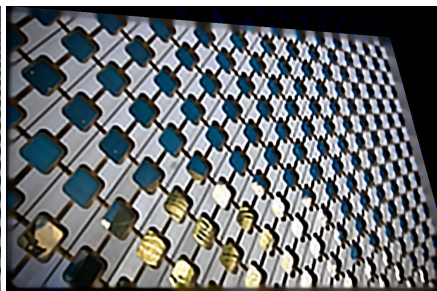


Ours

Figure 106. Visual comparison for 4x SR.



LR (NN interpolation)



TI-DTV [2]

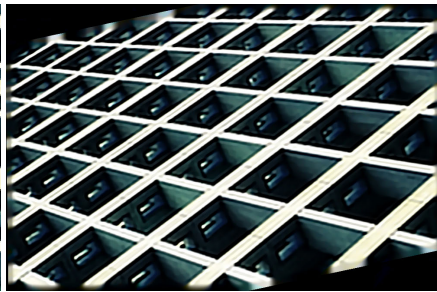


Ours

Figure 107. Visual comparison for 4x SR.



LR (NN interpolation)



TI-DTV [2]



Ours

Figure 108. Visual comparison for 4x SR.



LR (NN interpolation)



TI-DTV [2]



Ours

Figure 109. Visual comparison for 4x SR.

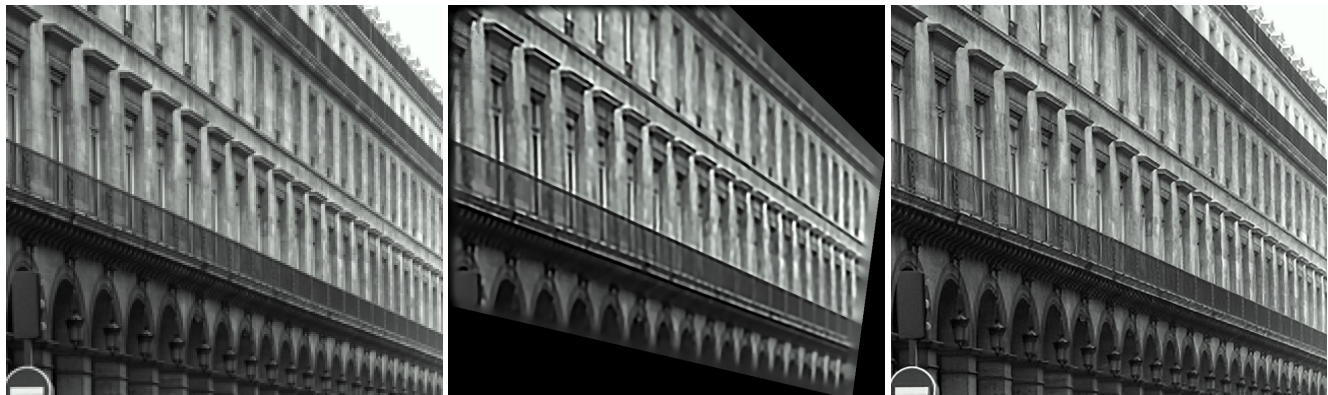


LR (NN interpolation)

TI-DTV [2]

Ours

Figure 110. Visual comparison for 4x SR.



LR (NN interpolation)

TI-DTV [2]

Ours

Figure 111. Visual comparison for 4x SR.



LR (NN interpolation)

TI-DTV [2]

Ours

Figure 112. Visual comparison for 4x SR.

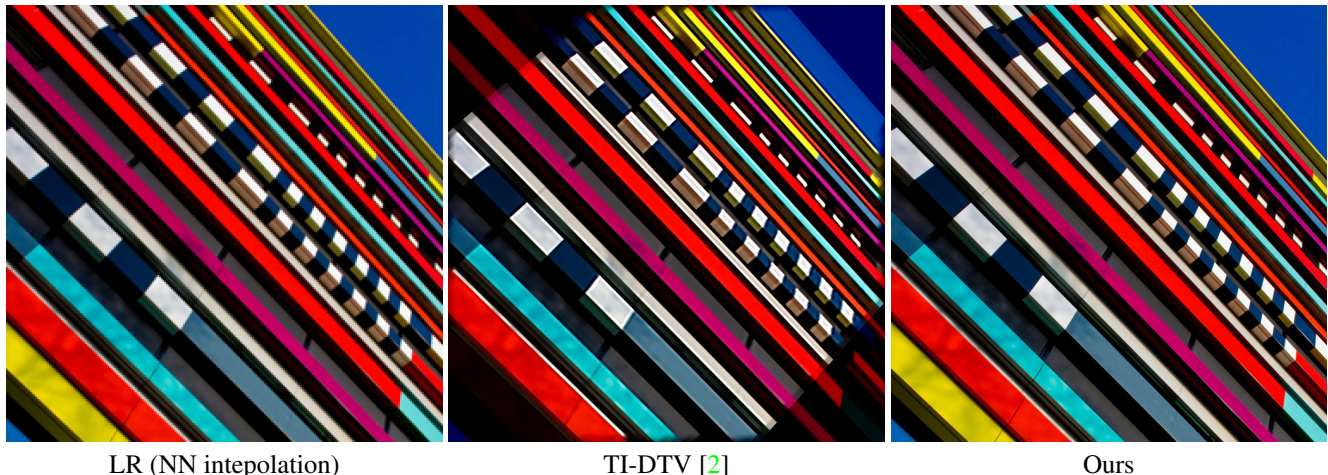


LR (NN interpolation)

TI-DTV [2]

Ours

Figure 113. Visual comparison for 4x SR.



LR (NN interpolation)

TI-DTV [2]

Ours

Figure 114. Visual comparison for 4x SR.

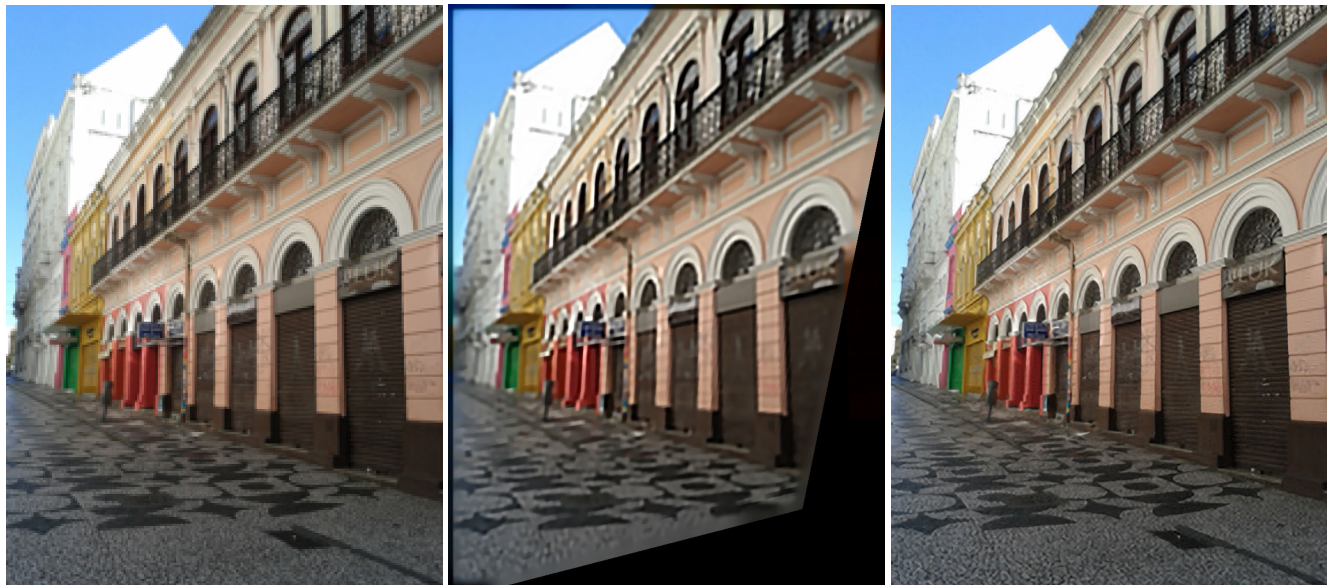


LR (NN interpolation)

TI-DTV [2]

Ours

Figure 115. Visual comparison for 4x SR.



LR (NN interpolation)

TI-DTV [2]

Ours

Figure 116. Visual comparison for 4x SR.

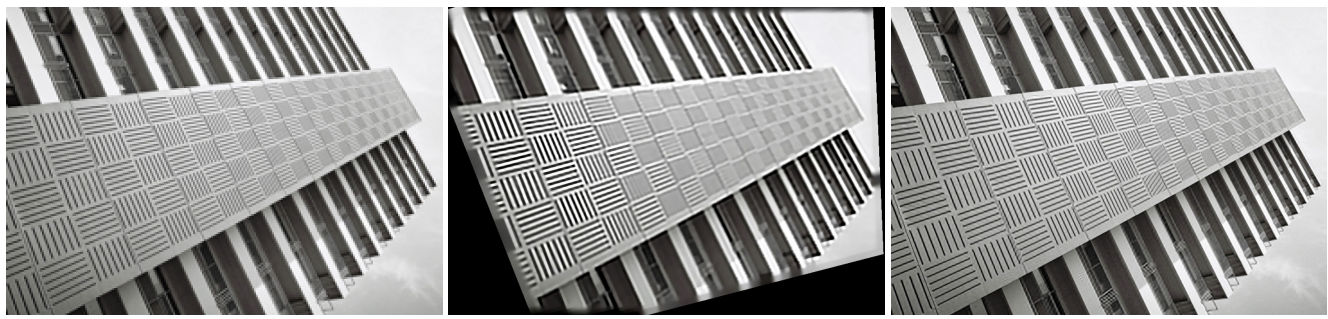


LR (NN interpolation)

TI-DTV [2]

Ours

Figure 117. Visual comparison for 4x SR.



LR (NN interpolation)

TI-DTV [2]

Ours

Figure 118. Visual comparison for 4x SR.



LR (NN interpolation)

TI-DTV [2]

Ours

Figure 119. Visual comparison for 4x SR.



LR (NN interpolation)

TI-DTV [2]

Ours

Figure 120. Visual comparison for 4x SR.

References

- [1] C. Dong, C. C. Loy, K. He, and X. Tang. Learning a deep convolutional network for image super-resolution. In *ECCV*, 2014. 1, 2, 3, 4, 5, 6, 7, 8, 9, 10, 11, 12, 13, 14, 15, 16, 17, 18, 19, 20, 21, 22, 23, 24, 25, 26, 27, 28, 29, 30, 31, 32, 33, 34, 35, 36, 37, 38, 39, 40, 41, 42, 43, 44, 45, 46, 47, 48, 49, 50, 51, 52, 53, 54, 55, 56, 57, 58, 59, 60, 61, 62, 63, 64, 65, 66, 67, 68, 69, 70, 71, 72, 73, 74, 75, 76, 77, 78, 79, 80, 81, 82, 83, 84, 85, 86, 87, 88, 89, 90, 91, 92, 93
- [2] C. Fernandez-Granda and E. J. Candès. Super-resolution via transform-invariant group-sparse regularization. In *ICCV*, 2013. 1, 94, 95, 96, 97, 98, 99, 100, 101, 102, 103, 104, 105, 106
- [3] D. Glasner, S. Bagon, and M. Irani. Super-resolution from a single image. In *ICCV*, 2009. 1, 2, 3, 4, 5, 6, 7, 8, 9, 10, 11, 12, 13, 14, 15, 16, 17, 18, 19, 20, 21, 22, 23, 24, 25, 26, 27, 28, 29, 30, 31, 32, 33, 34, 35, 36, 37, 38, 39, 40, 41, 42, 43, 44, 45, 46, 47, 48, 49, 50, 51, 52, 53, 54, 55, 56, 57, 58, 59, 60, 61, 62
- [4] K. I. Kim and Y. Kwon. Single-image super-resolution using sparse regression and natural image prior. *IEEE Trans. on Pattern Analysis and Machine Intelligence*, 32(6):1127–1133, 2010. 1, 2, 3, 4, 5, 6, 7, 8, 9, 10, 11, 12, 13, 14, 15, 16, 17, 18, 19, 20, 21, 22, 23, 24, 25, 26, 27, 28, 29, 30, 31, 32, 33, 34, 35, 36, 37, 38, 39, 40, 41, 42, 43, 44, 45, 46, 47, 48, 49, 50, 51, 52, 53, 54, 55, 56, 57, 58, 59, 60, 61, 62, 63, 74, 75, 76, 77, 78, 79, 80, 81, 82, 83, 84, 85, 86, 87, 88, 89, 90, 91, 92, 93
- [5] A. Singh and N. Ahuja. Super-resolution using sub-band self-similarity. In *ACCV*, 2014. 1, 2, 3, 4, 5, 6, 7, 8, 9, 10, 11, 12, 13, 14, 15, 16, 17, 18, 19, 20, 21, 22, 23, 24, 25, 26, 27, 28, 29, 30, 31, 32, 33, 34, 35, 36, 37, 38, 39, 40, 41, 42, 43, 44, 45, 46, 47, 48, 49, 50, 51, 52, 53, 54, 55, 56, 57, 58, 59, 60, 61, 62
- [6] L. Sun and J. Hays. Super-resolution from internet-scale scene matching. In *ICCP*, 2012. 1, 63, 64, 65, 66, 67, 68, 69, 70, 71, 72, 73
- [7] R. Timofte, V. De Smet, and L. Van Gool. A+: Adjusted anchored neighborhood regression for fast super-resolution. In *ACCV*, 2014. 1, 2, 3, 4, 5, 6, 7, 8, 9, 10, 11, 12, 13, 14, 15, 16, 17, 18, 19, 20, 21, 22, 23, 24, 25, 26, 27, 28, 29, 30, 31, 32, 33, 34, 35, 36, 37, 38, 39, 40, 41, 42, 43, 44, 45, 46, 47, 48, 49, 50, 51, 52, 53, 54, 55, 56, 57, 58, 59, 60, 61, 62
- [8] J. Yang, J. Wright, T. S. Huang, and Y. Ma. Image super-resolution via sparse representation. *IEEE Trans. on Image Processing*, 19(11):2861–2873, 2010. 1, 2, 3, 4, 5, 6, 7, 8, 9, 10, 11, 12, 13, 14, 15, 16, 17, 18, 19, 20, 21, 22, 23, 24, 25, 26, 27, 28, 29, 30, 31, 32, 33, 34, 35, 36, 37, 38, 39, 40, 41, 42, 43, 44, 45, 46, 47, 48, 49, 50, 51, 52, 53, 54, 55, 56, 57, 58, 59, 60, 61, 62, 63, 64, 65, 66, 67, 68, 69, 70, 71, 72, 73, 74, 75, 76, 77, 78, 79, 80, 81, 82, 83, 84, 85, 86, 87, 88, 89, 90, 91, 92, 93